To the Graduate Council:

I am submitting herewith a thesis written by Richard F. Eldreth entitled "Control of Melt Spinline Diameter and Birefringence Using a Novel Sensor." I have examined the final copy of this thesis for form and content and recommend that it be accepted in partial fulfillment of the requirements for the degree of Master of Science, with a major in Chemical Engineering.

Duane D Bruns

Duane D. Bruns, Major Professor

We have read this thesis
and recommend its acceptance:

John F. Fellers

DeBorgue

Accepted for the Council:

Lawrence Minkel

Vice Provost
and Dean of The Graduate School

STATEMENT OF PERMISSION TO USE

In presenting this thesis in partial fulfillment of the requirements for a Master's degree at The University of Tennessee, Knoxville, I agree that the Library shall make it available to borrowers under rules of the Library. Brief quotatations from this thesis are allowable without special permission, provided that accurate acknowledgment of source is made.

Permission for extensive quotation from or reproduction of this thesis may be granted by my major professor, or in his absence, by the Head of Interlibrary Services when, in the opinion of either, the proposed use of the material is for scholarly purposes. Any copying or use of the material in this thesis for financial gain shall not be allowed without my written permission.

Signature Richard F. Eldredt

Date February 25, 1985

CONTROL OF MELT SPINLINE DIAMETER AND BIREFRINGENCE USING A NOVEL SENSOR

A Thesis

Presented for the

Master of Science

Degree

The University of Tennessee, Knoxville

Richard F. Eldreth

March 1985

ACKNOWLEDGEMENTS

The author would like to express his sincere appreciation to the many people who aided him during the course of this research. He wishes to thank his advisor, Dr. Duane D. Bruns, for his continued support and assistance in the completion of this work. He would also like to thank Dr. John F. Fellers for his invaluable suggestions and encouragement that initiated this project and helped it through to completion. The author's indebtedness goes to Dr. Donald C. Bogue who provided considerable support and served as a member of his supervisory committee.

For special assistance in data acquisition for the project, the author would like to thank Ken Zieminski. Special thanks are also extended to James Hackney for sharing his vast wealth of knowledge in process control and to Phyllis Davis for her superior editing and typing of this manuscript.

Finally, the author's sincere appreciation goes to his parents, Fred and Margaret Eldreth, brother, Wayne, and sister, Lisa for their unending support and patience during the course of this work.

ABSTRACT

Process control techniques have been expanded to include polymer processing operations. This work demonstrated control of melt spinline diameter and birefringence in real-time on an operating spinline. Two control loops have been utilized--diameter and birefringence, respectively, controlled by the take-up velocity of the spinline. Control was accomplished using a prototyped novel sensor for on-line measurement of both diameter and birefringence. The sensor closed the control loop and also indicated spinline position and tension.

The growing awareness of the polymer processing industry to the advantages of applied process control has contributed greatly to the motivation of the project. The lack of process control research in the area of polymer processing, relative to the chemical industry, has given the inspiration for quickly developing new technology. Also, previous work (Lindenmeyer hypothesis) has indicated that energy perturbations of the spinline produce changes of the birefringence, so potential is offered for a new control variable. These changes have been confirmed and explored in this work.

Research on the melt spinline control demanded a minicomputer to serve as a data acquisition facility and controller. The computer interacts with the novel sensor to set parameters for analysis and recording of fiber diameter, birefringence, tension, and position. Also, the computer is used as a research data base for spinline modeling and optimization. Controlling algorithms are encoded in

the computer's memory for manipulating a sound wave perturbation and take-up motor to maintain a specific setpoint of diameter or birefringence.

The on-line measurements and capabilities of the novel sensor interfaced with a minicomputer has established a highly functional real time research facility. The real time data acquisition can provide a research data base for process optimization and is a basis for continuing research of the Lindenmeyer hypothesis. Also, the control loop is closed and a research control facility for developing advanced multivariable control strategies has been established. A demonstration of its utility has been made with the successful control of diameter and birefringence.

TABLE OF CONTENTS

CHAPTER		PAGE
I.	INTRODUCTION	1
II.	BACKGROUND	4
	2.1 Process Modeling	4
	2.2 Process Optimization	6
	2.3 Control Theory	9
	2.4 Data Filtering for Process Control	25
	2.5 Properties of Melt Spun Fibers	27
	2.6 Melt Spinning	41
III.	SENSOR DEVELOPMENT	59
	3.1 Sensor Specification	59
	3.2 Background Studies	61
	3.3 Bench Scale Research and Data Acquisition	63
	3.4 Hardware Development	65
	3.5 Sensor Calibration	74
IV.	CONTROL DEVELOPMENT	83
	4.1 Open Loop Analysis	83
	4.2 Model Development	88
	4.3 Control Techniques	95
V.	EXPERIMENTAL RESULTS AND DISCUSSION	104
	5.1 Operating Conditions	104
	Melt spinline	104
	Sensor	106

CHAPTER PAGE

V. (Continued)

5.2 Computer Data Acquisition 109

5.3 Open Loop Results 112

5.4 Control Loop Responses 122

VI. CONCLUSIONS AND RECOMMENDATIONS 132

6.1 Conclusions 132

6.2 Recommendations 135

LIST OF REFERENCES 143

APPENDIX 148

VITA 155

LIST OF TABLES

TABLE		PAGE
2.1	Closed Loop Setpoint and Disturbance Transfer Functions	23
3.1	Aperture Data for Laser	64
3.2	Comparison of Values Obtained at Hercules Inc. with Those at University of Tennessee (UT) for Polypropylene Fiber Samples	78
3.3	Comparison of Values Obtained at Hercules Inc. with Uncalibrated Sensor Readings at University of Tennessee (UT) for Polypropylene Fiber Samples	79
3.4	Spinline Data for Calibrated Sensor and Compensatory Microscope	80
3.5	Stability of Sensor Electronics (Static Spinline)	82

LIST OF FIGURES

FIGURE		PAGE
2.1.	Three-dimensional map indicating possible process optimums	7
2.2.	Two examples of feedback control	12
2.3.	Response of a first order process with dead time or second or higher order process (with or without dead time and no significant right hand plane zeros) to a step disturbance with P, PI, and PID controllers	18
2.4.	Negative feedback control	19
2.5.	Die swell	29
2.6.	Draw resonance	30
2.7.	Transmitted intensity vs. retardation for light passing through a polymer film between crossed polarizers	35
2.8.	Variation of stress-optical coefficient with temperature for several polymers	37
2.9.	Elastic recovery after 50% extension as a function of spinline stress	42
2.10.	Melt spinline process	44
2.11.	Heat transfer from the melt spinline	47
2.12.	Surface temperature as a function of distance from the spinneret for polyethylene fibers	49
2.13.	Crystallinity as a function of distance from the spinneret for polyethylene	51
2.14.	Unit cell of polyethylene	52
2.15.	Morphological model for melt spun linear polyethylene	54
2.16.	Mechanical properties of polyethylene as a function of crystalline orientation in the c-direction	55

FIGURE PAGE

2.17. Orientation factor as a function of spinline stress for melt spun polyethylene and polypropylene fibers 56

2.18. Tensile strength and elongation to break versus crystalline orientation in the c-direction for polypropylene 58

3.1. Birefringence measurements on polymer films using the intensity method 62

3.2. Intensity profile with uncrossed polarizers 66

3.3. Intensity profile with crossed polarizers 67

3.4. Lens system for the new sensor 69

3.5. Unidirectional translators designed for fiber positioning 70

3.6. Electronic scheme for sound wave and fiber instruments 72

3.7. Prototype diameter and birefringence detector for melt spinline 75

3.8. Melt spinline with diameter and birefringence instrumentation 76

4.1. Speaker-parabolic reflector system for perturbing the melt spinline with sound waves 85

4.2. Speaker, sensor and controller configuration 86

4.3. Response of birefringence to frequency of perturbing sound waves 94

4.4. Block diagram of closed loop fiber diameter control . . 96

4.5. Equipment for spinline diameter and birefringence control 97

4.6. Flowsheet of controlling program (integral control) 100

5.1. Spinline process with all computer interfaced instrumentation 105

FIGURE PAGE

5.2. Intensity profile with threshold 108

5.3. Steady state stability of diameter and birefringence 113

5.4. Open loop response of diameter to a step change in take-up velocity 115

5.5. Diameter as a function of motor speed for melt spinning under the research operating conditions 117

5.6. Open loop response of birefringence to a step change in take-up velocity 118

5.7. Birefringence as a function of motor speed for melt spinning under the research operating conditions 119

5.8. Response of birefringence to frequency of perturbing sound waves 121

5.9. Closed loop response of diameter with integral control and varied controller gain 125

5.10. Block diagram for proportional negative feedback control with feedforward indication of setpoint bias 127

5.11. Closed loop response of diameter with proportional control and varied controller gain 128

5.12. Closed loop response of birefringence with integral control 131

6.1. Control configuration for future work 137

CHAPTER 1

INTRODUCTION

Applied process control has developed as an important area of research during the past twenty-five years. The rapid growth is due to the increasingly complex structure of chemical processes, the high cost of materials, energy, etc. and the attractiveness of digital computers. State-of-the-art control techniques are advanced and permit control of many chemical processes. It is the knowledge gained from the successful control of classical chemical unit operations that has inspired the expansion of control techniques to include polymer processing operations.

A process of interest at this time is the polymer melt spinning operation. The melt spinning operation has been identified as the process of initial focus for several reasons:

1. There are a great number of multivariable process control opportunities on the fiber spinning process.
2. The potential for developing new technology is vast due to a previous lack of research utilizing process control on polymer processing operations.
3. The polymer processing industry is growing more aware of the advantages of applying process control on melt spinning operations (i.e., quality control, new product development, etc.).
4. Equipment and expertise for operating a research melt spinline is presently available from the Materials Science

Department, The University of Tennessee, Knoxville.

5. Materials and expertise for constructing sensors and computer interfaces to control the spinline are available from the Chemical Engineering Instrument Development Shop and Applied Control Laboratories.
6. Recent research demonstrates that the use of designed energy perturbations may change the physical properties of crystallizing polymers. Understanding of this phenomena may allow fibers with more optimal properties to be spun and provide additional process inputs to consider as manipulated variables in advanced control strategies.

Exploring process control opportunities with the melt spinline requires that a set of goals be established. The goals define the spinline control objectives and offer directives for the study. As consistent with most control studies, the ultimate goal is to achieve good control of at least some of the process output variables, in this case, spinline diameter and birefringence. Meeting the ultimate goal requires accomplishing several intermediate goals:

1. development of a novel on-line sensor for diameter and birefringence measurements to permit collection of data for these process response variables in real time;
2. establishment of a data acquisition system to store data for filtering, model development, process optimization, and study of the new energy perturbation phenomena;

3. investigation of energy perturbations designed to change the fiber morphology, evaluation of the feasibility for its use as a manipulated variable for process control, and indication of the level of effort needed in future research devoted to the Lindenmeyer hypothesis, "Designed Energy Perturbations";
4. demonstration of fiber diameter control and subsequent fiber birefringence control.

To reach the intermediate goals, a number of tasks must be performed such as enhancing a diameter measurement technique to include on-line fibers, undertaking a major development effort to prototype a sensor for on-line birefringence measurement, interfacing the peripheral equipment to an Applied Micro-technology minicomputer, and assimilating polymer processing principles so that good applied control could be accomplished. The tasks are numerous and have presented the basis for an on-going research project in spinline control. The background for understanding the diverse areas of this research is brought together in Chapter 2. Explanations of the complicated phenomena or birefringence, different process control techniques, and a variety of related theory is presented. The goals and tasks of the project are discussed in Chapters 3 and 4 while the results and directives for future work are given in Chapters 5 and 6.

CHAPTER 2

BACKGROUND

The expansion of process control techniques to include polymer processing operations requires knowledge of both process control and polymer processing technology. These fields are technically complex and until recently polymer processing has interacted to a much lesser degree with applied control theory than most other unit operations. It is desirable to comprehend central aspects of each field to better identify the possible opportunities for interactions between the two.

2.1 Process Modeling

A method of predicting and studying how a system may function is by mathematical modeling and simulation. A model can give an understanding of the system and offers insight that provides a basis to better operate or solve problems with the system. A typical model is a representation, to the best of our ability, to show the process response as a function of its inputs and the basic interactions between inputs and outputs of the process.

Process models can be classified by several characteristics, including how they are developed. Theoretical and empirical models represent two extremes in formulating a model. Theoretical models are developed from first principles (conservation of mass, energy, and momentum, and thermodynamic laws) generally under some assumptions or idealizations. These models typically require a very good

understanding of the process. Empirical models are developed by searching for any functional relationships which best fit the available data from the process. These relationships, however, are only as accurate as the data available (measurement error, etc.) and should only be expected to describe the process under processing conditions encompassed by the data. Models between these extremes, often called semi-empirical, contain aspects of both. In semi-empirical modeling, as much as is known about the process from first principles is included in the model and data are used to fill out the model, for example, to identify undetermined coefficients or used to illustrate where the model is inaccurate.

Another important classification of process models is by the type of mathematical equations used in the model, such as algebraic equations, ordinary differential equations, partial differential equations or a combination of equation types. The type of model equations also depends on whether the model is steady state or dynamic, i.e., whether the time derivatives are retained in the model. The type of equations in the model dictate the type of solution procedures needed to solve or simulate the model. For example, at the present time, the development of a model for predicting property changes of a melt spun fiber (12,19) as a function of sound wave change is one of an empirical nature. As the crystal structure of a polymer fiber varies, it is known that the fibers' properties can change greatly. However, models are not available which, if given the crystal structure, can predict the fibers' properties. The effect of sound waves (or other energy

perturbations) on crystal structure and fiber properties are even less well understood. However, an empirical model can be developed through use of sound wave data obtained from a system operating within specified operating conditions. Such a model can be used for process analysis and control design for the given operating conditions. It may also direct research into the fundamental mechanisms involved in the fiber's response to sound waves and set up directives for future sound wave experiments.

2.2 Process Optimization

Process optimization refers to driving a system to a desired, perhaps extreme, state to maximize or minimize an objective function or functions. The objective could be to maximize profit, system efficiency, or product characteristics. An optimization study generally needs to be tailored for the process under investigation. If the process is well understood, the optimization study probably starts using a mathematical model of the process coupled with a numerical search algorithm. When the process is poorly understood and an operating process is available, open loop search routines would likely be applied to the operating process. In general, both modeling and on-line testing are likely to be used simultaneously to guide each other and the total optimization study. These search routines ideally result in a multi-dimensional map that indicates the maxima and minima of the process variables (Figure 2.1).

If a mathematical model is available and used, there are several numerical schemes available for seeking an optimum, i.e.,

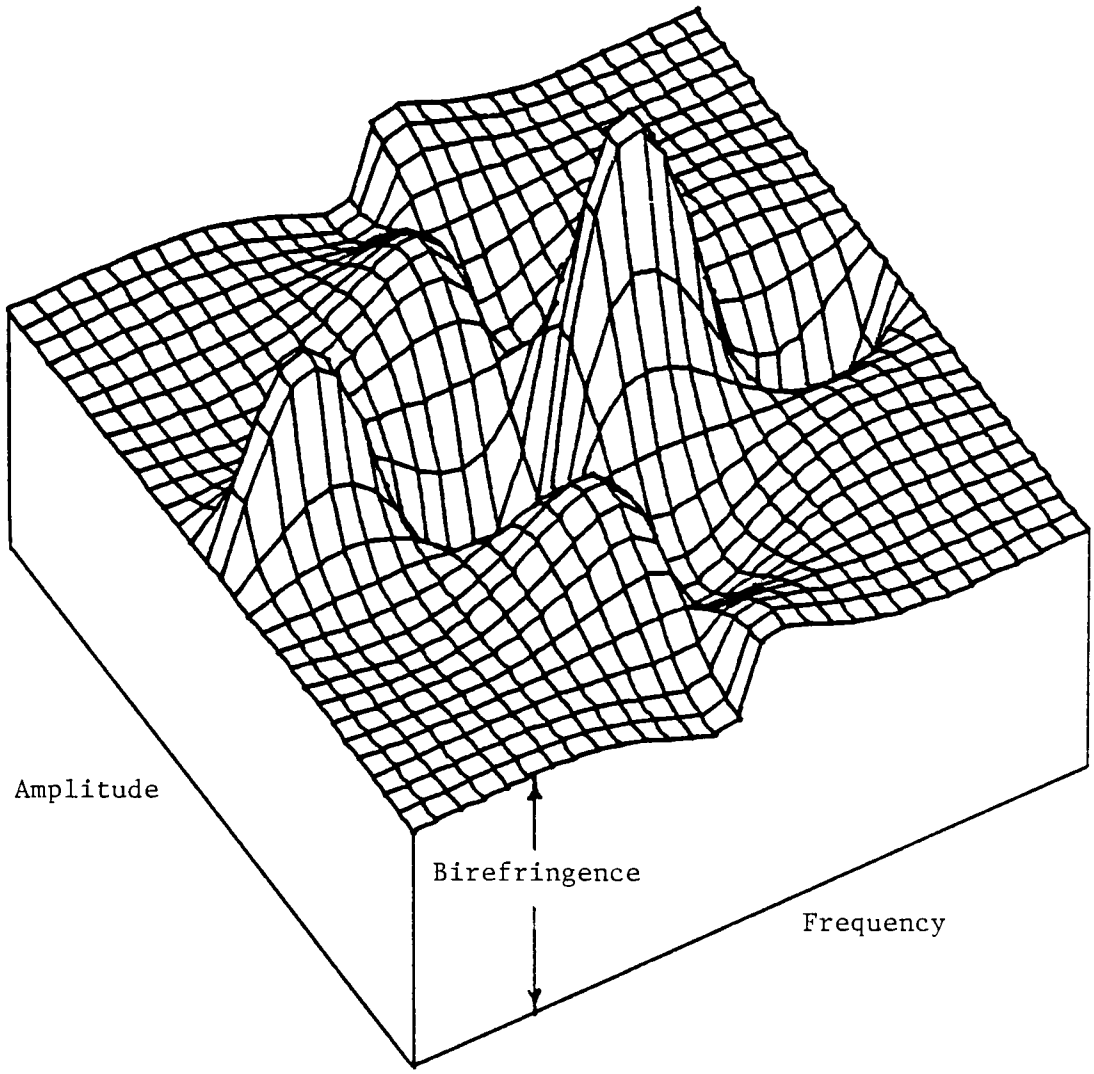


Figure 2.1. Three-dimensional map indicating possible process optimums.

an objective is defined (8,24). The numerical algorithms employed depend on the type of equations used in the model, such as linear algebraic, nonlinear algebraic, linear ordinary differential equations, etc. For optimization problems represented by a model, such as those involving nonlinearities and constraints, the computer codes PATERN and CMPLX are often used.

If an operating process is to be optimized using process data rather than mathematical modeling, there are several maximum-seeking procedures available. The object of each procedure is to achieve a maximum response by examining the effects of various factors that determine the response (8). Since a process model is not used, an estimate of the factors that combine to form an optimum is made using responses obtained experimentally. The methods used for making these estimates include factorial design, univariate procedures and methods of steepest ascent.

A common means of seeking an optimum is with evolutionary operation (EVOP) (2,10,16,21,22). EVOP provides a system for exploring the relationships between independent variables (process inputs) and dependent variables (process outputs). It consists of the systematic introduction of small changes in selected independent variables which affect a process. Generally, the best EVOP design is the multi-level factorial in which each independent variable will be held at a low and a high level and examining all possible combinations of highs and lows. Several sets of experimental runs (cycles) which include each of the designed combinations are used in determining which combination gives the desired optimum.

An optimum obtained by mathematical modeling or experimental data can be verified by operating the process under the predicted optimum conditions. An optimization study could be used on the polymer melt spinline to improve spinline quality and offer insight into a generation of experiments to improve process control.

Once an optimum is defined, a more accurate process model can be developed around the optimum operating point for use in formulating control strategies. The model needed for process control studies varies from that needed for optimization in at least two important aspects. The process control model should encompass dynamic or transient behavior as well as steady state behavior and a linear model is usually satisfactory. If the process is held near the desired operating point, the nonlinear characteristics are of less importance.

2.3 Control Theory

The control strategy for a given process is dependent upon several factors including the complexity of the system, the number of outputs to be controlled, the degree to which the controlled outputs need to be held at their setpoints, the number of inputs used as manipulated variables, whether advanced control concepts such as decoupling, feedforward, dead time compensation are to be used, etc. As the number of process outputs to be controlled gets larger, the control problem generally becomes more difficult, i.e., the control scheme may become very sensitive to interaction between the process variables. The manipulation of a single system input

may have a broad range of effects on several system outputs. The development and design of a control strategy must include these effects as well as any nonlinearities associated with the system's response to both manipulated and disturbance inputs. After the process model, control objectives, possible measurements, and available manipulated variables have been identified to a reasonable degree, the problem of defining a control configuration can be addressed.

Depending on the number of controlled outputs and manipulated inputs specified for the process, the control configuration can be classified as either single-input, single-output (SISO) or multiple-input, multiple-output (MIMO) (5,6,13). When one output is measured and only one input is manipulated, the control system is called SISO. The SISO systems are usually the simplest control structures because there is no problem with variable interactions or knowing which input controls which output, as in the case when two or more control loops are used (5). Analogously, when more than one output is measured and more than one input is manipulated, the control structure is called MIMO. MIMO systems are more sophisticated because the control loops can often interact with one another (6,13). The control action taken in one loop to compensate for an error in that loops output, also effects the outputs of the other loops. Due to this interaction, the pairing of which inputs control which outputs becomes very important. Often by correct input-output pairing the interaction can be avoided, if not, additional features such as decouplers must be added to the control scheme.

The development of most control strategies is based on a feedback control structure. The feedback structure is formed from measuring an output and comparing it to the desired value (setpoint). If an error exists, an input variable is manipulated by a controller to attempt to remove the error. The objective is to keep the controlled variables at desired levels, or setpoints (36). Examples of feedback control are shown in Figure 2.2. There are several reasons for using the feedback structure but most importantly it requires the least understanding of the process interactions, that is, a less than accurate process model is required. As the output of the operating process is monitored, the errors from the setpoint are known and can be accounted for, no matter what their origin, as long as the closed loop process remains stable.

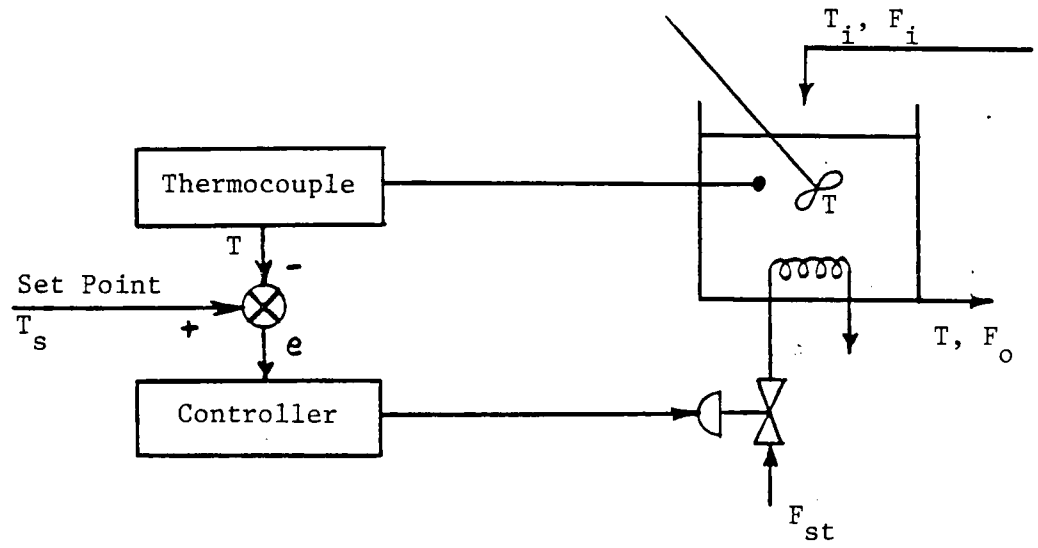
The function of a feedback controller is to receive the measured output signal and after comparing it with the setpoint, if an error exists, to produce an actuating signal that drives the output toward the setpoint. There are several feedback mechanisms for performing this function. The standard industrial feedback controller is the Proportional-Integral-Derivative (PID) controller whose control law is:

$$X(t) = X_{ref} + K_C\left(e(t) + \frac{1}{T_I}\int e(t)dt + T_D\frac{de(t)}{dt}\right) \qquad (2.1)$$

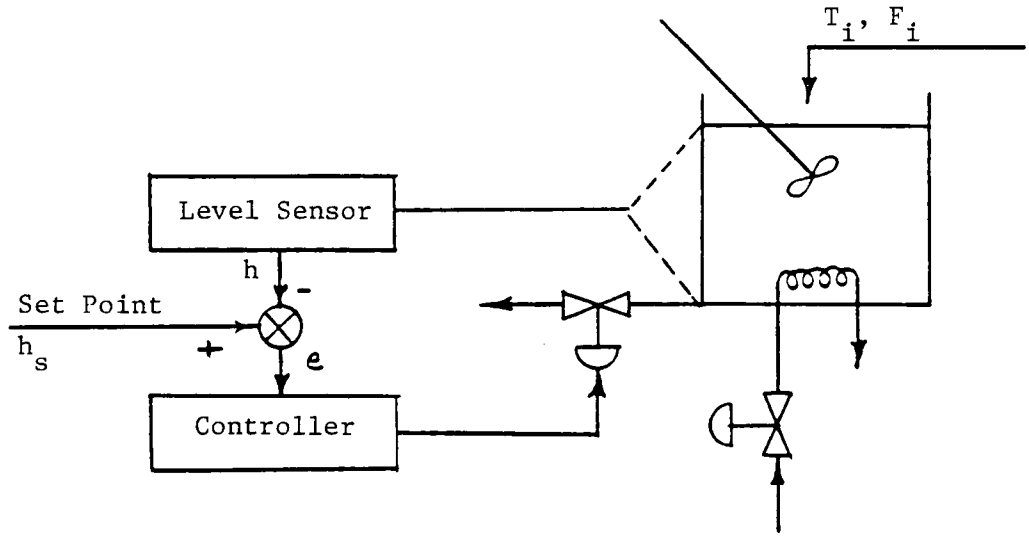
where $e(t)$ = process output setpoint - process output, the error

$X(t)$ = actuating signal

X_{ref} = reference value for actuating signal



(a)



(b)

Figure 2.2. Two examples of feedback control.
(a) Temperature control for a tank heater.
(b) Liquid level control for a tank.

K_C = controller gain or proportional constant

T_I = integral tuning constant

T_D = derivative tuning constant.

K_C, T_I, and T_D are adjustable parameters in the control law, often called tuning constants. For analysis of linear systems, transfer functions are often used. A transfer function is defined as the deviation in output (Laplace domain or s-domain) to the deviation in input (s-domain) with all initial conditions equal to zero (36). Noting that the PID control law is a linear equation, its transfer function can be obtained. Writing the equation in deviation variable form gives

$$X'(t) = K_C(e'(t) + \frac{1}{T_I}\int e'(t)dt + T_D\frac{de'(t)}{dt}) \qquad (2.2)$$

where $X'(t)$ = deviation in $X = X - X_{ref}$

$e'(t) = e(t)$ as the reference error is 0.

Taking the Laplace transform of the equation under zero initial conditions gives

$$\bar{X}'(s) = K_C(\bar{e}(s) + \frac{1}{sT_I}\bar{e}(s) + sT_D\bar{e}(s)) \qquad (2.3)$$

where $\bar{X}'(s)$ = deviation in X in the s-domain

$\bar{e}(s)$ = deviation in e in the s-domain.

Solving for the ratio of output to input in the previous equation results in the PID controller transfer function.

$$G_C(s) = \frac{\bar{X}'(s)}{\bar{e}(s)} = K_C(1 + \frac{1}{sT_I} + sT_D) = K_C(\frac{s^2T_IT_D+sT_I+1}{sT_I}) \qquad (2.4)$$

The simplest and most common implementation of a PID controller is to use only the P-mode or proportional control ($\frac{1}{T_I} = 0.0$ and $T_D = 0.0$). That is, the actuating signal is proportional to the error from the setpoint or, equations 2.1 and 2.4 reduce to

$$X(t) = X_{ref} + K_C e(t) \qquad (2.5)$$

$$G_C(s) = \frac{\bar{X}'(s)}{\bar{e}(s)} = K_C \quad . \qquad . \qquad (2.6)$$

The P-mode or proportional controller is described by either its controller gain, K_C, or its proportional band, PB.

$$P_B = \frac{100}{K_C} \qquad (2.7)$$

The proportional band is the range over which the error must change to drive the controller output over its full range. The higher the proportional band, the lower the gain and vice versa. Proportional feedback control is attributed with being very simple and usually effective, but at steady state, an error (offset) exists after a step change in setpoint or load variable.

Another type of feedback controller is one that operates in an I-mode or integral control only. That is, its output exhibits a time integral over the error rather than a proportion of its present magnitude. Most PID controllers have a switch to set it to I-mode only (P-mode switched to off). With the P-mode removed and $T_D = 0$,

equations 2.1 and 2.4 define the actuating signal as:

$$X(t) = X_{ref} + \frac{K_C}{T_I} \int e(t)dt \tag{2.8}$$

$$G_C(s) = \frac{X'(s)}{\bar{e}(s)} = \frac{K_C}{sT_I} \tag{2.9}$$

The purpose of the integral action is to drive the process back to its setpoint after it has been disturbed (25). The I-mode will take action as long as an error exists, that is, it will search for an appropriate actuating signal that will force the error to zero. This is called zero steady state error, or no offset. Its primary advantage is that it has no steady state error if the closed loop process is stable. The major disadvantage of the pure integral controller is that it often makes the process output oscillatory and even unstable (growing oscillation).

The second most common type of controller is one that uses a combination of the previous two, or a proportional-integral (PI) controller. Its actuating signal is defined as follows (equations 2.1 and 2.4 with $T_D = 0$:

$$X(t) = X_{ref} + K_C(e(t) + \frac{1}{T_I} \int e(t)dt) \tag{2.10}$$

$$G_C(s) = \frac{X'(s)}{\bar{e}(s)} = K_C(\frac{sT_I+1}{sT_I}) \tag{2.11}$$

Note that as T_I gets large, the integral action drops out. The biggest advantage of this controller is that the integral mode is active as long as there is any error, therefore, even small errors

can be eliminated. The basic control action is from the P-mode so the integral action can be kept small, avoiding oscillatory output problems. However, there is a condition called integral windup that exists when errors cannot be eliminated fast enough and the integral term grows until it saturates the actuator, manipulating the manipulated variable. If the actuator signal is allowed to grow beyond the fully opened or closed point of the actuator, the actuator can stay saturated even when the error has changed sign. This condition would continue until the integral has time to operate on the error after the sign change and bring the actuator back into its operating range. This condition is called reset windup. Most commercial industrial controllers have anti-reset windup which limits the actuator signal so that saturation of the actuator is minimal.

PID control or implementation of all modes of the controller is described by equations 2.1 and 2.4. The purpose of the derivative mode is generally one of anticipatory control. That is, it applies control proportional to the rate of change in the error or, it anticipates error. A major disadvantage to this mode is that noisy signals with little error give large derivatives resulting in large controller action, i.e., it destroys the PI control.

The attributes associated with the various modes of the PID controller given in the above summary can be misleading. These attributes are in terms of a "stereotype process," an overdamped second or higher order process with or without deadtime. The

stereotype process is what is typically encountered in chemical process control. Specifically, the attributes are essentially corrected for the first order process with dead time and second or higher order overdamped processes with or without dead time (which have few zeros in their transfer functions and no large right hand plane zeros). Figure 2.3 shows the typical behavior expected for such stereotype processes.

Examples where the attributes are not correct are pure gain processes with or without dead time, first order processes under P-mode control, second order significantly underdamped processes, sagging or wrong-way behavior processes (significant right hand plane zeros) and open-loop unstable processes. This discussion is pursued because one of the non-conforming types of transfer functions is found in the operation of the melt spinline; that of a pure gain process (even with large values of controller gain, K_C). It is expected that behavior very close to the first order without dead time, even with high controller gains, will also be encountered in future work.

Figure 2.4 shows the block diagram form of a process under negative feedback control. The diagram shows all of the transfer functions for control including only one disturbance transfer function. It should be noted that K_T is the same gain as in the transmitter transfer function allowing the operator to work in engineering units. This feature is available with most digital programmable controllers with the exception of single loop analog

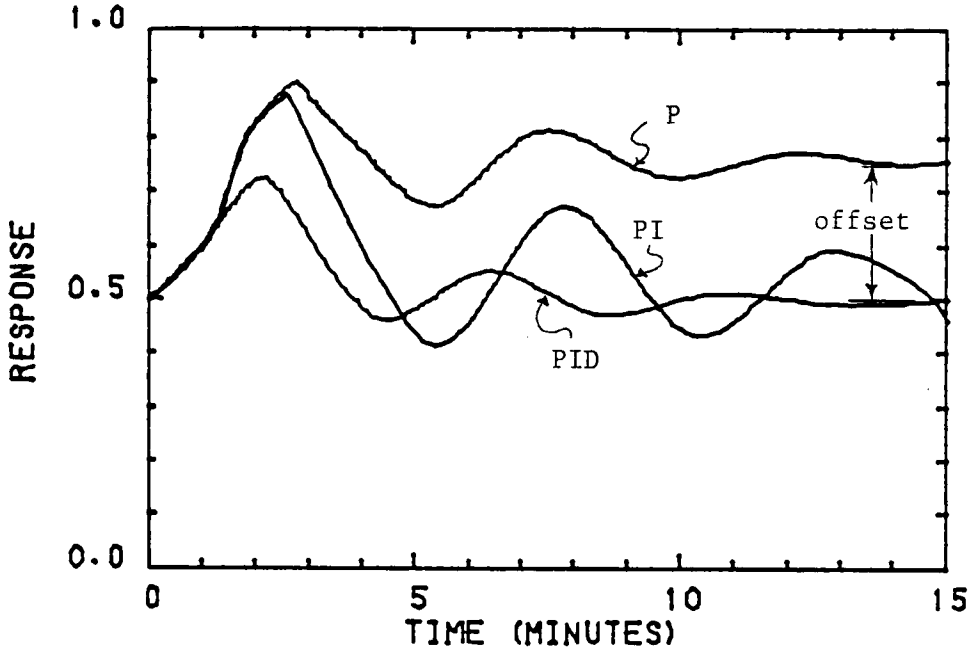


Figure 2.3. Response of a first order process with dead time or second or higher order process (with or without dead time and no significant right hand plane zeros) to a step disturbance with P, PI, and PID controllers.

Figure 2.4. Negative feedback control.
(a) Block diagram for negative feedback control.
(b) Response to a setpoint change for a pure gain process with I and PI control and a first order process with P control.

Definition of Block Diagram Variables:

$G_c(s)$ = controller transfer function

$G_v(s)$ = actuator transfer function

$G_p(s)$ = process transfer function

$G_d(s)$ = disturbance transfer function

$G_T(s)$ = transmitter transfer function

K_T = gain of transmitter transfer function

$\bar{Y}'(s)$ = process output signal

$\bar{Y}'_T(s)$ = transmitted process signal

$\bar{Y}'_{sp}(s)$ = setpoint signal

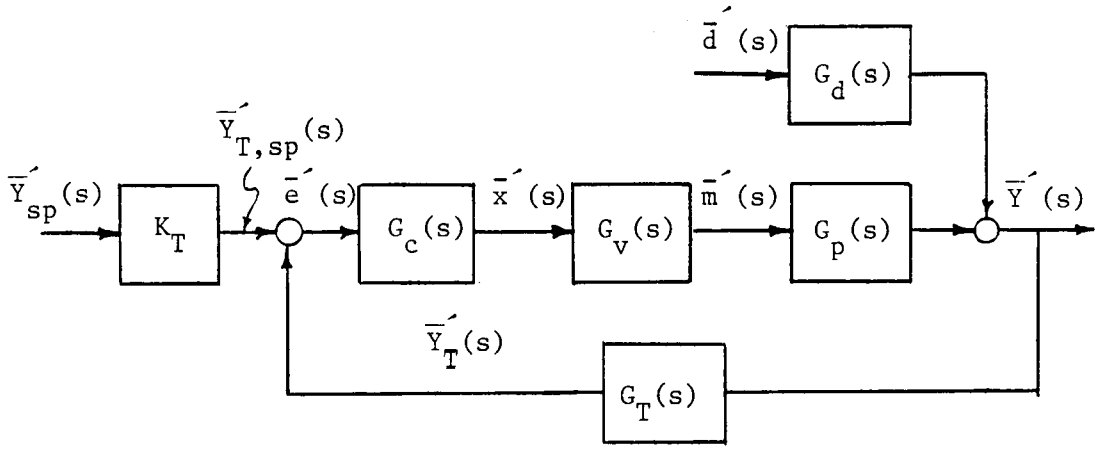
$Y'_{T,sp}(s)$ = transmitted setpoint signal

$\bar{e}'(s) = \bar{Y}'_T(s) - \bar{Y}'_{T,sp}(s)$ = error signal

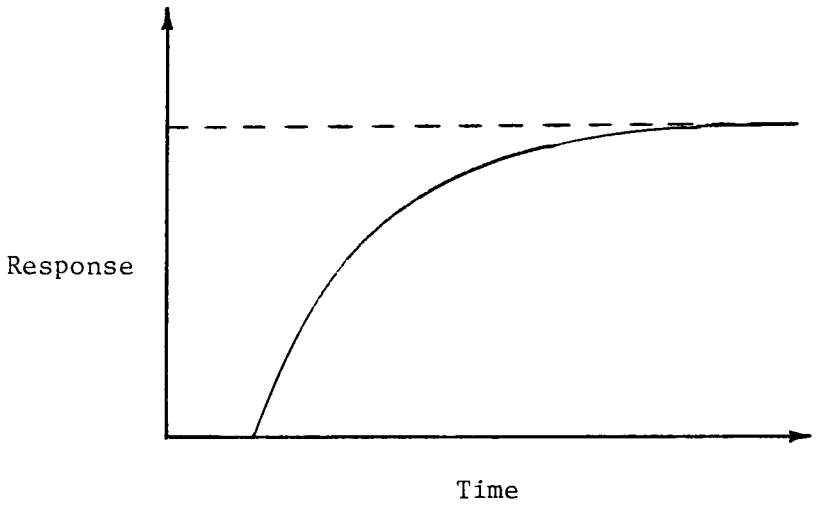
$\bar{x}'(s)$ = actuator input signal

$\bar{m}'(s)$ = process input signal

$\bar{d}'(s)$ = disturbance signal


$\bar{d}'(s)$
$G_d(s)$
$\bar{Y}'_{T,sp}(s)$
$\bar{Y}'_{sp}(s)$
K_T
$\bar{e}'(s)$
$G_c(s)$
$\bar{x}'(s)$
$G_v(s)$
$\bar{m}'(s)$
$G_p(s)$
$\bar{Y}'(s)$
$\bar{Y}'_T(s)$
$G_T(s)$

(a)


Response
Time

(b)

Figure 2.4

controller often require the operator to work in non-engineering units. The transfer functions, G_P, G_D, G_T and G_V represent linear models of various elements in the closed loop process and are usually linearized approximations of the actual models. The linearization is usually made around the design or operating point.

The closed loop process, with the feedback loop in place, behaves different than the open loop process. Recalling that the goal of applied process control is to obtain the best behavior in the closed loop mode, it becomes necessary to investigate a means of improvement. The closed loop behavior can be investigated in terms of the overall transfer function. The overall transfer function is defined as the ratio of one deviation variable input to one deviation variable output, both in the s-domain and all other input deviations at zero (with initial conditions equal to zero) (36). For the process shown in Figure 2.4, the overall transfer function for the response, $Y'(s)$, to the disturbance, $d'(s)$ is

$$\frac{\overline{Y}'(s)}{\overline{d}'(s)} = G_{d,CL}(s) = \frac{G_D}{1+G_C G_V G_P G_T} \tag{2.12}$$

where the subscript CL is used to denote the closed loop process. The overall, or closed loop, transfer function is the simultaneous solution of all equations represented by the block diagram, with $Y'sp(s) = 0$ and $d'(s) = 0$. The overall transfer function for set-point changes is

$$\frac{\bar{Y}'(s)}{\bar{Y}'_{sp}(s)} = \frac{K_T G_C G_V G_P}{1+G_C G_V G_P G_T} \tag{2.13}$$

Using the closed loop relations of equations 2.12 and 2.13, Table 2.1 has been developed. In Table 2.1, the transfer functions for G_T and G_V have been taken as constants, which is often a good approximation.

$$G_T(s) = K_T \tag{2.14}$$

$$G_V(s) = K_V \tag{2.15}$$

Also, the table is written to consider the cases where $G_p(s) = K_P$ (pure gain) and $G_P(s) = \frac{K_P}{T_p s+1}$ (first order). For a non-typical case in which I-mode control only is used, where $G_C(s) = \frac{K_C}{sT_I}$, equation 2.6 can be solved to give the following relationship for setpoint changes,

$$G_{sp,CL}(s) = \frac{K_T(\frac{K_C}{sT_I})K_V K_P}{1+\frac{K_C}{sT_I}K_V K_P K_T} = \frac{K_O}{sT_I+K_O} = \frac{1}{\frac{T_I}{K_O}s+1} \tag{2.16}$$

where $K_O = K_C K_V K_T K_P$, the open loop gain.

Analogously, the disturbance transfer function, equation 2.12, can be solved to give,

TABLE 2.1

CLOSED LOOP SETPOINT AND DISTURBANCE
TRANSFER FUNCTIONS

Controller	Transfer Function	
	Setpoint, $(G_{sp})_{CL}$	Disturbance, $(G_d)_{CL}$
	Pure Gain Process: $G_p = K_p$	
P-mode: $G_c = K_c$	$\frac{K_o}{1+K_o}$	$\frac{K_d}{1+K_o}$
I-mode: $G_c = \frac{K_c}{sT_I}$	$\frac{1}{(\frac{T_I}{K_o})s+1}$	$\frac{\frac{K_d T_I s}{K_o}}{(\frac{T_I}{K_o})s+1}$
PI-mode: $G_c = \frac{K_c(sT_I+1)}{sT_I}$	$\frac{sT_I+1}{s(\frac{T_I}{K_o}+T_I)+1}$	$\frac{\frac{K_d T_I s}{K_o}}{s(\frac{T_I}{K_o}+T_I)+1}$

TABLE 2.1 (continued)

Controller	Transfer Function: Setpoint, $(G_{sp})_{CL}$	Transfer Function: Disturbance, $(G_d)_{CL}$
	First Order Process: $G_p = \frac{K_p}{\tau_p s+1}$	
P-mode: $G_c = K_c$	$\frac{\frac{K_o}{1+K_o}}{(\frac{\tau_p}{1+K_o})s+1}$	$\frac{\frac{K_d}{1+K_o}}{(\frac{\tau_p}{1+K_o})s+1}$
I-mode: $G_c = \frac{K_c}{sT_I}$	$\frac{1}{(\frac{\tau_p T_I}{K_o})s^2+(\frac{T_I}{K_o})s+1}$	$\frac{\frac{K_d T_I s}{K_o}}{(\frac{\tau_p T_I}{K_o})s^2+(\frac{T_I}{K_o})s+1}$
PI-mode: $G_c = \frac{K_c(sT_I+1)}{sT_I}$	$\frac{T_I s+1}{(\frac{\tau_p T_I}{K_o})s^2+(\frac{T_I}{K_o}+T_I)s+1}$	$\frac{\frac{K_d T_I s}{K_o}}{(\frac{\tau_p T_I}{K_o})s^2+(\frac{T_I}{K_o}+T_I)s+1}$

$$G_{d,CL}(s) = \frac{\frac{K_d}{K_0}(sT_I)}{\frac{T_I}{K_0}s+1} = \frac{\frac{K_d T_I}{K_0}s}{\frac{T_I}{K_0}s+1} \quad . \tag{2.17}$$

The entries in Table 2.1 are derived from simple control theory, however, some of the entries are not consistent with the stereotype attributes of Figure 2.3. Namely, P-mode control on pure gain processes are still pure gain. The transfer functions for I and PI-mode for setpoint changes of pure gain processes behave as first order without dead time and never become oscillatory no matter what values are used for the tuning constants (the same applies to P-mode control of first order processes). Also, I and PI-mode control for disturbances of pure gain processes behave as first order processes without dead time only there is zero steady state gain. The example of a first order process with PI control behaves as indicated in Figure 2.3 and the closed loop process is second order.

2.4 Data Filtering for Process Control

Filters are used in process control for smoothing a noisy process signal. A smooth signal is desired so the best process control can be achieved. Noise generated by most processes can be filtered by one of several methods including moving number averages, moving weighted averages, non-linear differential equations, etc. The moving number average is the simplest filter because it requires only summing a range of most recent data and dividing by the number of data points in the range, k.

$$\text{Moving Number Average} = \frac{\sum_{i=n+1-k}^{n} y_i}{k} \tag{2.18}$$

where n = current sample number

k = number of points used in the average

y_i = process output at sample i, i = 1,2, ..., n
range of the average = n+1-k to n

the average is then used in the control strategy.

More advanced filtering uses a moving weighted average. The moving weighted average is explained by considering the summation of a number of data points, k, each multiplied by a weighting factor, f_i. The sum of the weighting factors is one. As desired, one may wish to weight more current data points heavier than previous points.

$$\text{Moving Weighted Average} = \sum_{i=n+1-k}^{k} y_i f_i \tag{2.19}$$

where f_i = weight factor for sample i, $\sum f_i = 1$.

A type of moving weighted average filter which is commonly used in process control applications where inputs and outputs are discrete-time signals is the first order discrete filter. This filter is written into the controlling software and eliminates the need for analog filters which use RC circuits to damp out high-frequency noise. The filter is described by a first-order linear difference equation (36),

$$y_n = (1-a)y_{n-1}+ax_n \tag{2.20}$$

where x_n = discrete-time input to filter with noise

y_n = discrete-time output from filter without noise

a = a constant called a filtering parameter.

For melt spinline control with the current equipment, a typical filter used in data smoothing could be encoded into the controller memory and could filter up to 50 data points if a one second sample time is used, i.e., each output to the controller would be an average of up to 50 raw data points. Analysis of the character of the spinline noise is necessary before filtering is to begin. Also, it could be that a statistical filter that discards points lying outside one or two standard deviations of the mean will be desired.

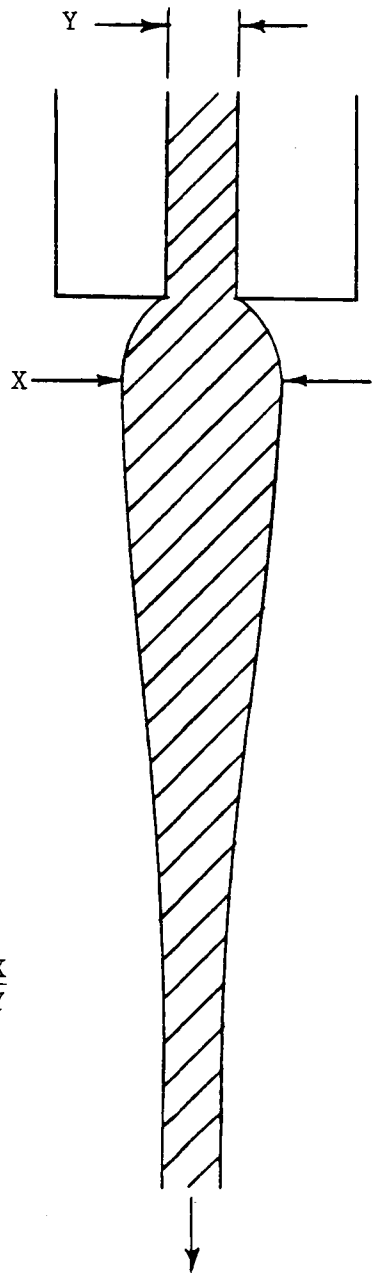
2.5 Properties of Melt Spun Fibers

Polymers have properties that differ greatly from other carbon bearing chemicals. The entanglement and cross-tying of the long carbon chains form a material that solidifies to have vast mechanical properties or can be melted to have flow (or rheological) properties. In either case, it alters the nature of light passing through it because of its inherent optical properties. The properties to be discussed are those associated with the polymer when it is melt spun. Such properties include viscoelasticity, birefringence, tensile strength and Young's modulus.

Viscoelasticity refers to the ability of a material to flow, yet, retain some of its elasticity. This property is observed in

polymer melts because of the intrinsic chain structure. As a gradual force is applied, the chains will elongate, stretch, and slip along one another allowing the melt to flow. Upon relaxation of the force, the melt will partially retract allowing the chains to settle into more stable positions. The extent of this phenomenon is dependent upon temperature and type of polymer. It is viscoelasticity that contributes to the die swell (Figure 2.5) of the melt spinning process. That is, the polymer is pushed through a small hole, orienting the chains, then into the atmosphere where the chains partially recoil into more stable positions. The die swell is closely associated to the spinline instability called draw resonance (Figure 2.6) which is a periodic swelling of the fiber.

Another important property is the double refraction of light as it passes through the fiber, or birefringence. Birefringence is a complicated phenomenon occurring in anisotropic materials. That is, because of their atomic structure, these materials have different optical properties for light traveling in different directions through the crystal (37). One light ray may strike the crystal and propagate through it as though it were an isotropic medium while another may strike at a different direction and travel through it at a different velocity. The ray that propagates through the crystal as it would in an isotropic medium, velocity constant in all directions, is called the ordinary (o) ray. The o-rays can best be visualized as a pebble dropped into a pool of water and waves leaving the point of impact with the same speed in all directions. The ray that propagates through the crystal at a speed



$$\text{Die swell} = \frac{X}{Y}$$

Figure 2.5. Die swell.

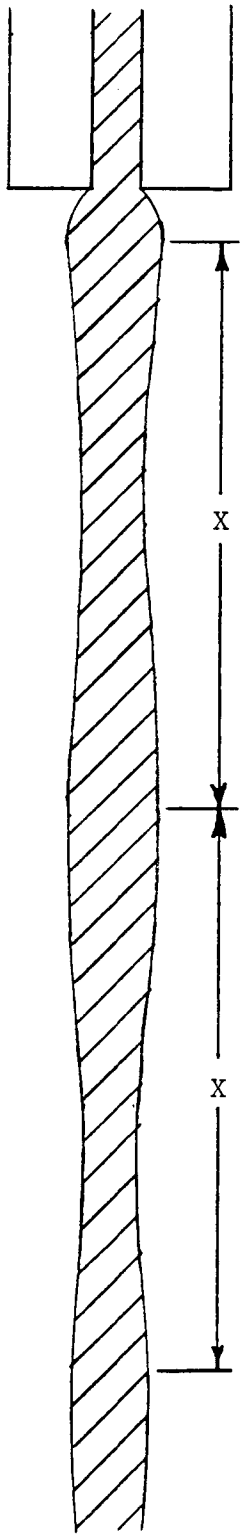
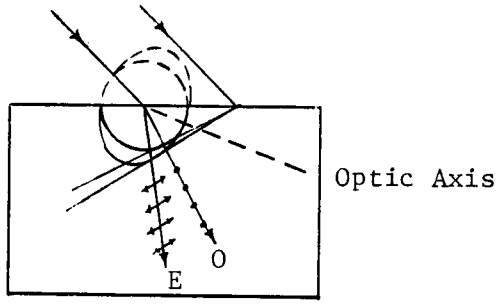


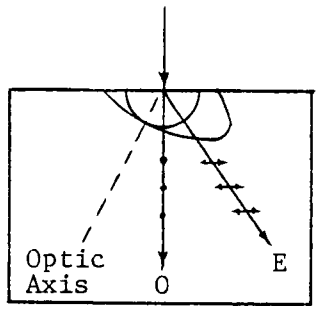
Figure 2.6. Draw resonance.

dependent upon its direction is called an extraordinary (e) ray. The waves of the e-ray are called ellipsoids of revolution and polarized mutually perpendicular to the o-rays. They can best be visualized as a pebble striking an anisotropic medium with the waves surrounding the point of impact forming ellipses and leaving at speeds dependent on the direction of travel.

The propagation of both o and e-rays can be illustrated by construction of Huygens' wavelets for the rays,



where the axis of revolution is the optic axis. The o-ray is polarized with its electric field perpendicular to the plane formed by the optic axis and the direction of propagation while the e-ray has its electric field in the plane of the optic axis and the direction of travel. The rays striking the crystal along the optic axis travel with the same speed and direction. Analogously, the rays striking perpendicular to the optic axis travel in the same direction but at the maximum difference in speeds. For the case of rays striking at an obscure angle, the e and o-rays separate, traveling in different directions and different speeds.



From this analysis, it can be said that since a birefringent material propagates light in two directions polarized perpendicular to one another which travel at different speeds that the material has two refractive indices. One refractive index is in the direction of the optic axis and is the ordinary refractive index for the material. The other is perpendicular to the optic axis and permits travel of light at a higher velocity, V_2.

$$\text{(a)} \quad n_1 = \frac{c}{V_1} \qquad \text{(b)} \quad n_2 = \frac{c}{V_2} \tag{2.21}$$

where c = speed of light in a vacuum.

In the case of a birefringent film, the optic axis is in the direction that the film was extruded (drawn). Striking the film with polarized light in a direction perpendicular to the plane of the film will cause the light to separate into o and e-rays, polarized perpendicular to one another, traveling the same direction but at different speeds depending on the magnitude of birefringence. Upon exiting the film the rays are out of phase by an amount depending on the thickness of the film and the difference in the refractive indices in the two directions. The light rays recombine to form light that is polarized at a different angle than it entered,

i.e., a resultant wave has been formed. This is to say that the film has imposed a rotation of the plane of polarization. This phenomenon is called the retardation of the light and it can be measured by three different methods.

The first is to observe the birefringent crystal under a microscope between crossed polarizers. The sample rotates the light so that an amount of light may pass through the second polarizer, depending on the magnitude of birefringence. A compensator containing a birefringent crystal plate is placed near the sample and rotated to compensate for the retardation imposed by the sample. Rotation of the plate is proper when there is no light transmitted through the second polarizer and a reading is taken from the scale attached to the birefringent plate. Appropriate calculations are then performed to obtain the retardation (according to compensator specifications). The birefringence, Δn, is obtained by dividing the retardation, Γ, by the sample thickness, x. This method is used for fibers as well as films.

$$\Delta n = \frac{\Gamma}{x} \tag{2.22}$$

The second method for obtaining the retardation is by striking the birefringent sample with polarized, monochromatic light of known intensity, I_o. This method has been developed and employed on polymer film extrusion processes. The light is rotated by the sample and allowed to strike a polarizer that is rotated perpendicular to the original plane of polarization. The amount of light

transmitted by the second polarizer, I, is then recorded by a radiometer head and used in the expression for retardation (26):

$$I = I_o \sin^2\left(\frac{\pi \Gamma}{\lambda}\right) \tag{2.23}$$

where λ = wavelength of the light

x = sample thickness

Γ = retardation.

This expression follows from the analysis because the intensity will vary from bright to dark (periodic) as retardation increases through 360 degree orders. Intuitively, it is known that as the retardation increases from 0 to 360 degrees, 360 to 720 degrees, etc., it rotates the plane of polarized light by that same amount. Therefore, the transmitted intensity goes through two periods of maximum light and two periods of darkness with each rotation through 360 degrees of retardation, i.e., I = maximum at 90 and 270 degrees (Figure 2.7).

A final method of determining the orientation of a melt spinline is through the use of rheo-optical laws relating the stress to the molecular orientation (or birefringence) of the carbon chains. For years it has been known that deforming a polymer creates changes in the birefringence. The subject of rheo-optics makes quantitative use of this fact to give insight into the stress fields developed within the polymer when it is deformed. Rheo-optics, in short, is the association of the principle axes of the stress tensor with the ellipsoidal wave normals that describe the refractive indices in

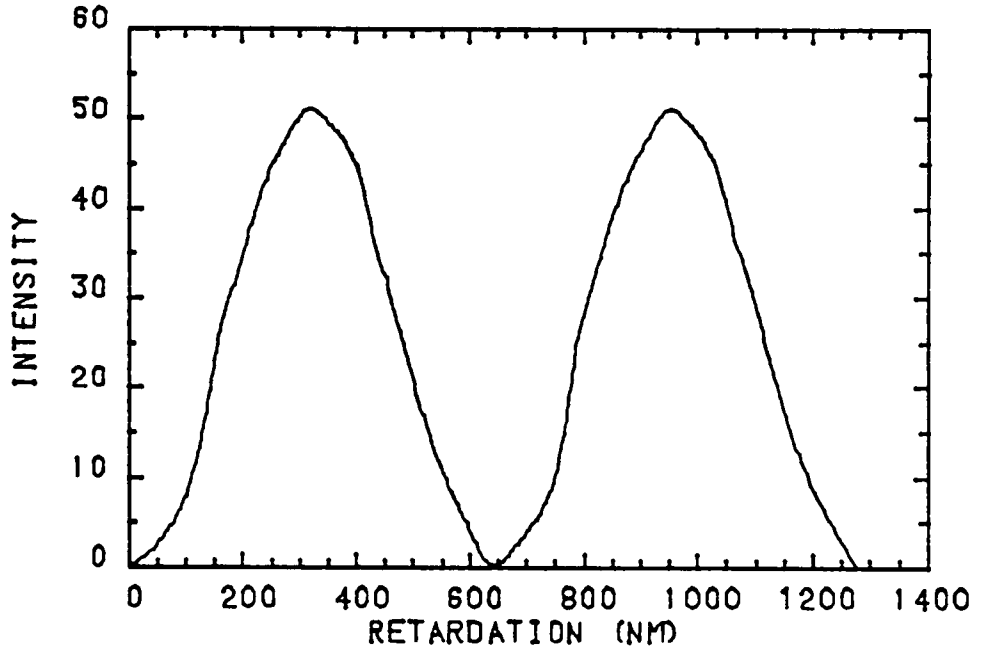


Figure 2.7. Transmitted intensity vs. retardation for light passing through a polymer film between crossed polarizers.

the direction of the principle axes. This relationship has been dealt with theoretically, as well as, empirically and it has been shown that the principle birefringences are proportional to the differences in principle stresses, i.e.,

$$n_i - n_j = C(\sigma_i - \sigma_j) \tag{2.24}$$

where C = stress-optical coefficient

n = refractive index

σ = stress

where C is called the stress-optical coefficient. The association of this law with a melt spinline is best described by considering a spinline of radius, r, under tension, T. Substitution into the previous equations yields the following:

$$\Delta n = C\left(\frac{T}{\pi r^2}\right) \quad . \tag{2.25}$$

The stress-optical coefficient, C, is a function of both polymer type and temperature. Studies have given C as a function of temperature for several polymers (Figure 2.8).

An important consideration when studying the nature of birefringence, retardation, or wave propagation is the effect of electromagnetic waves on a melt spun fiber. Analysis of the propagation of electromagnetic waves through an anisotropic medium such as a synthetic fiber begins with an understanding of the propagation through an isotropic medium. Isotropic materials, meaning the speed of

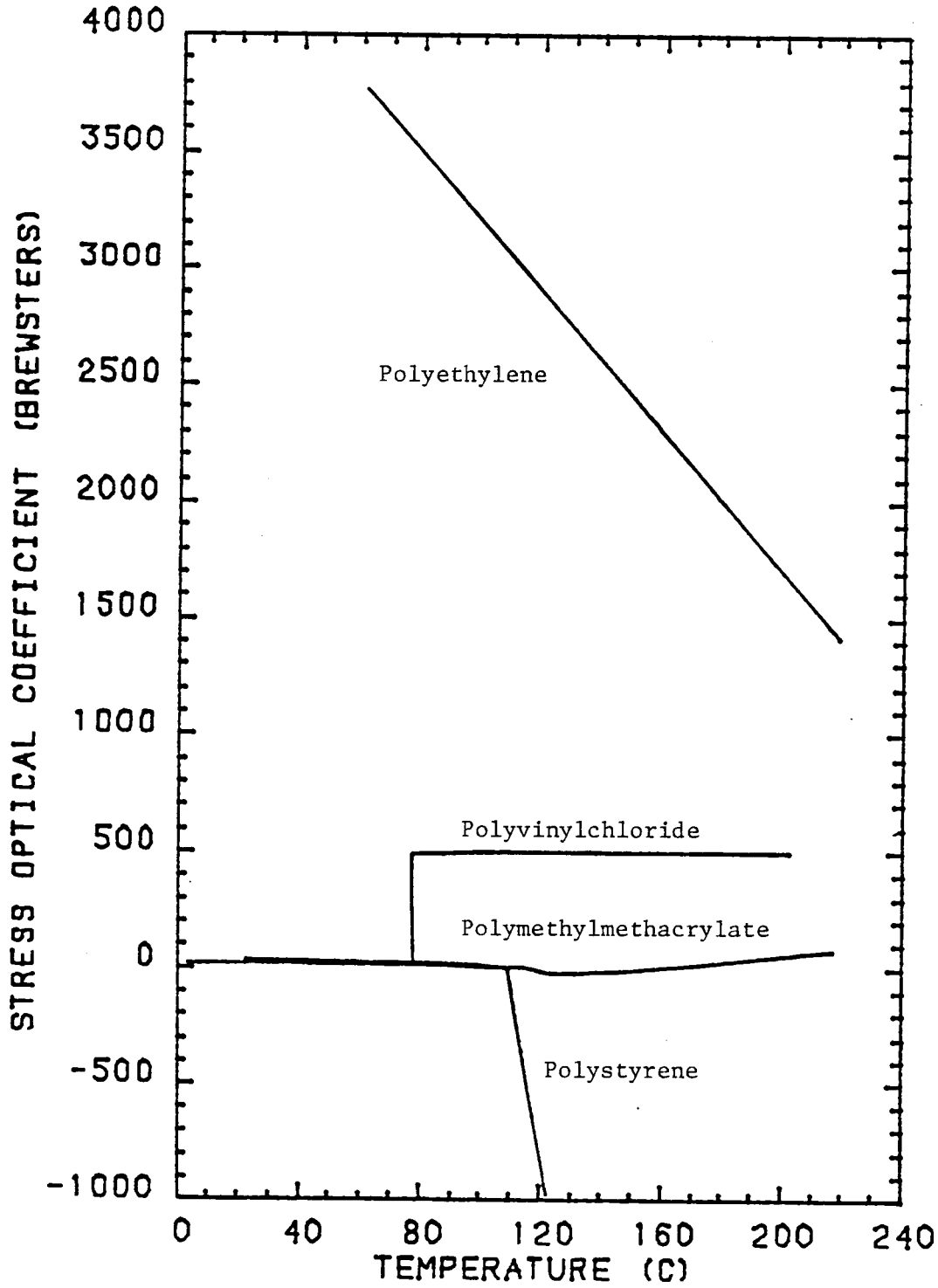


Figure 2.8. Variation of stress-optical coefficient with temperature for several polymers.

waves in all directions is the same, under the influence of electromagnetic radiation show a behavior that is described using Maxwell's differential equations (37,42).

$$\oint E \cdot \hat{n} dA = \frac{1}{\varepsilon_o} Q \tag{2.26}$$

$$\oint B \cdot \hat{n} dA = 0 \tag{2.27}$$

where E = electric field vector

B = magnetic field vector.

These equations relate the electric and magnetic field vectors to their sources which are electric charges, currents, and changing fields. In principle, all problems in electricity and magnetism can be solved from Maxwell's equations. As these equations are solved, it can be shown that the electric and magnetic fields are mutually perpendicular to one another and perpendicular to the direction of propagation. The velocity, V, of the waves in the direction of propagation is given by:

$$\frac{dE}{dt} = V = \frac{1}{\mu\varepsilon} \tag{2.28}$$

where μ = magnetic permeability

ε = dielectric constant.

Supposing two waves, out of phase, traveling through the medium with the same velocity were resolved into principle directions, say two and three, the propagation of each wave would be given by:

$$E = E_2(x_1-vt+\delta_2)\varepsilon_2 + E_3(x_1-vt+\delta_3)\varepsilon_3 \tag{2.29}$$

where E = electromagnetic flux.

The left term on the right hand side of the equation is the magnitude in the second principle direction and the right is the magnitude in the third. This breakdown of Maxwell's equations is simple because the velocities and dielectric constants are the same in all directions.

The analysis for electromagnetic radiation through an anisotropic medium is not as simple. The primary reason for this is the dielectric constant takes the form of a second order tensor (42). The mathematics are similar to the isotropic and the second order tensor is simplified by considering only one direction.

A primary result of the analysis is Fresnel's equation of wave normals.

$$\sum^{j} \frac{s_j}{V^2 - \frac{1}{\varepsilon_j \mu}} = 0 \tag{2.30}$$

where s = cross product of the electric and magnetic fields.

Note that since this is a quadratic expression, there are two velocities which satisfy the equation. Namely,

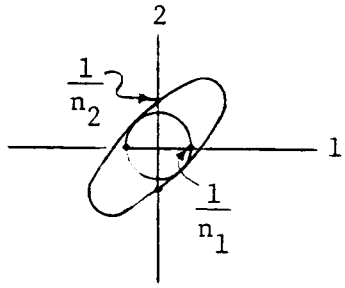
$$\text{(a)}\quad V_1 = \frac{1}{\mu\varepsilon_2} \qquad \text{(b)}\quad V_2 = \frac{1}{\mu\varepsilon_3} \tag{2.31}$$

$$(a)\quad n_1 = \frac{C}{V_1} \qquad (b)\quad n_2 = \frac{C}{V_2} \tag{2.32}$$

where n = refractive index

C = velocity of light in a vacuum.

A graphical representation of the two-dimensional electromagnetic propagation defines the refractive indices and shows Fresnel's ellipsoid.



The result of the analysis is that birefringence, Δn, has been defined for electromagnetic radiation through an anisotropic material. On a final note, the birefringence is observed using any frequency of the electromagnetic spectrum including x-rays, long radio waves and high frequency sound waves.

The mechanical properties of a melt spun fiber include tensile strength, elongation to break, Young's modulus, and elastic recovery. Each of these properties offer insight into the degree of orientation of the fiber. Analogously, each property has a direct dependence on the spinning conditions such as tension, die size, drawdown, etc. As the fiber is drawn, the carbon chains become oriented, occupying less space and reducing the cross-sectional area. The result is a higher tensile strength and a higher Young's modulus

(stress/strain). Some of the previous work with polyethylene and polypropylene is presented in the following section. The elastic recovery (plastic deformation/sum of elastic and plastic deformation) for polyethylene is presented (Figure 2.9) and it is noted that it increases with spinline stress.

2.6 Melt Spinning

This work focuses on the application of process control techniques to the polymer melt spinning operation. In the polymer industry, there are several methods for processing polymers to produce different products, from ram injection to blow molding. One of the most important of these is the production of synthetic fibers by melt spinning. This process is a fundamental one for the textile industry.

The polymer melt spinning process originated in 1932 and has grown to be a commercial means of producing clothing, carpets, cigarette filters, etc. The primary materials used in producing these fibers are polyethylene, polypropylene, polyethylene terephthalate (PET) and various polyamides. The one most commonly used for experimental purposes is polyethylene because other polymers have too low a viscosity to subject them to varying experimental techniques. Also, the stretched polyethylene filaments have a molecularly entangled structure that recoils when the load is removed, indicating there is a high elastic recovery which is ideal for melt spinning.

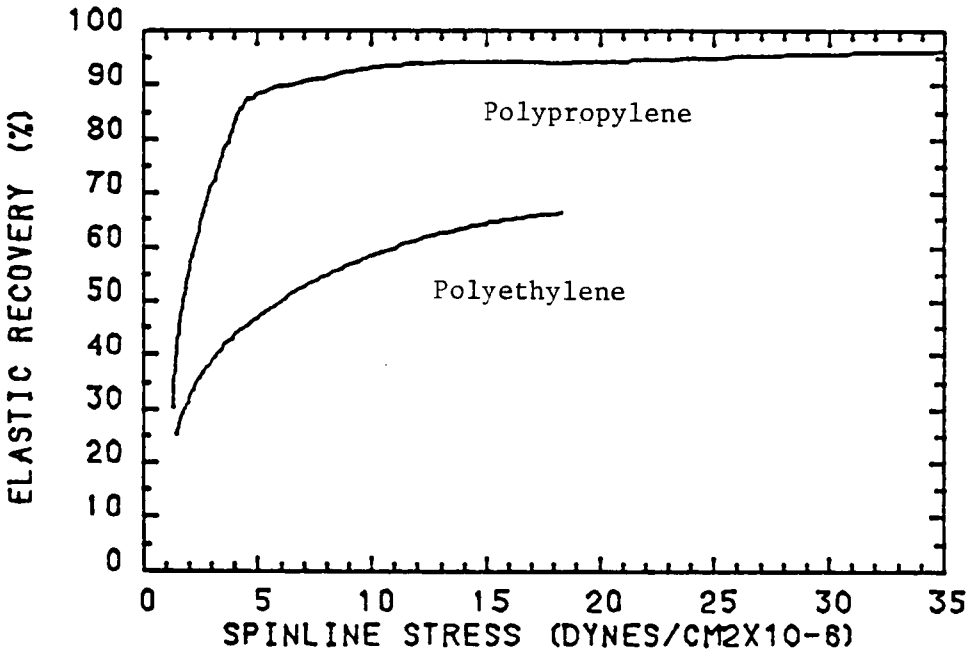


Figure 2.9. Elastic recovery after 50% extension as a function of spinline stress.

A typical process of spinning synthetic fibers begins with the introduction of pelletized polymer into the feed hopper (Figure 2.10). The hopper feeds the polymer into the screw chamber where it is heated and slowly churned toward the end of the extruder. At the end, the molten polymer enters the metering pump. This pump sets the mass flow rate and pushes the polymer through a die (spinneret) to form a fiber. At this point, the carbon chains of the polymer become slightly oriented, compressed, and released to the atmosphere (creating a die swell) where it travels to the take-up winder, being cooled by convection along the way. The point where the molten polymer becomes opaque is sometimes called the frost point. The take-up winder often exerts a force on the spinline which can alter the morphology as it develops during the process and produces draw-down of the fiber. These changes are usually accompanied by significant mechanical property changes. It should be mentioned that increased crystallization (cooling) rates also produce changes in the morphology of the spinline.

There have been studies that offer insight into the behavior of the melt spinline with constant and transient system parameters. These include heat transfer (43), structure development (1,15,23, 28,32,33,43,44), light transmission (20,26,35) and stress (18,26, 39,40,41). Each of these deal, in part, with the scope of this work.

Heat is transferred from the spinline to the atmosphere by convection. Thus, movement of the spinline results in a temperature

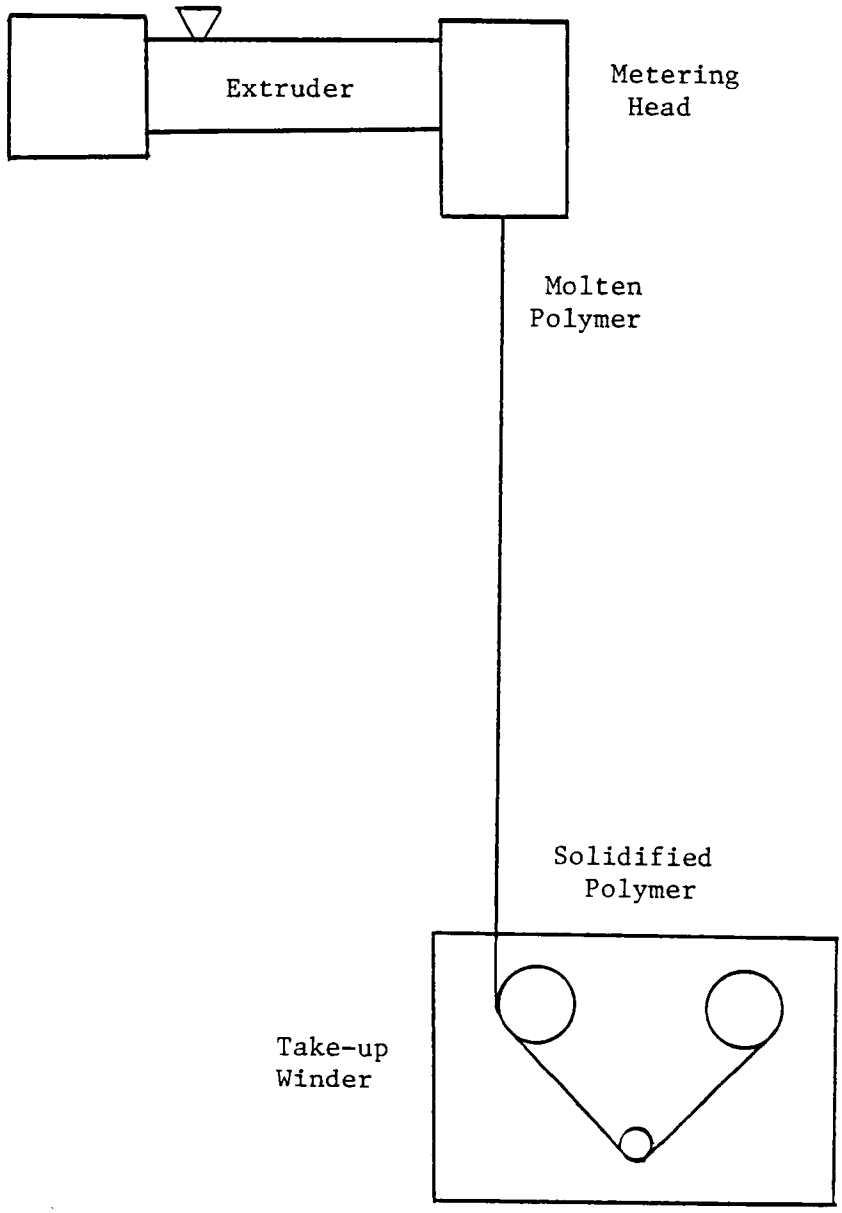


Figure 2.10. Melt spinline process.

gradient, both axially and radially, as it cools en route to the take-up winder. As the gradient is increased or decreased, the orientation of the carbon chains at any point increases or decreases. This results in a frost point that moves with the temperature gradient. By the same analogy, the cooling takes place radially, from the outside toward the center of the fiber, creating a radial distribution of birefringence values. The result is an axial and radial spinline birefringence.

In this work, it is important to know the temperature along the spinline because one of the three methods for measuring the spinline birefringence requires determination of the polymers stress-optical coefficient. This coefficient is temperature dependent and must be determined at the point where the stress is being measured. The stress-optical coefficient, when multiplied by the spinline stress, gives birefringence.

The simplest means of considering the heat transfer from a moving spinline is to assume a constant temperature across the fiber cross section. Therefore, the analysis becomes one-dimensional (43). The energy balance can be written as follows:

$$\rho Qc \frac{dT}{dx} = -C[h(T-T_{surr}) + \varepsilon k(T^4-T^4_{surr})] \qquad (2.33)$$

where T = temperature of spinline at x

T_{surr} = temperature of surroundings

h = heat transfer coefficient

c = heat capacity

C = circumference of spinline at x

ε = emissivity

k = Stefan-Boltzmann constant

This analysis follows the laws of energy conservation and permits calculation of the temperature at any point, x, along the spinline (Figure 2.11), however, it does not consider the enthalpy of crystallization.

For this work, it is important for the spinning research and hardware to permit a change of polymer type. Making a change of polymer type will change the thermal capacity of the spinline and result in a change of the temperature gradient. The change in gradient is defined by the above equation by changing the values for emissivity, heat capacity, and heat transfer coefficient to those representing the new polymer. Most of these values can be found in polymer texts and reference books. However, it is necessary to calculate the heat transfer coefficient because it varies with different spinline operating conditions, i.e., spinneret size and velocity. Experimental studies (43) of heat transport from moving filaments to ambient air have given an acceptable expression for the heat transfer coefficient.

$$\frac{hd}{k_{air}} = 0.42\left(\frac{d\bar{V}\rho_{air}}{\eta_{air}}\right)^{1/3} \qquad (2.34)$$

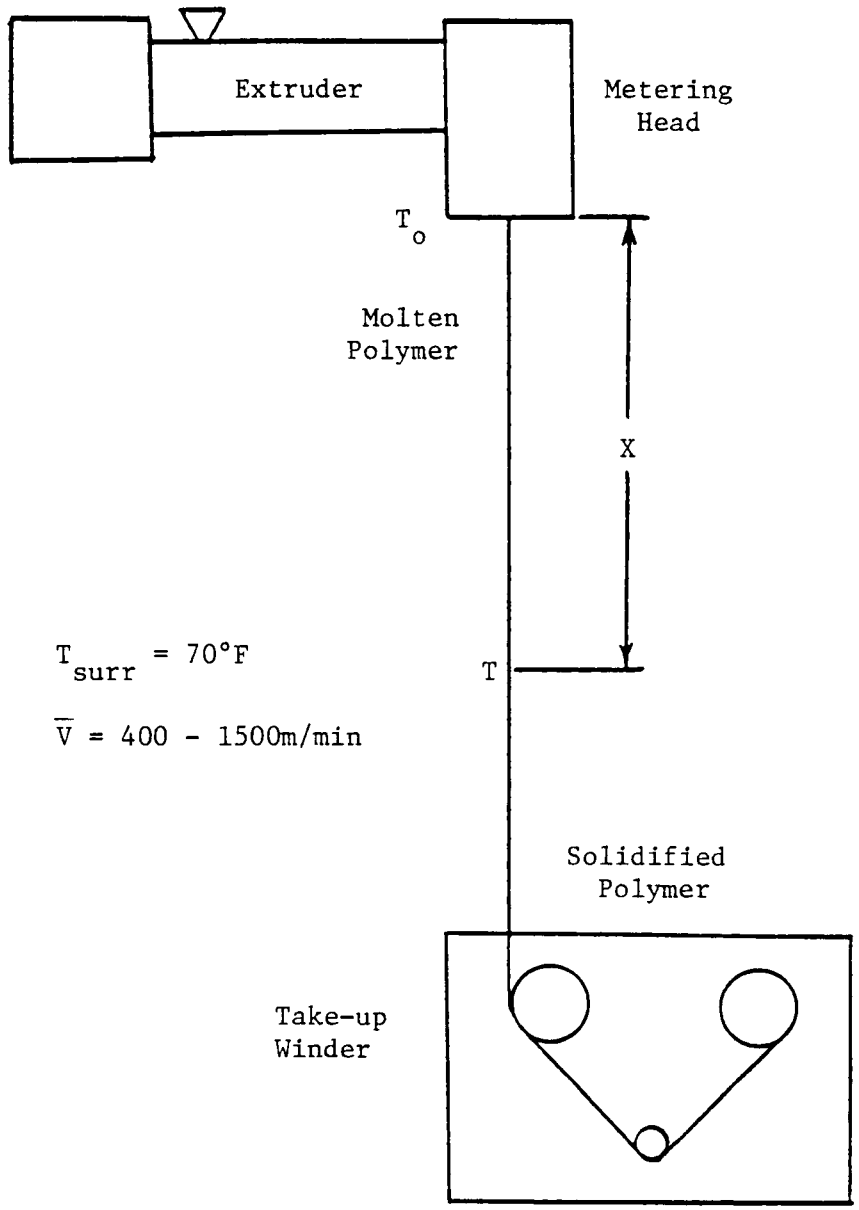


Figure 2.11. Heat transfer from the melt spinline.

where k = thermal conductivity of air

η = viscosity of air

ρ = density of air

h = heat transfer coefficient

d = diameter of spinline.

With all polymers, the fiber surface temperature decreases as a function of distance from the spinneret as shown in Figure 2.12. The fiber cools rapidly from the spinneret to the frost piont, where crystallization begins. At the frost point, the enthalpy of crystallization is liberated causing a temperature plateau, or temperature increase. After approximately 60 percent of the crystallization takes place, the fiber continues to cool, only more slowly, as it approaches ambient temperature (9).

The structure developed in melt spinning defines the relationship between the spinning conditions and the structure and properties of the spun fiber (32). The fiber of interest, polyethylene, has long been known to crystallize rapidly from the melt and is a good polymer for studying structure development.

As polyethylene is spun, the melt is pumped through a spinneret to regulate the size of the fiber. This process begins with randomly coiled carbon chains that become slightly oriented when pressed through a small diameter opening. The melt is drawn down at an extremely high rate causing more orientation of the chains. This orientation then becomes a function of take-up velocity (or drawdown). Crystallization begins above the frost point where

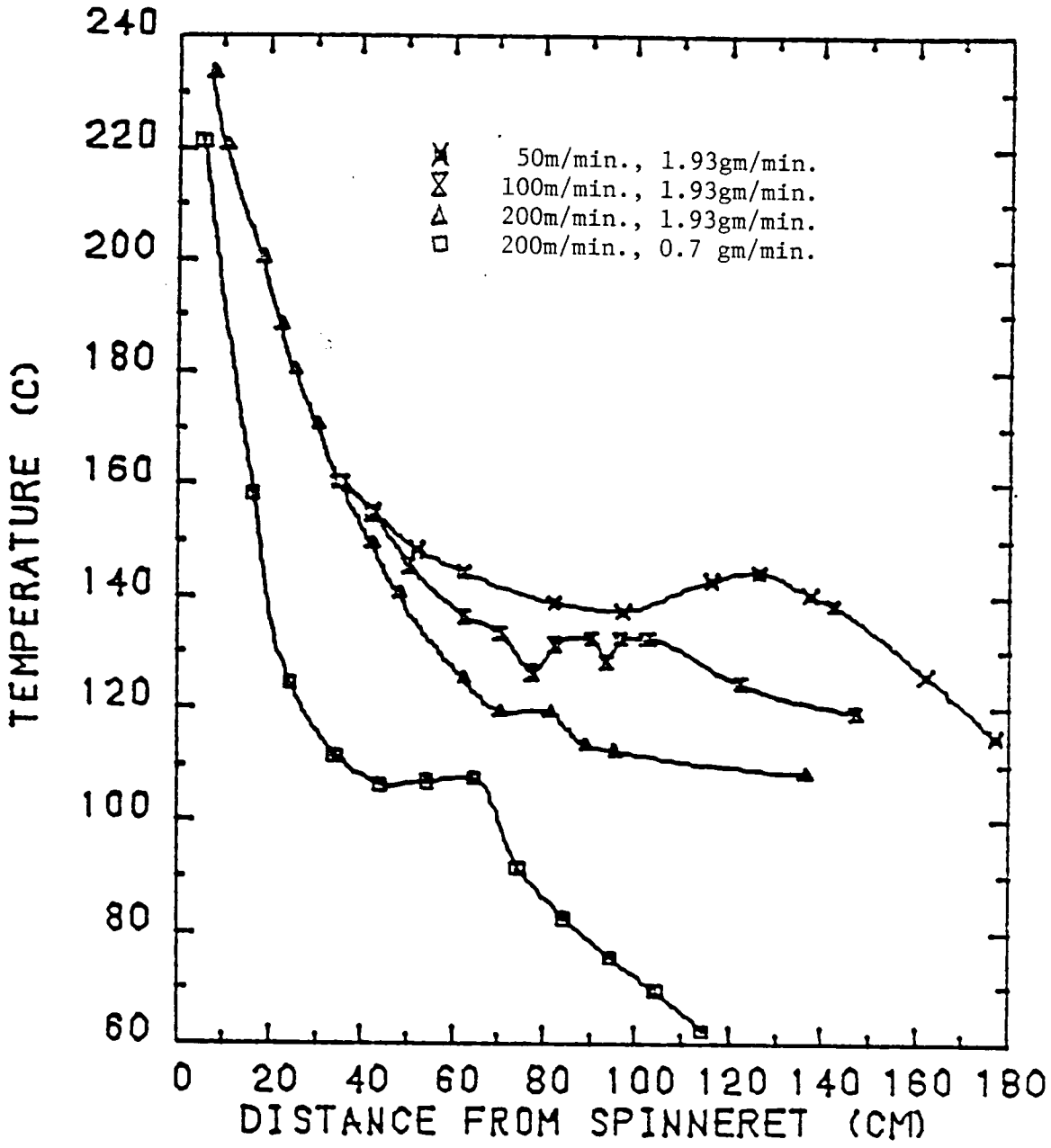


Figure 2.12. Surface temperature as a function of distance from the spinneret for polyethylene fibers.

nucleation sites are numerous and continues as the filament moves to the take-up winder. Almost 60 percent of the final crystallinity is developed, however, before the fiber begins to cool from the temperature at the frost point. In the general case, the polymer starts crystallizing further down the spinline, and progresses to an ultimate crystallinity, as the take-up velocity increases. The effect of increasing the take-up velocity at a constant mass flow rate is an increase in both stress and cooling rate which leads to an increase in crystallization rate (Figure 2.13). The effect of increasing the mass flow rate at constant take-up rate is an increase in cross-sectional area and a slight change in tension with a net decrease in stress. Also, the cooling and crystallization rates will decrease.

A more detailed look at the spinline orientation, requires orientation factors to be considered. The unit cell of polyethylene has three principle directions (a, b, and c) mutually perpendicular to one another (Figure 2.14). In each direction, there is an orientation factor (f_a, f_b, and f_c) that corresponds to the change in orientation as it is stretched (or drawn). The orientation factor, f, is represented as follows:

$$f = \frac{\overline{\alpha_{\parallel} - \alpha_{\perp}}}{\alpha_1 - \alpha_2} \qquad (2.35)$$

where α = polarizability along the principle axes of the unit cell.

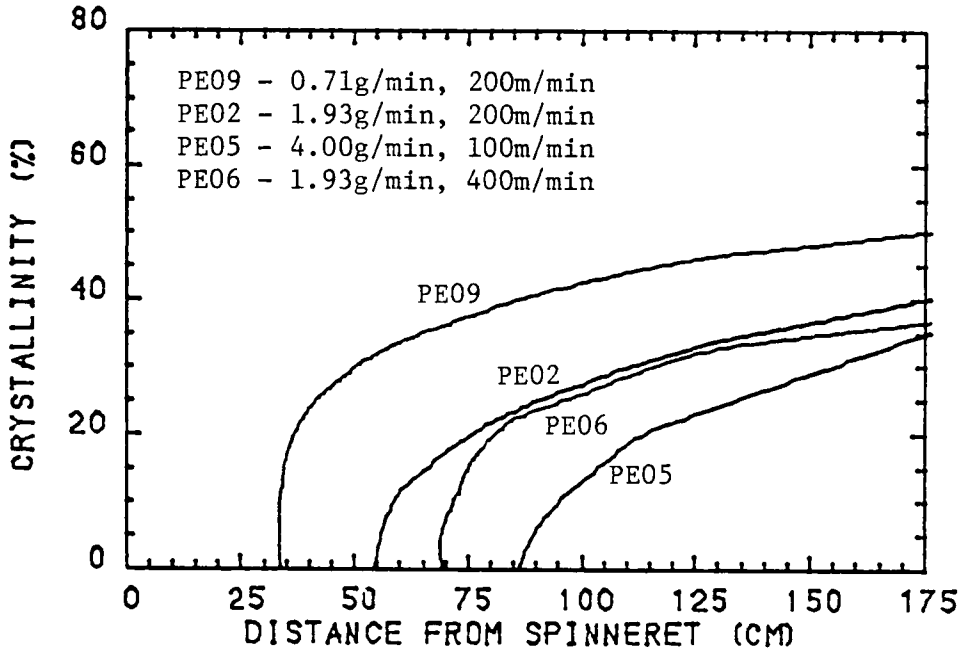


Figure 2.13. Crystallinity as a function of distance from the spinneret for polyethylene.

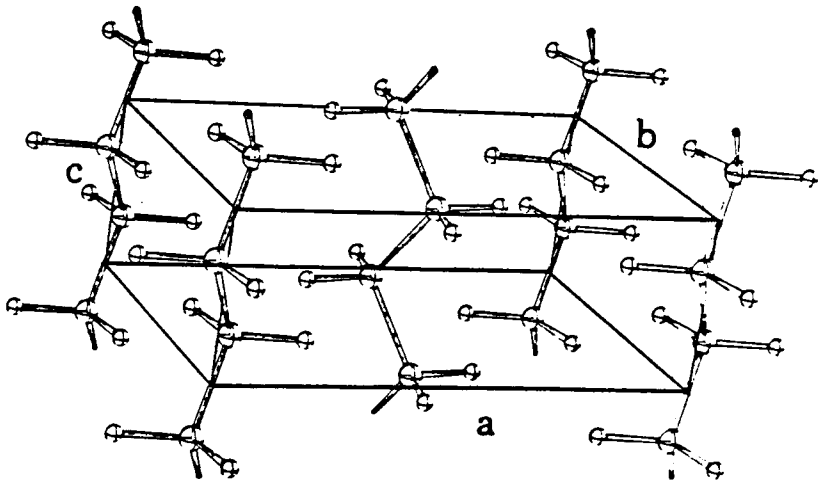


Figure 2.14. Unit cell of polyethylene. Principle directions are indicated by a, b, and c.

Due to continuity, the sum of the factors must equal zero. A negative f indicates a decrease in spacing (or increase in orientation) while a positive f indicates an increase. At a sufficiently low take-up rate, the f-values are zero because there is no preferred orientation. As the take-up rate increases, f becomes negative: $f_b = -0.45$, $f_a = f_c = 0.22$. Ultimately, at the highest drawdown, the orientation is best along the fiber axis where $f_c = 0.65$, $f_b = -0.45$, $f_a = -0.20$.

Using a scanning electron microscope, it has been possible to examine the morphology of polyethylene. The microscope studies have shown a surface lamellar texture perpendicular to the fiber axis. As take-up velocity increases, the surface becomes finer and more uniform. A morphological model can be seen in Figure 2.15 (32).

Studies on polyethylene have also shown significant changes in the mechanical properties of the fiber with orientation. Uniaxial stretching of the fibers treated under different spinning conditions has indicated that tensile strength, elongation to break, and Young's modulus change with variations in orientation along the c-axis, or drawdown. As the orientation along the fiber axis increases, the modulus and tensile strength change as indicated in Figure 2.16 (32). These changes in mechanical properties correlate well with spinline stress (Figure 2.17) (29). Therefore, on-line tension monitoring is an important variable for process control.

Several researchers (4,11,32) have performed tests identical to those in this discussion on polymers such as polypropylene,

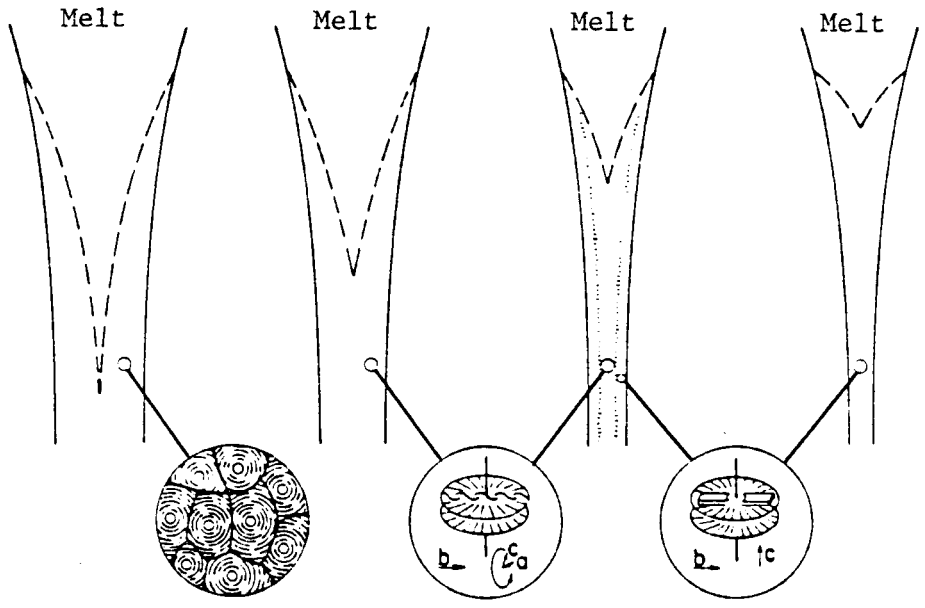


Figure 2.15. Morphological model for melt spun linear polyethylene.

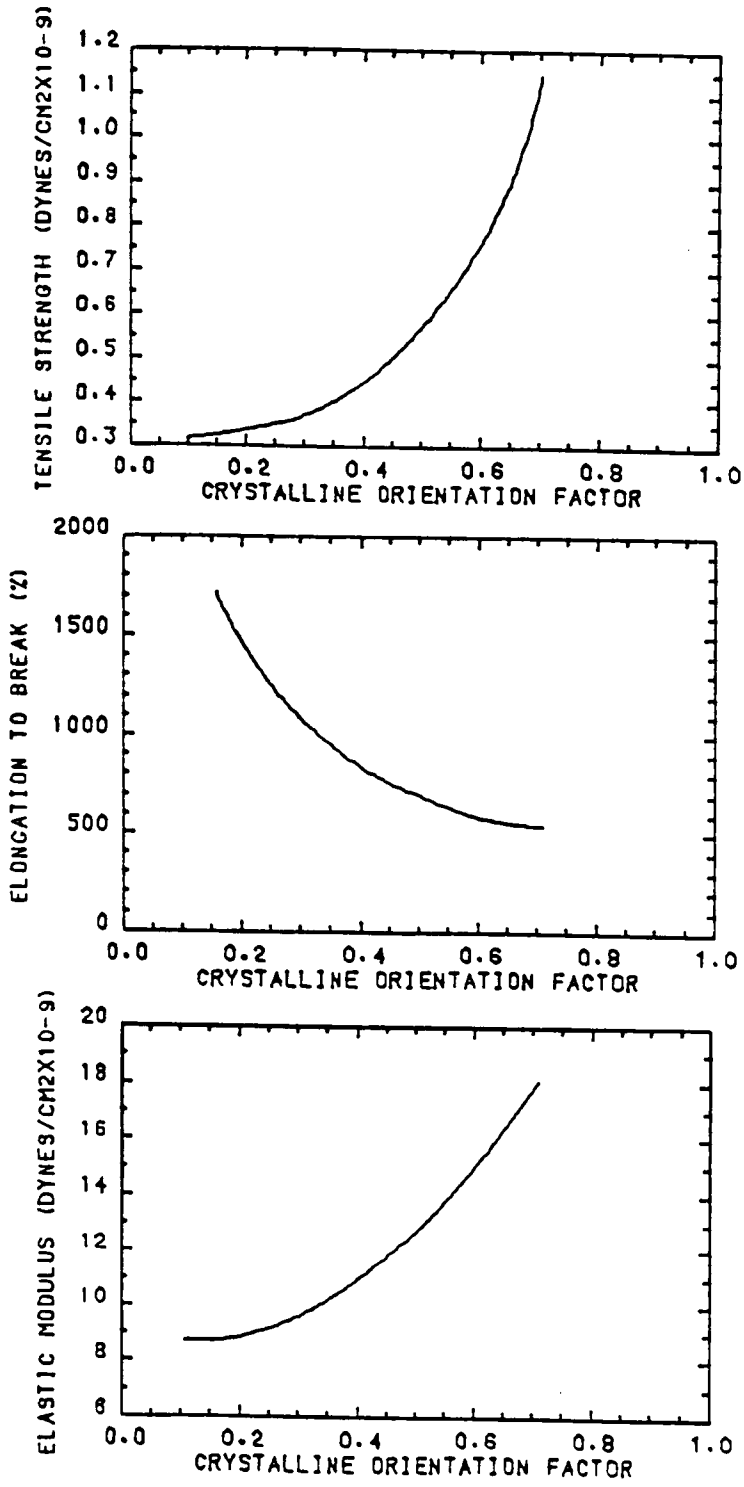


Figure 2.16. Mechanical properties of polyethylene as a function of crystalline orientation in the c-direction.

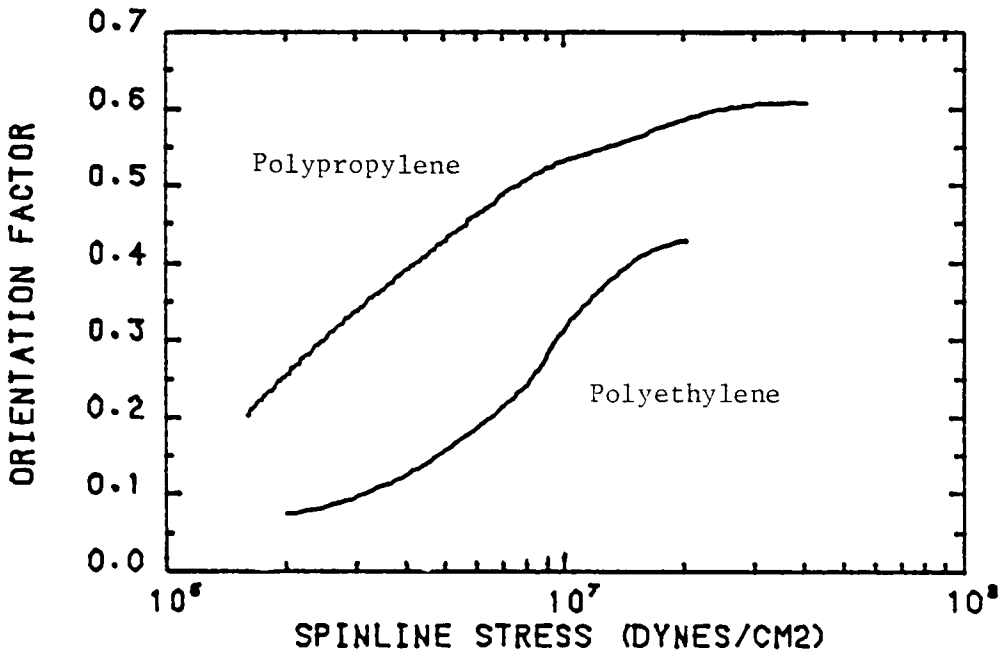


Figure 2.17. Orientation factor as a function of spinline stress for melt spun polyethylene and polypropylene fibers.

Nylon 6, PET, and polyoxymethylene. The test results, although not identical for obvious reasons, follow the same trends as the polyethylene samples (example, Figure 2.18) (33). Therefore, in this work it is reasonable to assume that designed equipment for on-line measurement of physical properties can accommodate with slight modifications, a change in polymer type.

As polymers are melt spun under transient spinline conditions, significant changes are noted in spinline tension (38). For instance, an increase in melt temperature gives a lower viscosity melt which elongates easier and reduces the tension. Also, an increase in mass flow rate under constant take-up velocity decreases tension as predicted by continuity.

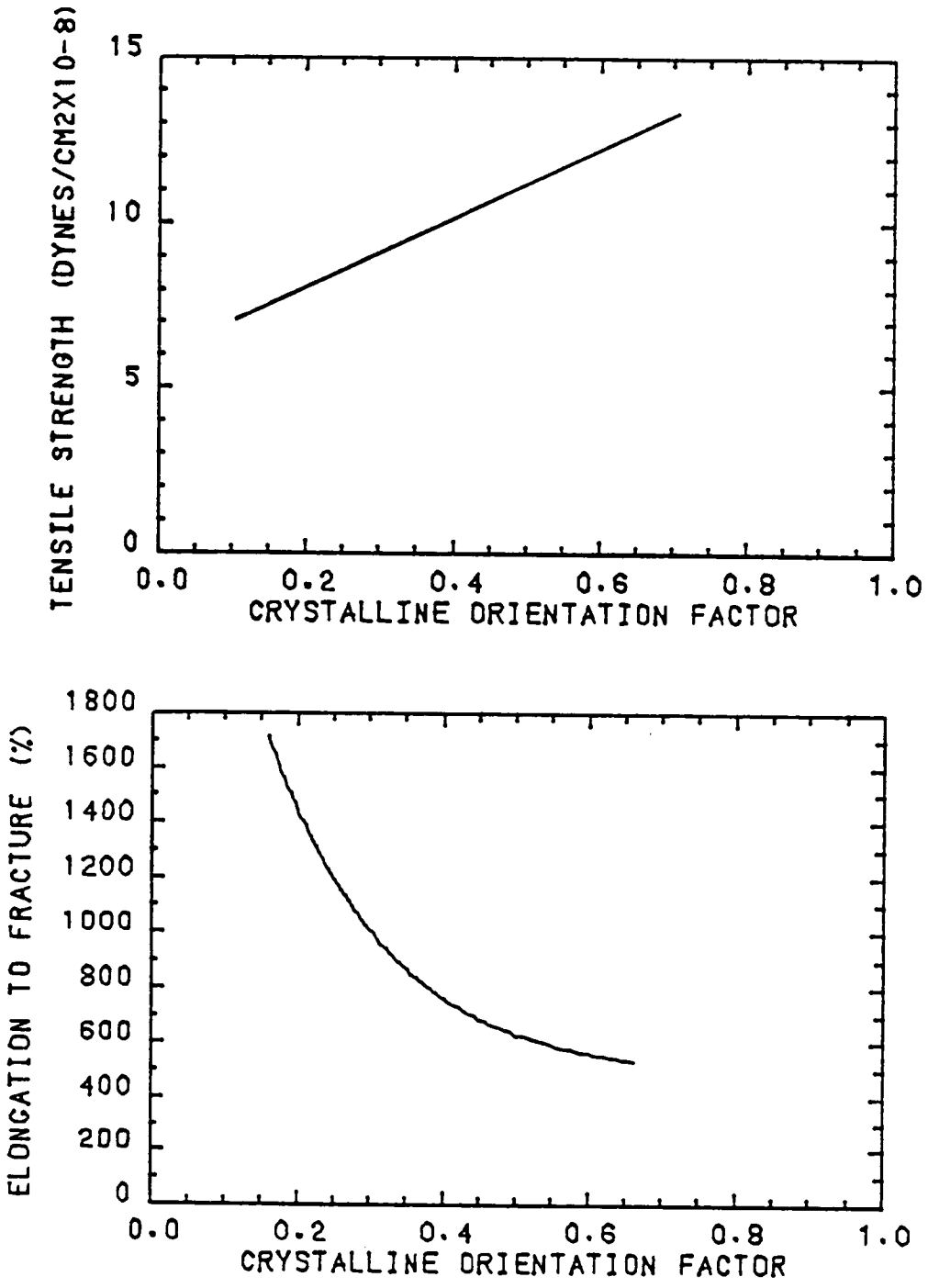


Figure 2.18. Tensile strength and elongation to break versus crystalline orientation in the c-direction for polypropylene.

CHAPTER 3

SENSOR DEVELOPMENT

The accuracy of tests performed on a melt spinline is directly dependent on the ability to monitor the desired characteristics of the polymer as it is melt spun. Also, a requirement for process control is the ability to measure the process outputs that are to be controlled. Therefore, it is essential that an accurate and reliable sensor be developed. The sensor must measure and send out signals corresponding to the properties that are monitored, in this case, diameter and birefringence. The signals will be monitored by a minicomputer which will either incorporate a controlling strategy (closed loop) to maintain a setpoint or record the values for open loop analysis.

3.1 Sensor Specification

Development of a prototype sensor begins with defining the desired characteristics of the sensor. Ultimately, the sensor is to send out voltages that represent the properties to be monitored, that is, diameter and birefringence. A major requirement is that measurements must be made close to real-time so that the values can be used in a control strategy. Also, the sensor must be small enough to be portable and fit within the physical constraints of the laboratory. The sensor should utilize as much presently available equipment as possible due to the financial constraints of the project. Finally, it is desirable that the sensor have fairly tight

tolerances, say ± 1 percent of the actual value, using any practical filtering (electronic or statistical). An accurate, smooth measurement signal will also improve the ability to control the system.

The concept of on-line birefringence measurements has been studied using the mechanical aspect of the spinline. That is, measurement of the spinline stress and using the fibers stress-optical coefficient to calculate the birefringence. The major problem with this technique is that the stress-optical coefficient is temperature dependent and the state-of-the-art ability for measuring fiber temperature in real time make it difficult to know the precise spinline temperature at the point where stress is being measured. This makes it desirable to seek alternative means of birefringence measurement.

As presented in Section 2.4, there are three useful methods for determining birefringence. One of which, the tension measurement, offers only an approximate value. The other two methods--compensation and intensity, deal directly with the light transmission through the fiber. These are more precise measurements because they deal with birefringence on a molecular level. The compensation method is undesirable because it involves the use of a microscope and compensator plate to determine retardation of the spinline. This is not desired because the rotation of the compensator plate and reading of the diameter involve the human element. In real time sensor measurements and spinline computer control, the human element must be removed. Therefore, the remaining method--intensity, is

the one with the most potential for development of the prototype sensor. Also, studies (20,26) have proven the method useful on polymer film extrusion processes.

3.2 Background Studies

Recent research on the uniaxial and biaxial stretching of polymer films has required the use of an effective means of determining the stress birefringence and molecular orientation during transient conditions. This research has incorporated the theory of light transmission through solid polymers by Stein (34,35) which was presented, in part, in Section 2.4. A 0.5 mW He-Ne laser of wavelength 6328 Å was used as a light source because it has good intensity stability and is plane polarized (Figure 3.1). The laser beam strikes the film of thickness, d, and the plane of polarization is rotated due to the effects of retardation. A second polarizer (analyzer) is placed at the exit of the laser beam and rotated 90 degrees to the incident beam. If any light passes the analyzer and strikes the radiometer head, then the film is birefringent because it has caused some rotation of the polarized light. The amount of transmitted light is defined by the following relationship:

$$I = I_o \sin^2\left(\frac{\pi d \Delta}{\lambda}\right) \tag{3.1}$$

where I_o = intensity of incident beam

Δ = birefringence

λ = wavelength of the light source.

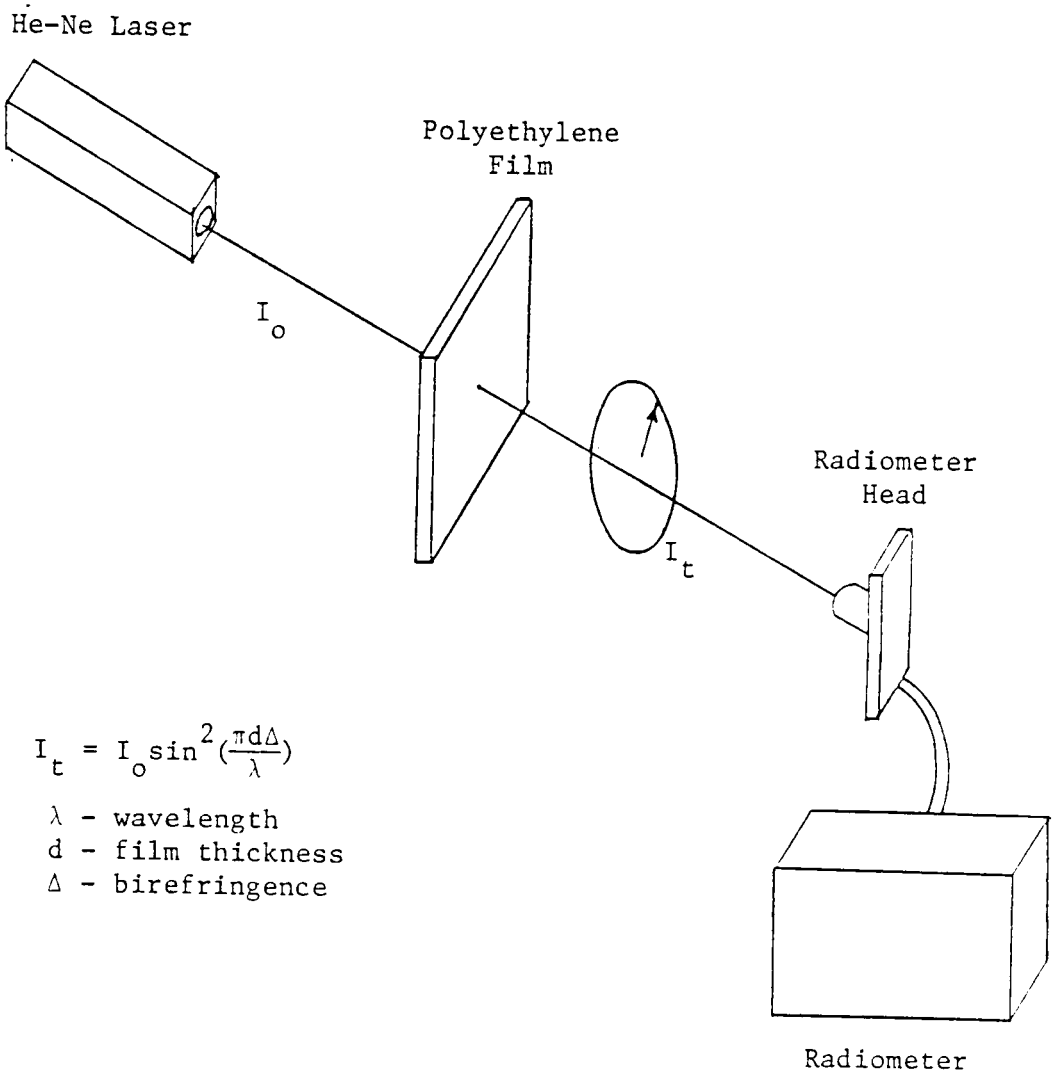


Figure 3.1. Birefringence measurements on polymer films using the intensity method.

This relationship worked accurately on the research by Hong (20) and Matsumoto (26) on polymer films and it seems plausible that it would work on fibers if only the center portion of the fiber were considered. Therefore, measuring the fiber diameter and retardation would give the birefringence. Now, an objective has been defined and an acceptable means of achieving it has been stated.

3.3 Bench Scale Research and Data Acquisition

The development of the sensor began with bench scale research. A 0.5 mW He-Ne laser and an International Light 700 Research Radiometer was available for preliminary work. The laser and radiometer head were attached to an optical bench to provide stability, accuracy and reliability to the work. Direct aim was taken at the radiometer head at a distance of two feet where the cross-sectional area of the laser beam is approximately twice the area of the photodiode in the radiometer head. The intensity of the beam is such that it saturates the photodiode even on the lowest sensitivity setting. It was thought that the introduction of the fiber and a crossed polarizer into the beam would alleviate the saturation problem, however, it did not. At this point, the options were to use a smaller laser, larger range detector such as a photomultiplier tube, or use filters and apertures to reduce the beam intensity. A new laser was not financially feasible, a larger range detector was tried but the loss of sensitivity was too great, finally some success was found with the use of apertures for reducing the beam. The results (radiometer readings) of various pinhole apertures are presented in Table 3.1.

TABLE 3.1

APERTURE DATA FOR LASER

Aperture Size (μ)	Radiometer Range*	Radiometer Reading***		
		No Fiber	Fiber 1**	Fiber 2**
300	A	9.74	2.65	3.76
200	A	5.16	0.41	0.93
	B	+	3.29	8.64
100	A	1.50	0.06	0.13
	B	14.92	0.23	0.98
	C	+	2.35	9.61
50	A	0.06	0.00	0.02
	B	0.64	0.02	0.16
	C	6.29	0.26	1.61
	D	+	2.65	15.64
25	A	0.00	0.00	0.00
	B	0.02	0.01	0.02
	C	0.18	0.08	0.10
	D	1.85	0.96	1.17
	E	14.57	6.87	8.79

* A x 10^{-3}, B x 10^{-4}, C x 10^{-5}, D x 10^{-6} $W/cm^2/nm$

Room Light: A=0.00, B=0.00, C=0.095, D=0.90, E=6.81

** Fiber 2 has a higher drawdown ratio (smaller diameter) than Fiber 1.

*** International Light 700 Research Radiometer.

The pinhole apertures seemed effective at the time until it was later discovered that the polarization of the laser beam was greatly distorted when light passed through them. Therefore, they became undesirable and the search continued for a means of sensing the intensity of the laser beam.

The search for a sensor has revealed a novel instrument containing a vector of 1024 photodiodes contained within one inch (EG&G Reticon Line Scan Camera). The output of the photodiodes is transmitted as a video signal and can be continuously indicated by an oscilloscope. Initial thoughts were to reduce the intensity of the beam by magnifying it to cover the one inch range. More research into this device revealed many exciting opportunities for the spinline research. The image of the laser beam incident upon a fiber, magnified several times and allowed to illuminate the vector of photodiodes, gives a highly resolved picture of the fiber intensity profile (Figure 3.2). Analysis of the profile indicates the diameter of the fiber as well as the amount of light transmitted through the center of the fiber. Recall, however, the analysis for birefringence must take place with an analyzer rotated 90 degrees with respect to the polarization of the incident beam. The intensity profile is then changed to that of Figure 3.3. The major noted change is the light intensity outside the fiber.

3.4 Hardware Development

Exploring the potential offered by the line scan camera required the development of several pieces of hardware. Namely, an

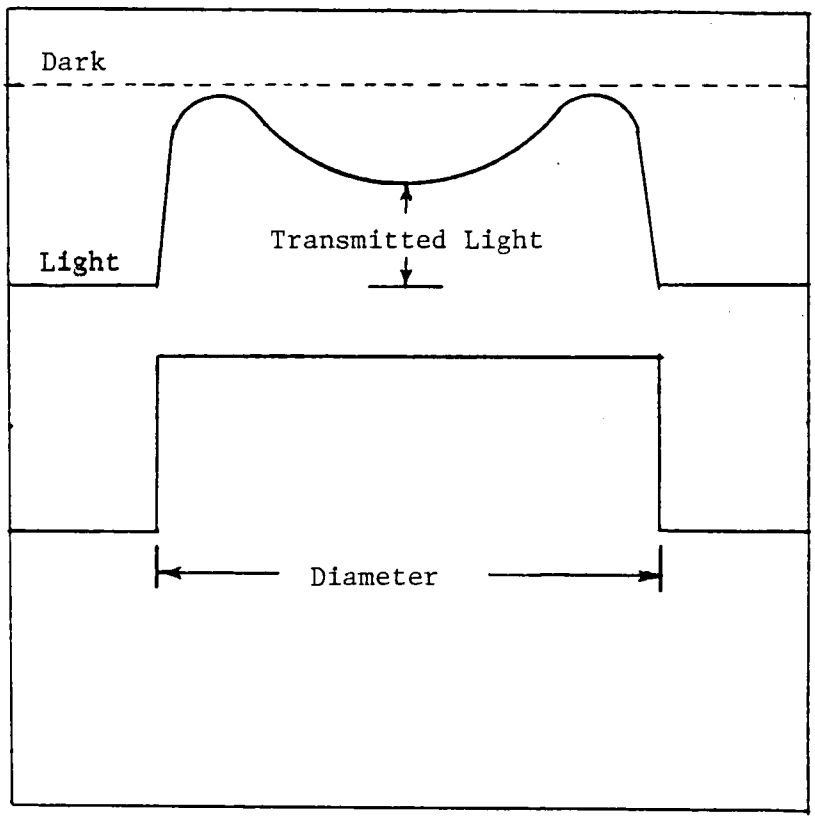


Figure 3.2. Intensity profile with uncrossed polarizers.

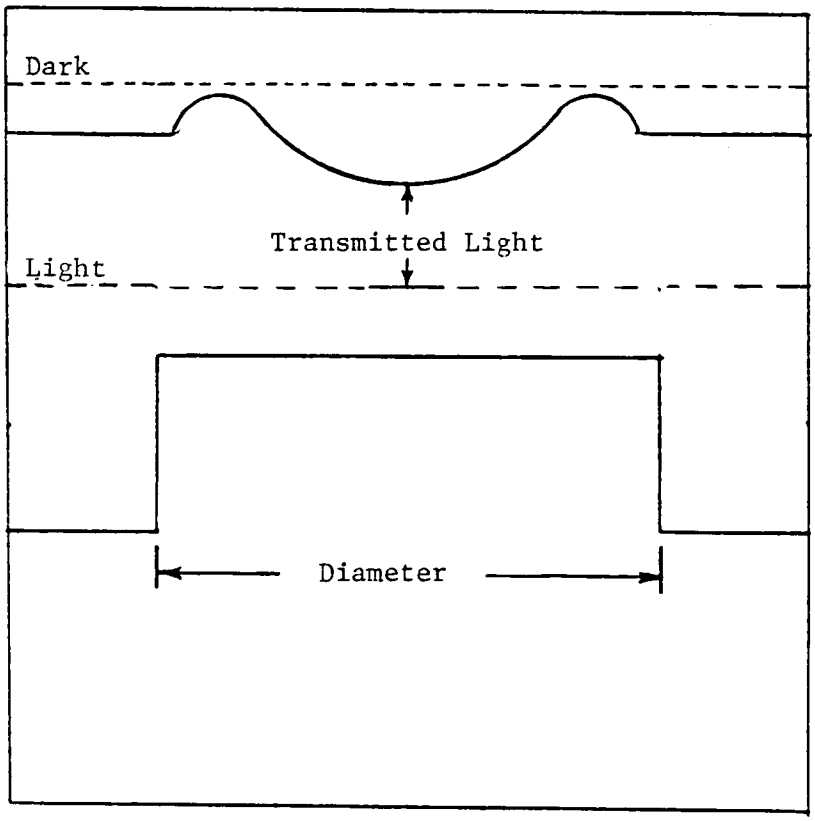
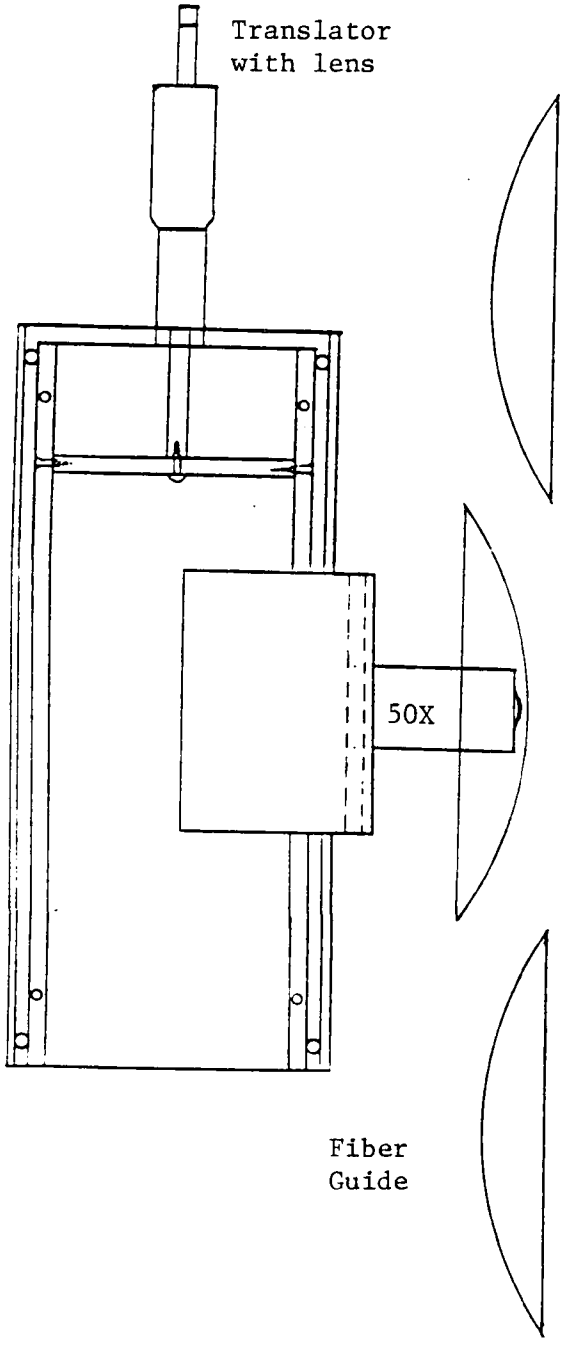


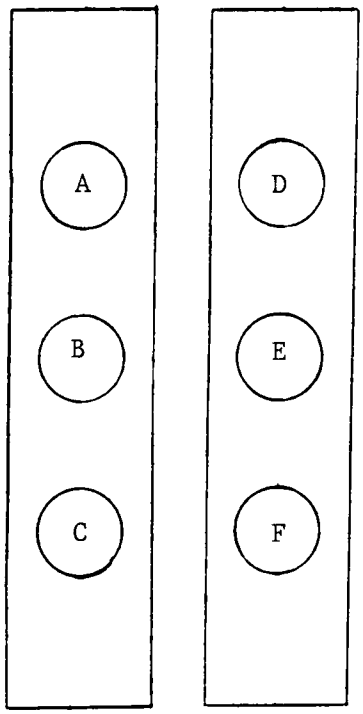
Figure 3.3. Intensity profile with crossed polarizers.

interchangeable lens system for magnifying the fiber and beam to the desired level (Figure 3.4), an x-y-z translator for positioning the fiber in the center of the lens system (Figure 3.5), and a system of three guides to stabilize the fiber and hold it in the field of focus as it passes across the lens. Working together, these items enabled one to observe on-line birefringence and diameter changes on the oscilloscope screen.

The next major task was development of an interface to allow an Applied Microtechnology minicomputer to "see" the on-line measurements. A set of specifications describing the desired interaction of the sensor and computer was presented to and discussed with the Chemical Engineering Instrument Development Shop. A plan was developed to monitor the scan rate (sync pulse) and video signal produced by the camera and using a signal analyzer the output would be voltages corresponding to diameter and light transmission through the central area of the fiber. The signal analyzer determines the fiber diameter using a clock to time the width of the fiber during one scan of the photodiodes. Detection of a dark photodiode starts the clock, the fiber's central transitions from dark to light to dark are ignored, and the detection of the next light photodiode stops the clock. The value of the clock is converted (using the scan rate of ten milliseconds) to a number of photodiodes occupied by the fiber and sent to the computer as a signal from 0-5V.

At the computer, the signal is converted to microns (0V = 0 photodiodes and 5V = 1024 photodiodes) via magnification factors (Figure 3.4).





Lens Specifications:

Lens	Diameter	Magnification
A	16.5mm	1.36X
B	17.0mm	1.52X
C	17.0mm	1.62X
D	17.0mm	1.76X
E	16.0mm	2.00X
F	13.0mm	2.18X

Figure 3.4. Lens system for the new sensor.

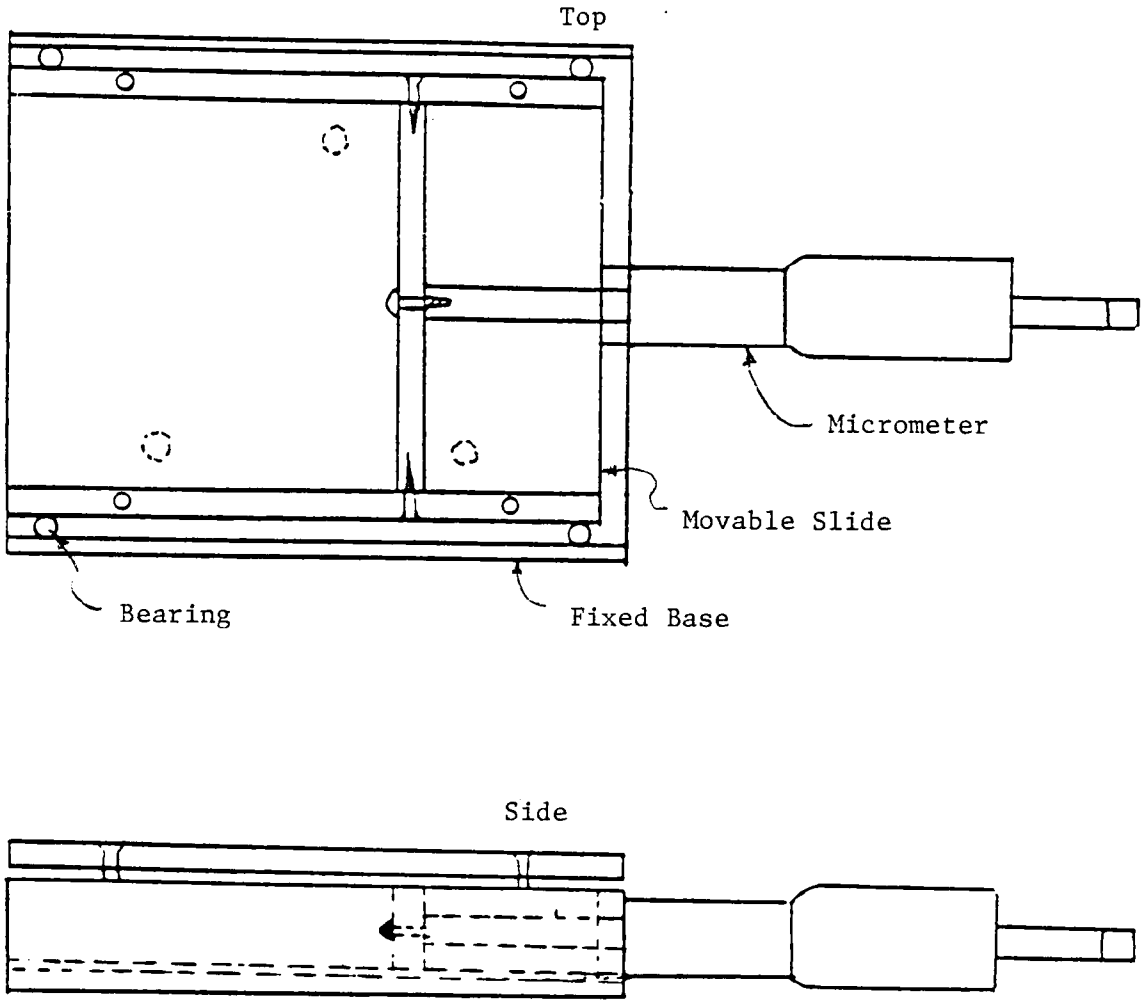


Figure 3.5. Unidirectional translators designed for fiber positioning. A combination of three forms an XYZ translator.

Obtaining a signal for the light transmission through the analyzer is considerably more complicated. Since it is desired to monitor only a portion of the fiber, such as the central section, the signal analyzer must be told which photodiodes to record. The equipment developed allows this to be done either manually or by the minicomputer. The minicomputer sends signals in parallel that correspond to the photodiodes where recording is to start and stop (as directed by a computer program). The analyzer then converts these values to clock times and begins monitoring each scan through the photodiodes. When the leading edge of the fiber is detected, two clocks are started--start and stop integration (Figure 3.6). As the start clock has the value set by the start signal, the analyzer begins recording photodiodes and integrating until the stop clock reaches the value set by the stop signal. The average value of the photodiodes is converted to a signal (0 - 1V) where 0 indicates all monitored photodiodes are dark and 1 indicates all are saturated. This value is a direct indication of the amount of light rotation by the fiber or transmission through the analyzer, I. Using the initial light intensity, I_o and equation 2.23, the retardation of the light is obtained. The two measurements of the sensor, diameter and retardation, indicate the spinline birefringence by equation 2.22. Laboratory testing of the analyzer was performed using a simple fiber simulation device and a white light source.

The Instrument Shop testing indicated proper operation of the signal analyzer, however, when the device was used with the laser

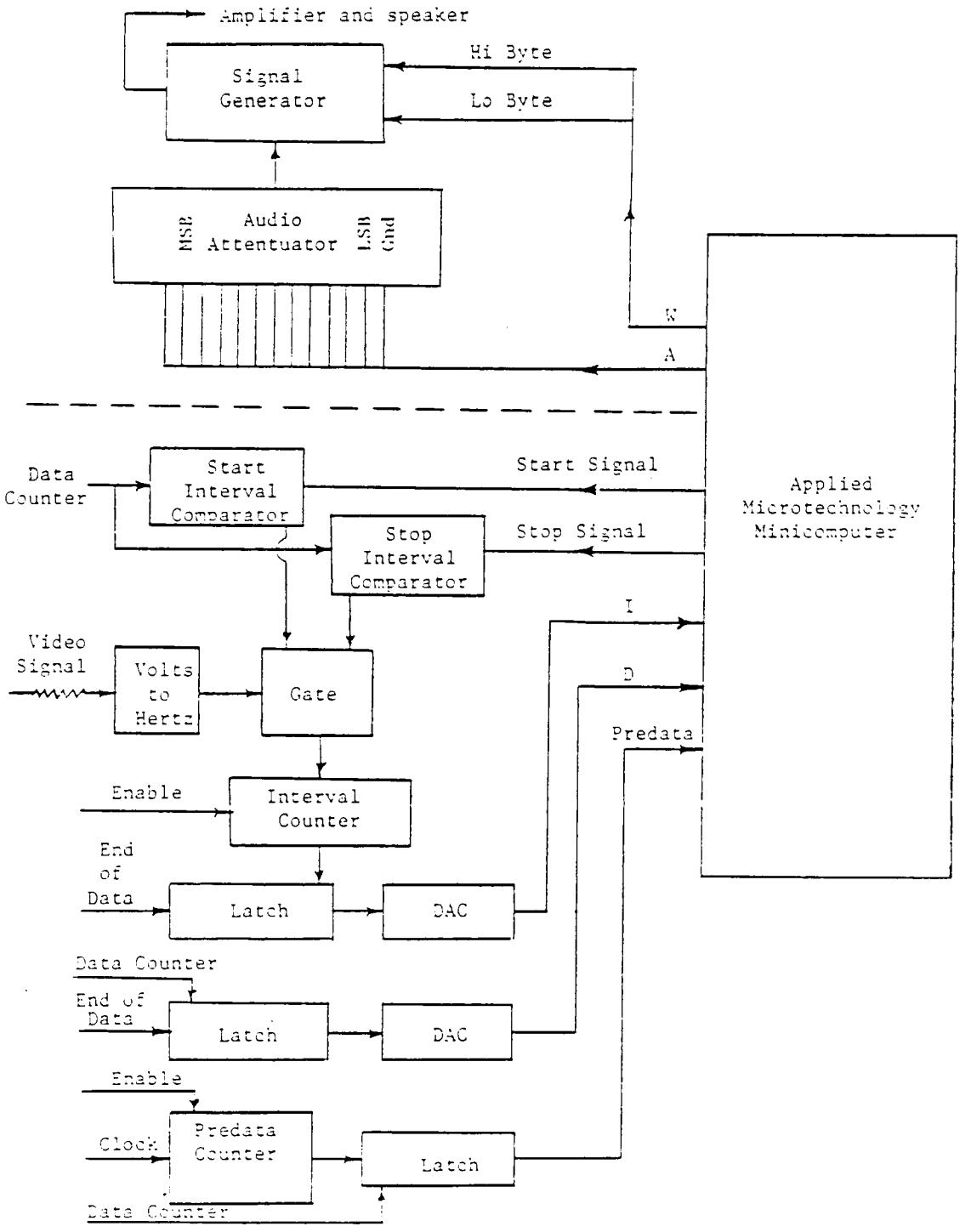


Figure 3.6. Electronic scheme for sound wave and fiber instruments.

and lensing system, a problem was detected. The line scan camera had a resolution high enough to send a noisy signal to the analyzer, the noise was created by the nonuniformity and inconsistency of the laser beam (undetectable in earlier research). The individual wavefronts of the laser beam were being detected due to the high magnification of the lens system. The solution was to replace the laser with a white light source (300W Tungsten - Halogen lamp), filter, and polarizer. The filter allowed a narrow band of light frequencies (approximately 10 nm) to propagate through the fiber to the camera eliminating any nonuniform wavefronts. The system now worked for any rotation through 90 degrees of retardation, or one-quarter of the wavelength of the light (Figure 2.7, page 35). Identification of this problem is understood by considering that the resultant wave formed by a crystal can be rotated through 360 degrees (one order) any number of times depending on the birefringence of the crystal.

Expansion of the sensor and analyzer capabilities to include more than 90 degrees retardation is accomplished through the stress-optical property of the fiber (Section 2.4). Monitoring the tension, diameter, and identifying the stress-optical coefficient indicates an approximate value for retardation.

$$\Gamma = C\sigma d \tag{3.2}$$

where C = stress-optical coefficient

σ = stress applied to sample

d = sample thickness.

The retardation calculated by this method is used to indicate which 90 degrees of which order the sensor is to operate in, i.e., 0 to 90, 90 to 180, 180 to 270, etc. Once the appropriate order is identified, a precise value is found through the intensity method. This expansion required obtaining a high resolution tensiometer (Rothschild Model V108407) to place on the spinline and all equipment associated with interfacing the tensiometer with the computer. The cooperation of the Instrument Development Shop resulted in a unique device that senses tension and sends a corresponding voltage to the computer (0-5V). No tension is indicated by 0V and 1gm of tension is indicated by 1V. The sensing elements are now complete (Figures 3.7-8).

3.5 Sensor Calibration

Calibration refers to the procedure of altering the system parameters to make the sensor output correspond to known values. The sensor calibration was performed empirically by comparison of the sensor output with fibers of known diameter and birefringence. This was accomplished off-line by manipulating system variables such as focus, camera threshold setting, integration parameters, and initial light intensity, I_o.

A variety of fibers donated to the project by Hercules Inc. were used for the calibration procedure. Each fiber was sent with a set of measurements obtained by the Hercules laboratory. Before using them for sensor calibration, it was important to measure the diameter and birefringence of each fiber using the equipment at

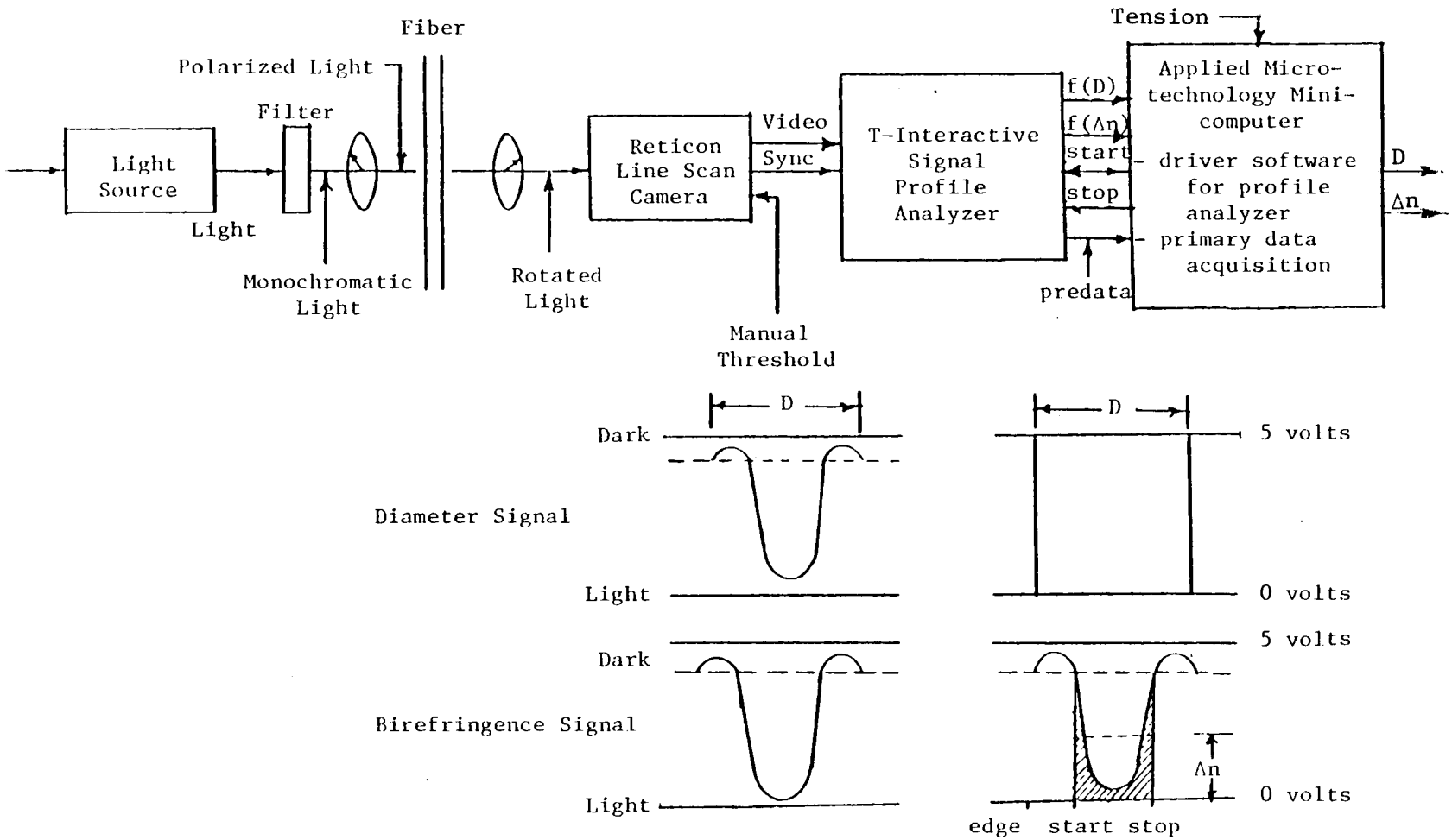


Figure 3.7. Prototype diameter and birefringence detector for melt spinline.

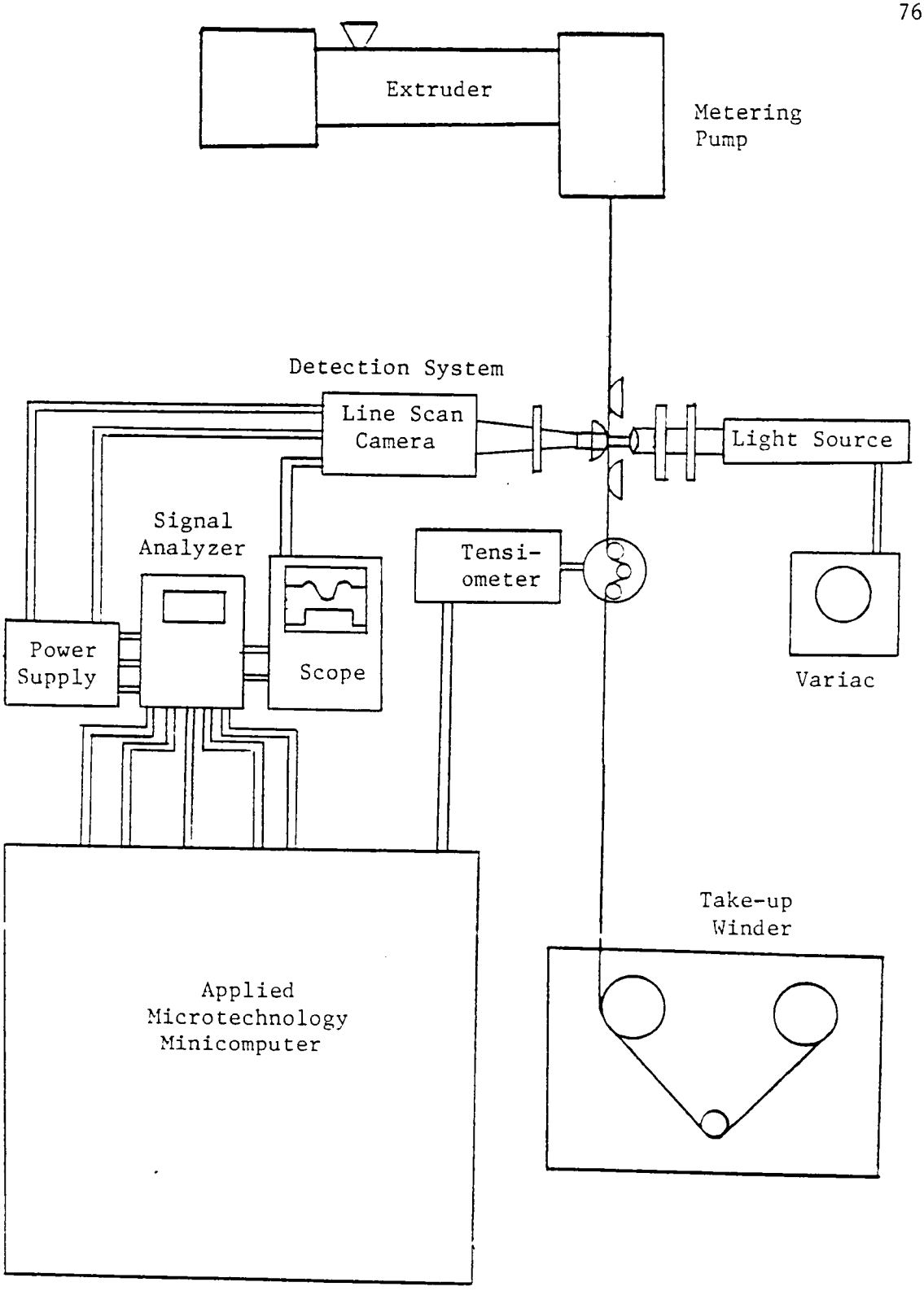


Figure 3.8. Melt spinline with diameter and birefringence instrumentation.

The University of Tennessee. These results are listed in Table 3.2. The percent difference is small indicating positive support for their use with the sensor. Each of the fiber samples were placed across the lens system and sensor readings were recorded (Table 3.3). Adjustments were made to partially compensate for any error between the sensor and an average of the UT and Hercules data. The primary adjustments were camera threshold for diameter, and tensiometer dynamic calibration and focus for birefringence. Each of these measurements were for a static fiber.

It was not known if the dynamics of the spinline would require recalibration of the sensor with a moving spinline. Therefore, tests were performed using an Olympus compensatory microscope mounted on-line directly below the sensor. The microscope permitted observation and measurement of the diameter and retardation of the spinline under dynamic conditions. The dynamic measurements indicated that slight recalibration of the sensor was necessary because the only difference in readings should be the difference resulting from the measurement positions. The recalibration brought the sensor within 3.0 percent of actual values (Table 3.4), where the actual values are those read by the author on-line with the Olympus Compensatory Microscope.

The proper control of the spinline requires that the sensor give accurate values and be electronically noise free. The electronic noise is observed by placing a fiber on the sensor, off-line, and activating the computer and camera. The system remained active

TABLE 3.2

COMPARISON OF VALUES OBTAINED AT HERCULES INC.
WITH THOSE AT UNIVERSITY OF TENNESSEE (UT)
FOR POLYPROPYLENE FIBER SAMPLES

Fiber Designation	Diameter (microns)			Birefringence		
	Hercules	UT*	% Diff.	Hercules	UT*	% Diff.
6026-59-1	63	61.7	2.1	0.008	0.0066	17.5
6026-59-2	37	37.8	2.1	0.027	0.0265	1.8
6026-59-3	34	33.5	1.4	0.031	0.0284	8.4
6026-59-4	103	109.6	6.0	0.006	0.0047	21.7
6026-59-5	83	76.7	7.6	0.017	0.0212	19.8
6026-59-6	62	58.7	5.3	0.029	0.0280	3.4
6026-59-7	19	22.3	14.8	0.017	0.0172	1.2

* Obtained using an Olympus compensating microscope with one eyepiece unit=87 microns.

TABLE 3.3

COMPARISON OF VALUES OBTAINED AT HERCULES INC.
WITH UNCALIBRATED SENSOR READINGS AT
UNIVERSITY OF TENNESSEE (UT) FOR
POLYPROPYLENE FIBER SAMPLES

Fiber Designation	Diameter (microns)			Birefringence		
	Hercules	UT*	% Diff.	Hercules	UT*	% Diff.
6026-59-1	63	52.2	17.1	0.008	0.0079	1.2
6026-59-2	37	31.9	13.8	0.027	0.0313	13.7
6026-59-3	34	28.3	16.8	0.031	0.0336	7.7
6026-59-4	103	92.6	10.1	0.006	0.0056	6.7
6026-59-5	83	64.8	21.9	0.017	0.0252	32.5
6026-59-6	62	49.6	20.0	0.029	0.0332	12.7
6026-59-7	19	18.8	1.1	0.017	0.0204	16.7

* Using sensor lens No. 1.

TABLE 3.4

SPINLINE DATA FOR CALIBRATED SENSOR
AND COMPENSATORY MICROSCOPE

	Diameter (microns)		Birefringence	
Reading	Sensor	Microscope*	Sensor	Microscope*
1	105.8	103.2	0.0010	0.0013
2	103.1	101.7	0.0020	0.0019
3	89.8	87.0	0.0045	0.0051
4	96.2	94.3	0.0035	0.0030
5	80.1	76.2	0.0057	0.0061
6	91.2	88.5	0.0053	0.0053

* The microscope was mounted one foot below the sensor. Compensations were made for sensor calibration.

for approximately five minutes with a sample time of one second. The measurements indicated very stable electronics (Table 3.5).

With this development accomplished, it was felt that the prototype sensor would provide a suitable means of monitoring control variables for use in process control strategies. The sensor has given the basis and incentive for continuing the on-line development work associated with spinline control.

TABLE 3.5

STABILITY OF SENSOR ELECTRONICS
(STATIC SPINLINE)

Time* (seconds)	Diameter** (photodiodes)	Time (seconds)	Diameter (photodiodes)
1	535	16	535
2	535	17	538
3	535	18	537
4	537	19	537
5	537	20	534
6	536	21	535
7	537	22	534
8	535	23	536
9	535	24	536
10	536	25	535
11	536	26	537
12	533	27	537
13	536	28	535
14	535	29	536
15	535	30	536

* For brevity, only 30 seconds of data are presented.

** Actual diameter $\cong$ 536 photodiodes.

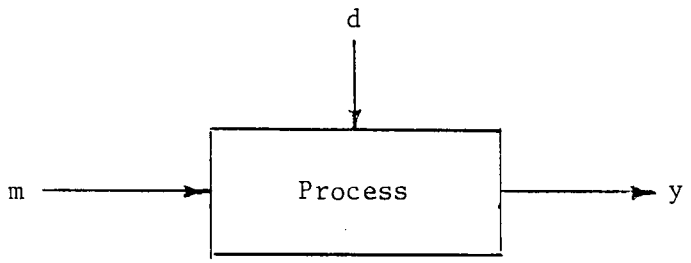
CHAPTER 4

CONTROL DEVELOPMENT

A functional control scheme for spinline diameter and birefringence has several phases of development. The development was separated into phases to promote the ease of derivation and understanding of the control scheme and its operation. Each of the phases is a separate entity that must be complete before the next is to begin. These phases include testing system response to various inputs, empirical model identification, definition of control objectives and feedback controller design.

4.1 Open Loop Analysis

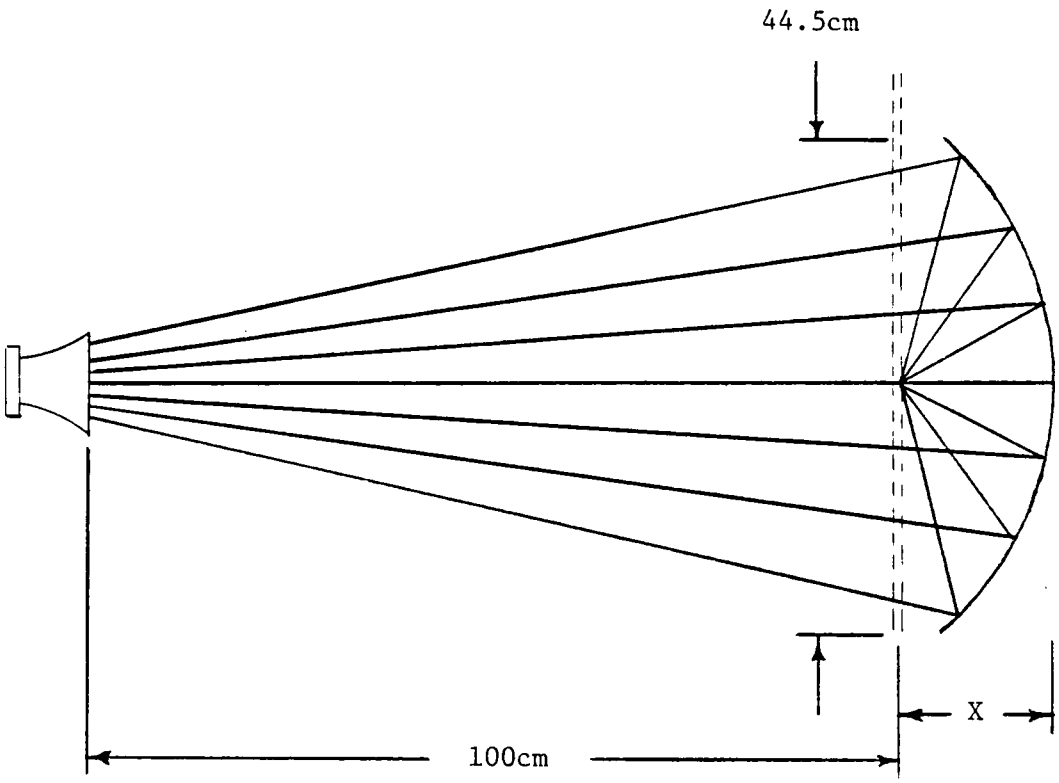
The development of a control strategy begins with an understanding of the dynamics of the process (3). One method of developing an understanding of the process is through a series of step tests. The dynamics of the melt spinning process are readily described as the process is introduced to a variety of input changes. That is, m (an input variable) is changed and the change in y (an output variable) or several outputs are recorded with all disturbances minimized as much as possible (d=0).



Inputs to the spinning operation which are of most interest at the present time are frequency and amplitude of sound waves and take-up velocity. It was speculated that the introduction of sound waves to a transforming or crystallizing anisotropic medium would produce a change of birefringence. That is, a physical vibration (or wave propagation) of specific magnitude and frequency imposed on the spinline would shift the orientation or crystallinity of the polymer. This spawned the development of a speaker - parabolic reflector system (focal point determination, Figure 4.1) for focusing a high power region of sound waves on the spinline. By placing the perturbation above the frost region, it would seem that changes caused by the energy perturbation might be "frozen" into the spinline (Figure 4.2). Thus, it is important to define the change of birefringence as a function of sound wave characteristics (frequency and amplitude).

It is known that changes of take-up velocity will produce changes in the drawdown of the fiber, i.e., the orientation is changed. This change in drawdown produces a fiber with different diameter and birefringence. An important consideration with step changes in motor speed is the effect of acceleration and deceleration of the motor because the acceleration may be faster than deceleration due to the physics of the motor operating under a load.

Therefore, the following relationships of inputs to outputs need to be explored if these inputs are to be used as manipulated variables in control strategies:



Speaker	Frequency	X
Tweeter	4,000Hz	13.2cm
Tweeter	7,500Hz	14.5cm
Tweeter	10,000Hz	14.0cm
15 in. Woofer	2,500Hz	13.2cm
15 in. Woofer	5,000Hz	13.6cm

Average X = 13.57cm

Figure 4.1. Speaker-parabolic reflector system for perturbing the melt spinline with sound waves.

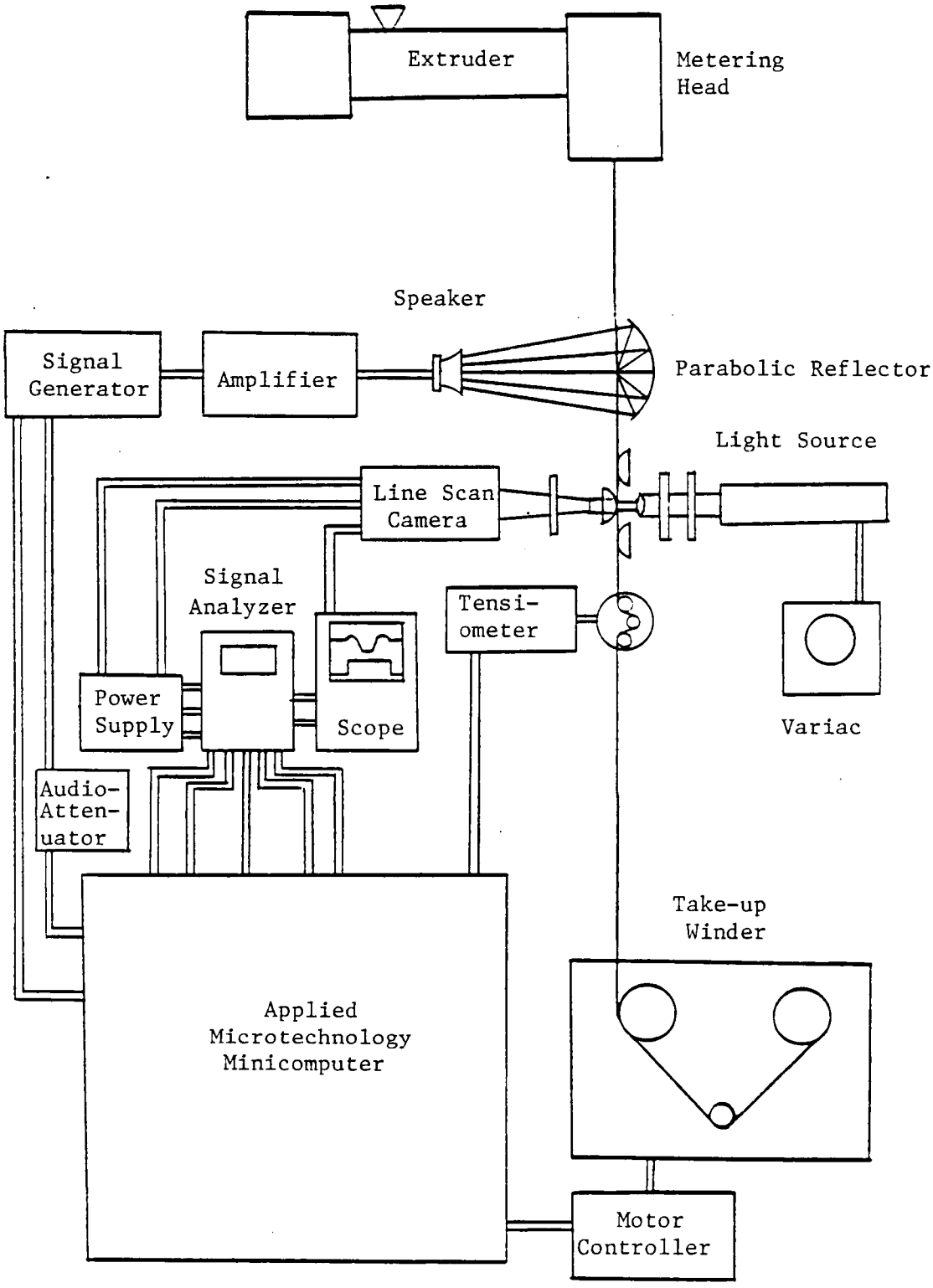


Figure 4.2. Speaker, sensor and controller configuration.

output		input
diameter	response to	take-up velocity
birefringence	response to	take-up velocity
birefringence	response to	sound wave frequency
birefringence	response to	sound wave amplitude

Ideally, a set of four functional relationships describing the listed output responses to the listed input changes for a set of other process inputs (mass flow rate, metering head pressure, etc.) is desired. For optimization of the process at steady state, the functional description needs to be able to describe the effect of changes in the listed inputs over large ranges and thus the non-linearities are of central importance. Also, the relationships help to describe the interactions of the process variables and offers insight into an overall process model. It is possible that domination or lack of definition of a relationship will cause it to be ineffective and undesirable as a manipulated variable.

For process control, the behavior of the process around the operating point at which the process is to be controlled is of main concern. Thus, a dynamic linear model encompasses most of the needs for an understanding of the process. This can be obtained via the step test procedure described above, with the step results fit to linear ordinary differential equations or transfer functions. The above list requires four transfer functions.

There are several methods for determining the transfer functions and process response characteristics. Namely, the three common types are stepping, ramping and pulsing the process inputs. These

techniques may adequately describe the behavior of the process and is generally the first step in building a process model. Often analysis of the test responses offers insight into the type of controlling strategy that is best for the process. These tests are performed to varying degrees on the three process inputs: sound wave frequency and amplitude and take-up velocity, while monitoring both birefringence and diameter.

The steady state character is another important consideration in defining process responses to input changes. If the process behavior shows variations even at the best steady state that can be obtained (no input changes to the best of our ability), the degree of inaccuracy, or real variations, of the data must be determined. It is possible that process variations, or noise, changes as a function of process inputs such as spinline velocity.

4.2 Model Development

Development of a model for control of the melt spinline is first addressed by considering the process to be single input-single output. Some level of a process model is essential to developing a controlling algorithm because it is an indication of the effect a manipulated variable has on the output of interest. For example, the process gain, the amount of output change with input change, describes how the input needs to be changed to reach a new steady state. The technique for developing the model is dependent on the particular input and output being considered (7,17,31). The empirical data correlating inputs with outputs are used to assist

the development of mathematical equations that represent the process. Also, certain relationships used in the model can be derived theoretically.

Consider the open loop analysis of take-up velocity vs. diameter. The systems' mass balance helps to describe this behavior.

$$\text{Mass in (at die)} = \text{Accumulation in the spinline} + \text{Mass out (at sensor)} \tag{4.1}$$

Since the density is constant and variations in spinline behavior are essentially negligible, there is no accumulation of mass in the spinline and the mass balance reduces to

$$V_1 A_1 \rho = V_2 A_2 \rho \tag{4.2}$$

$$\text{Drawdown} = \frac{V_2}{V_1} = \frac{A_1}{A_2} = \frac{d_1^2}{d_2^2} \tag{4.3}$$

where V_1 = extrusion velocity
V_2 = velocity at sensor
d_1 = die size, or extrusion diameter
d_2 = diameter at sensor

This represents a theoretical mathematical model. Though it is probably the simplest spinline behavior to describe, it offers many needed pieces of information. The model can be used to calculate the velocity needed for a desired diameter. With the die size, d_1, fixed and the mass flow rate, V_1, the velocity for a desired diameter, D_2, can be calculated.

$$V_2 = V_1\left(\frac{d_1^2}{d_2^2}\right) \tag{4.4}$$

This relationship can be used in spinline adjustment because it offers an opportunity for feedforward control. A feedforward scheme could entail the calculated adjustment in V_2 if an error in diameter is detected or, if a change is made in the diameter set-point, a feedforward controller could calculate the new velocity needed for the take-up winder.

The model, equation 4.4, could also be used to develop diameter, d_2, transfer functions for changes in inputs of die size, d_1, mass flow rate, V_1, and take-up velocity, V_2. Linearizing the model around an operating point provides these transfer functions. So, solving the model equation for d_2 gives

$$d_2 = d_1\left(\frac{V_1}{V_2}\right)^{1/2} \tag{4.5}$$

and linearizing around an operating point ($d_1 = D_{1,ref}$, $V_1 = V_{1,ref}$, $V_2 = V_{2,ref}$) gives

$$d_2 = \left(d_1^2 \frac{V_1}{V_2}\right)^{1/2}\Big|_{ref} + \frac{\partial d_2}{\partial d_1}\Big|_{ref}(d_1-d_{1,ref}) + \frac{\partial d_2}{\partial V_1}\Big|(V_1-V_{1,ref}) + \frac{\partial d_2}{\partial V_2}\Big|_{ref}(V_2-V_{2,ref}) \tag{4.6}$$

$$d_2' = d_2 - d_{2,ref} = \left(\frac{V_{1,ref}}{V_{2,ref}}\right)^{1/2} (d_1 - d_{1,ref})$$

$$+ \frac{d_{1,ref}}{2(V_{1,ref}V_{2,ref})^{1/2}} (V_1 - V_{1,ref})$$

$$- \frac{d_{1,ref}V_{1,ref}^{1/2}}{2V_{2,ref}^{3/2}} (V_2 - V_{2,ref}) \qquad (4.7)$$

The model, linearized around an operating point, is of the following form:

$$d_2' = K_{d_1} d_1' + K_{V_1} V_1' + K_{V_2} V_2' \qquad (4.8)$$

where $'$ = deviation variables, value-reference value

K = steady state gain constant

$$K_{d_1} = \left(\frac{V_{1,ref}}{V_{2,ref}}\right)^{1/2}$$

$$K_{V_1} = \frac{d_{1,ref}}{2(V_{1,ref}V_{2,ref})^{1/2}}$$

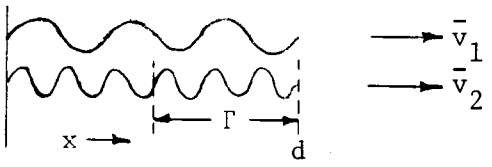
$$K_{V_2} = -\frac{d_{1,ref}^{2}V_{1,ref}^{1/2}}{2V_{2,ref}^{3/2}}$$

The transfer functions given by this model are as follows:

$$\frac{\bar{d}_2'(s)}{\bar{d}_1'(s)} = K_{d_1}, \quad \frac{\bar{d}_2'(s)}{\bar{V}_1'(s)} = K_{V_1}, \quad \frac{\bar{d}_2'(s)}{\bar{V}_2'(s)} = K_{V_2} \quad . \tag{4.9}$$

Since the accumulation term of the mass balance is negligible, the diameter response, at least to these variables, is a pure gain. Thus, a diameter control loop will have the nature of a pure gain process if G_V and G_T are also essentially pure gains (see Table 2.1, page 23). Tests of these results can easily be made with experimental data.

Other modeling to be considered include birefringence vs. V_1, V_2, D_1, as well as birefringence vs. sound wave frequency and amplitude. Birefringence, Δn, is a direct indication of the double refraction and orientation of the polymer. The retardation of waves propagating through the fiber is dependent on the length of travel and, therefore, diameter dependent. Dividing retardation by diameter indicates the birefringence. Further consideration shows the retardation dependence on diameter to be the difference of refractive indices in mutually perpendicular directions, Δn:



$$\Gamma = d(n_2 - n_1) = d\Delta n \tag{4.10}$$

where the velocities, $\bar{v}_1$ and $\bar{v}_2$, are a function of the material and its orientation and C is the velocity of light.

The functional descriptions for $\bar{v}_1$ and $\bar{v}_2$ are extremely complex. Thus, the description of retardation and birefringence, in terms of a model for inputs d_1, V_1 and V_2, is extremely complex (even at present state-of-the-art). The research for describing the effect of frequency and amplitude of sound waves on birefringence is only in the initial stage. Thus, for control and optimization purposes, experimental data and empirical models rule the degree to which it can be used. The effect of the perturbation is to disrupt the normal morphology of the fiber as it develops. The disruption could be in the form of increased or decreased crystallinity, changes in the number of nucleation sites for crystallization, or changes in orientation. For example, this may occur because a portion of the carbon chains will overcome the energy of activation that normally separates them and determines the orientation factor. However, as noted above, mathematically defining these changes, from a theoretical standpoint, is impractical at this time. Further work into this problem may, however, present a plausible empirical model for birefringence as a function of frequency. Preliminary test results for a range of frequencies has indicated a trend of birefringence changes that could be appearing at harmonic frequencies (Figure 4.3). A better description of this work can be given when new data is acquired and analyzed. As an example, the function may appear as:

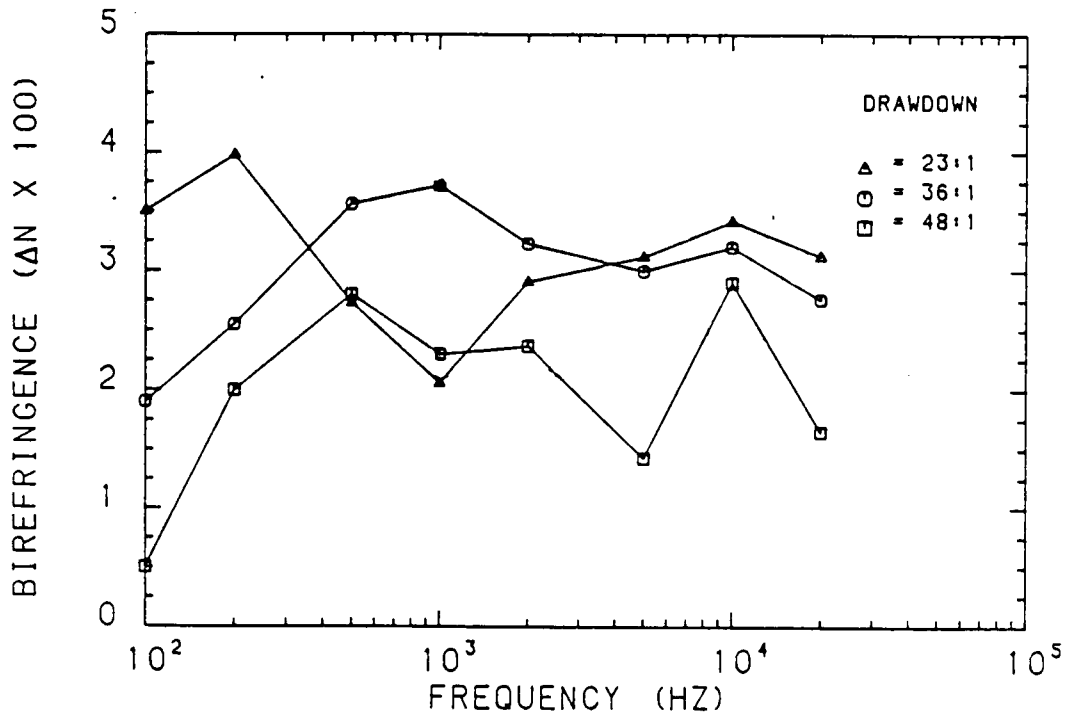


Figure 4.3. Response of birefringence to frequency of perturbing sound waves.

Source: Westbrook, P. A., and J. F. Fellers, "Some Results and Comments on the Experiment to Give a Primative Test to the Modified Lindenmeyer Hypothesis," Dept. of Chemical, Metallurgical and Polymer Engineering, University of Tennessee, 1983.

$$\Delta n = \sin^2(\omega d) \qquad (4.11)$$

This simplistic model for response to frequencies is provided that amplitude is constant. The interaction of frequency and amplitude must be considered because a response similar to Figure 2.1, page 7 may occur. Further research using on-line studies of this behavior may yield an empirical model relating frequency and amplitude to birefringence.

4.3 Control Techniques

The control objective of this work is to maintain spinline diameter or birefringence at setpoints by manipulating the take-up velocity and sound wave perturbation. The driving force behind the control development is the lack of research in this area and the need to improve the quality of melt spun fibers.

Development of a basic control strategy begins with considering the fewest number of inputs and outputs to the process. In this study, only control of a single output with a single input will be considered. The first control work is one with a readily defined mathematical model, diameter control by manipulating take-up velocity. A diagram of the signal flow is presented in Figure 2.4, page 19 , and a block diagram of this process is presented in Figure 4.4. An overall representation of the control equipment is given in Figure 4.5.

The first control loop implemented in the experimental work used integral control action only. The use of the integral mode

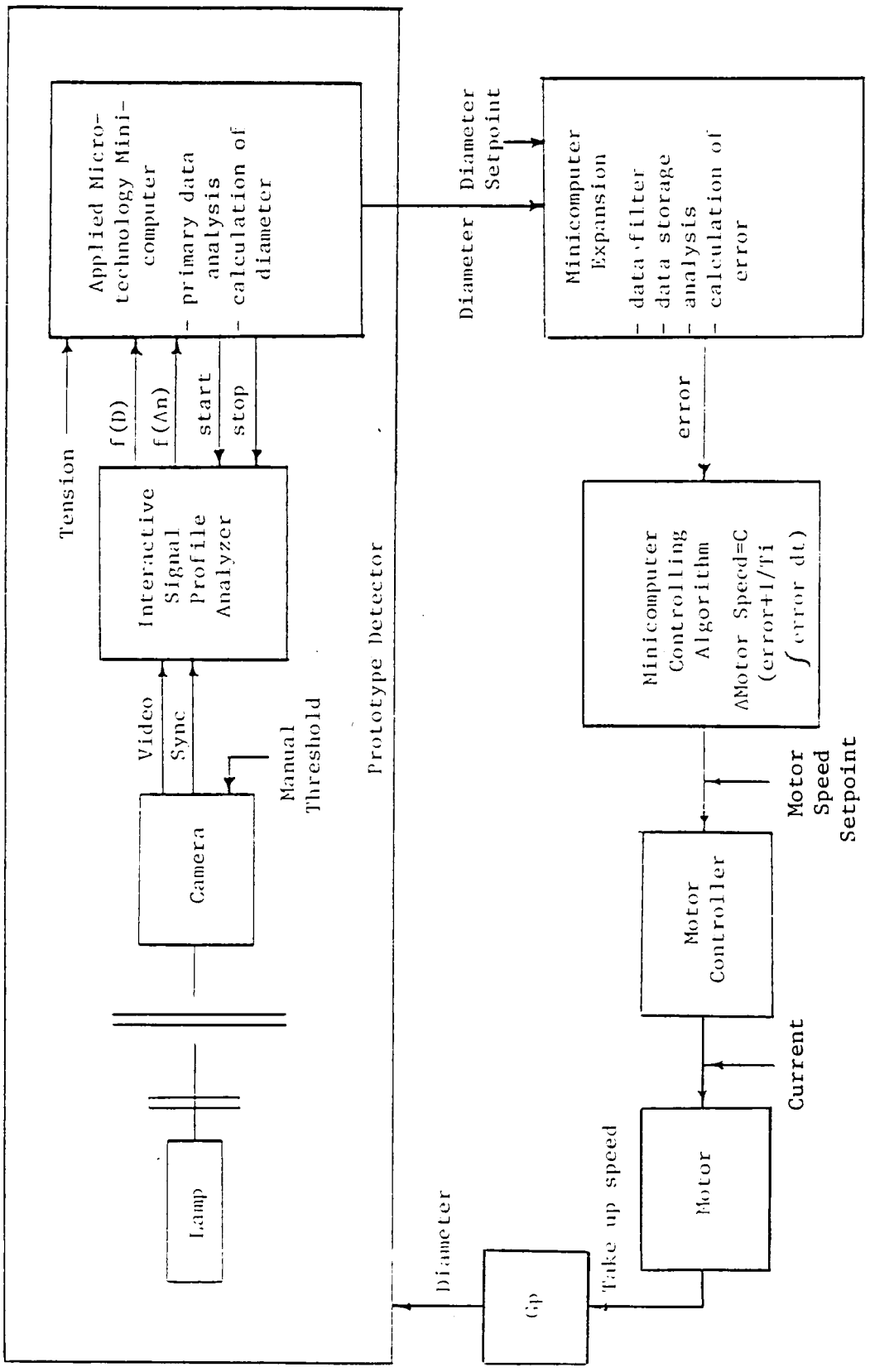


Figure 4.4. Block diagram of closed loop fiber diameter control.

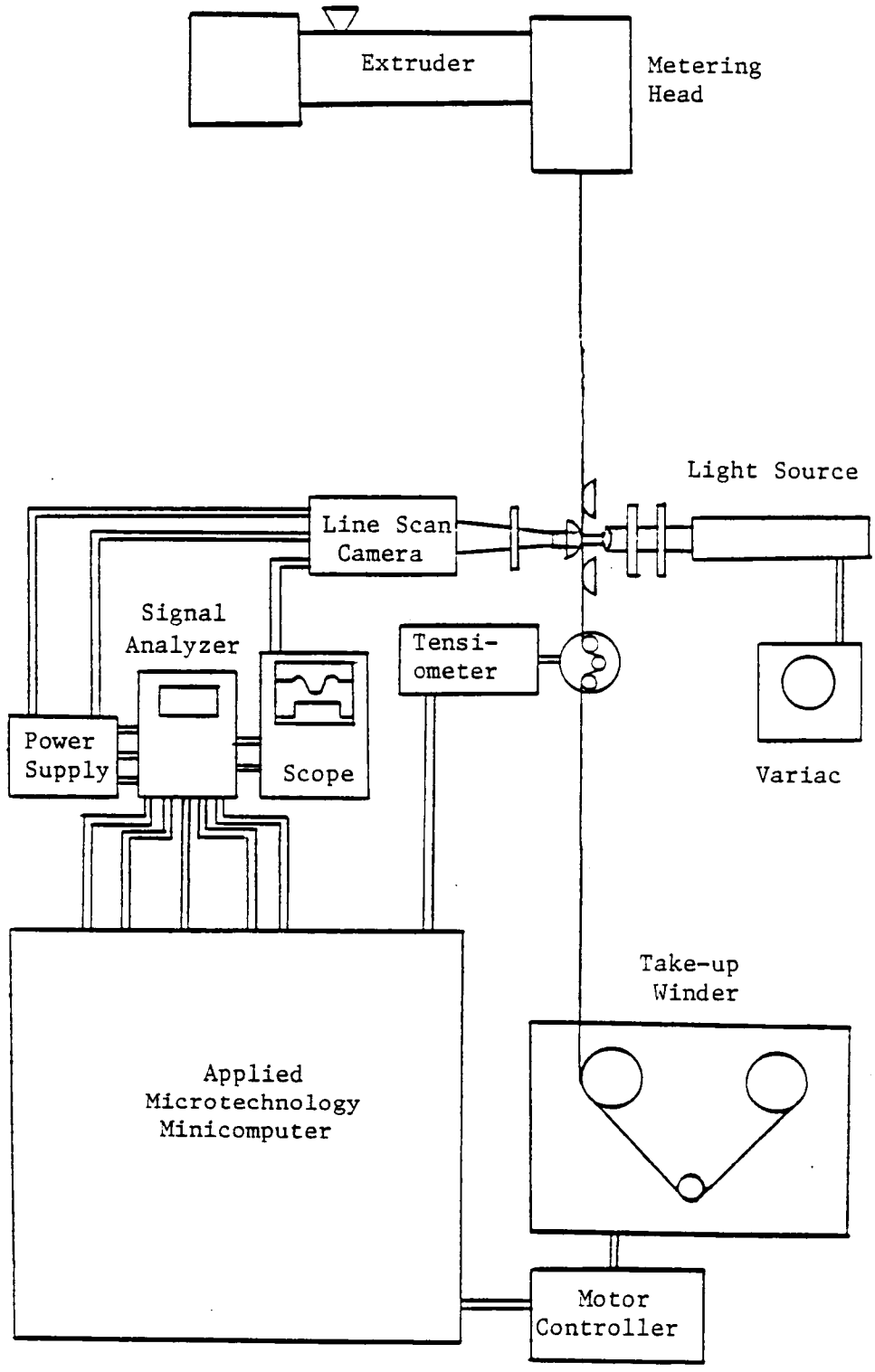


Figure 4.5. Equipment for spinline diameter and birefringence control.

for initial attempts at closed loop control was for mainly one reason. Due to the fast response of the motor, its transfer function is essentially a constant (response time is 13 milliseconds for a 10 percent step in speed) as is the transfer function for the sensor (scan rate is 10 milliseconds), that is, $G_V = K_V$ and $G_T = K_T$ when the typical proportional control is used. Therefore, for step changes in setpoint, or take-up velocity, V_2 changes in nearly a step fashion so the response in fiber diameter is essentially instantaneous. This is shown in Table 2.1, page 23 for $G_V = K_V$, $G_T = K_T$, $G_P = K_P$, and $G_C = K_C$, the closed loop transfer function is a pure gain. This type of manipulation of the spinline has a tendency to break the spinline as would be expected. When I-mode control is used, $G_C = \frac{1}{sT_1}$, the closed loop transfer function is first order, thus for step changes in setpoint, the response is not a sudden "jerk" on the spinline. Also with I-mode there is no offset from the desired setpoint. Later analysis of the results showed that I-mode had the effect of filtering the "noise" from the spinline data which was encountered from the on-line measurement system.

The discussion on the effect of closed loop control have been in terms of analog loops. The controller and sensor in this research are actually discrete, or digital. The sensor can collect a data point every 40 milliseconds and the controller was usually run at a sample time of one second. The behavior of a sample data control loop follows that of the analog results if the sample time

of the loop is small enough. This aspect may need to be pursued in future work but is only pointed out at the present time.

The digital form of the integral controller law is written as follows:

$$\text{New Motor Speed} = \text{Old Motor Speed} + K_C K_P (d_{2,ref} - d_2) \qquad (4.12)$$

where K_C = controller gain

K_P = process gain

$d_{2,ref}$ = diameter setpoint

d_2 = actual diameter measured at sensor

where motor speed is the manipulated variable and diameter is the control variable. Note that historical information is stored in "old motor speed" with each cycle of the control loop. The initial value of motor speed when the loop is first closed is termed the bias. A flowsheet of the controlling program is given in Figure 4.6.

This work will involve I-mode feedback control and P-mode feedback with feedforward indication of setpoint bias. The I-mode controller used on the spinline has a constant $\frac{K_C}{T_I}$ which amplifies the integral of the error. The process gain, K_P, can be obtained from step tests or from Equation 4.8, page 91. It was tuned with several values of $\frac{K_C}{T_I}$ and the closed loop response was recorded. The transfer function of the I-mode controller for both pure gain and first order processes are indicated in Table 2.1, page 23.

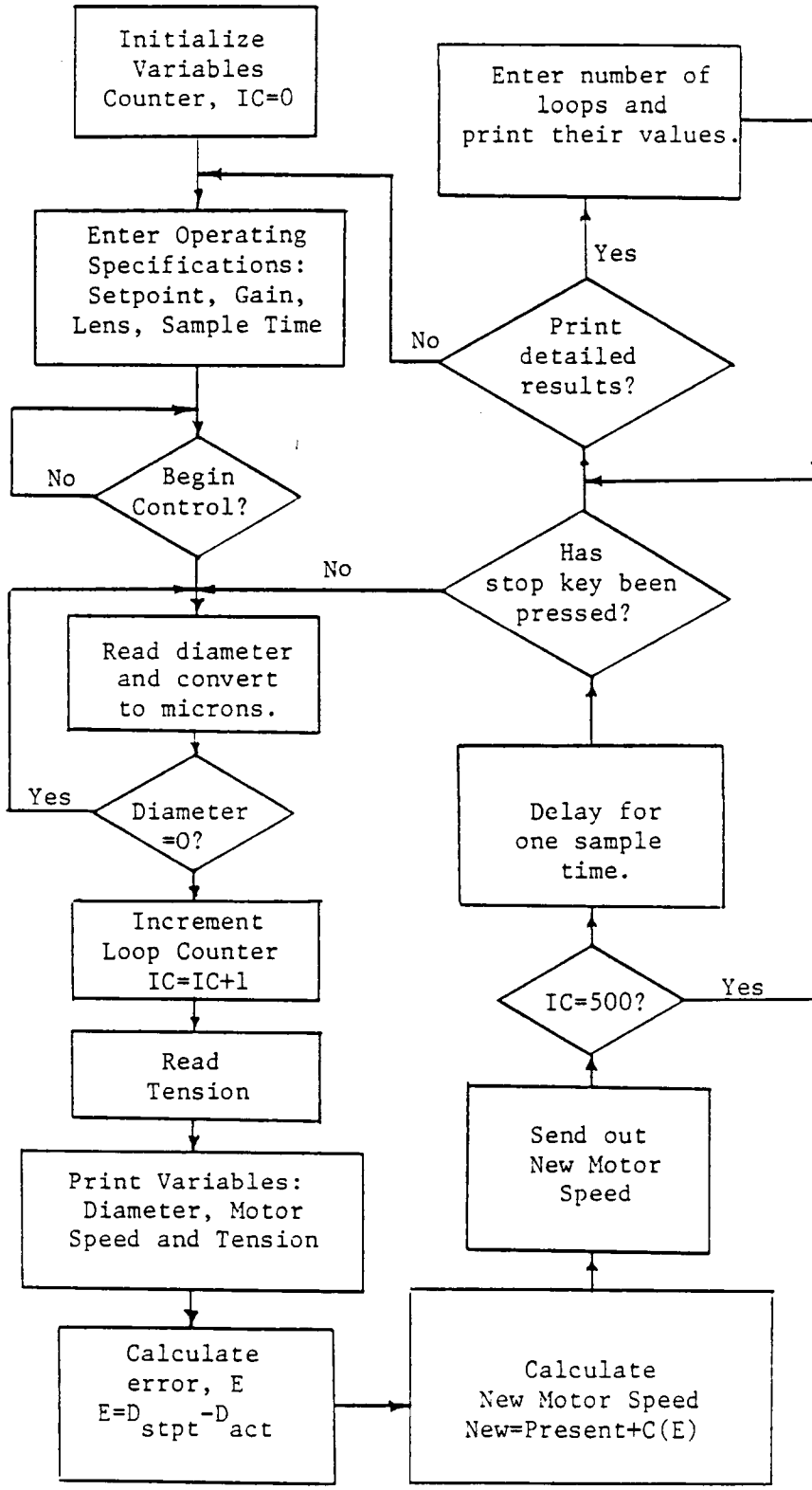


Figure 4.6. Flowsheet of controlling program (integral control).

Further study of the diameter vs. take-up velocity process leads to the conversion from I-mode to P-mode control with feedforward indication of a bias corresponding to the setpoint. The feedforward indication of bias uses the process model (Equation 4.4, page 90) to predict the new steady state motor speed (MS), $V_{2,ref}$ when a setpoint change is encountered.

$$\text{Motor Speed Bias} = \frac{K_P}{d_{2,ref}^2} \tag{4.13}$$

$$\text{New Motor Speed} = \text{Motor Speed Bias} + K_C K_P (d_{2,ref} - d_2) \tag{4.14}$$

The feedforward mechanism for determining a new bias for each setpoint permits a change of setpoint that would normally break the fiber because the step in motor speed was too large. The P-mode only controller, at times, could induce a large step in motor speed provided the error or step in setpoint were large. If the feedforward were removed and an arbitrary (but reasonable) value of bias was chosen, the P-mode control yields an offset from the setpoint due to the nature of the tuning parameters.

$$\text{Offset} = \frac{1}{1+K_P K_C} \tag{4.15}$$

With the feedforward activated and there is no error in successive loops, the fiber must be at the desired diameter. Tuning this controller is similar to the integral controller because there is only one tuning parameter, K_C. Also, the closed loop transfer functions

for the P-mode control of pure gain and first order processes are indicated in Table 2.1, page 23.

The dynamics of many processes make them difficult to control due to the long settling times. This problem is reduced by combining the proportional and integral modes into one controller. This technique is to be examined with the melt spinline. The effect of Proportional-Integral (PI) control will be an increase in the order of response (integral mode), elimination of the offset (integral mode), and a faster response with the use of large K_C's and small T_I's. The controller is described as follows:

$$\text{New Motor Speed} = \text{Motor Speed Bias} + K_C K_P \left(e(t) + \frac{1}{T_I}\int e(t)dt\right)$$

$$\text{where } e(t) = d_{2,ref} - d_2 \qquad (4.16)$$

As mentioned earlier, there are two tuning parameters, K_C and T_I. Tuning is performed by holding one constant while manipulating the other until the desired response is found or use tuning rules (25, 31,36).

The next control study is also a system that is defined empirically using experimental data, birefringence control by manipulating the take-up velocity. In this study, only I-mode control is considered due to its effectiveness in the previous experiment. The fit, as reported in Chapter 5, is as follows:

$$\text{Motor Speed Bias} = C_{\Delta n}\sqrt{\Delta n_{ref}} \qquad (4.17)$$

$$\text{New Motor Speed} = \text{Old Motor Speed} + K_C K_P(\Delta n_{ref} - \Delta n) \qquad (4.18)$$

where Δn_{ref} = birefringence setpoint

Δn = birefringence measured at sensor

The birefringence response to I-mode control was similar to the diameter response. The control strategy operates by monitoring tension to indicate the order of the retardation (Figure 4.5, page 97).

The final system with potential to support a controlling algorithm, birefringence vs. sound wave frequency, will not be studied at this time due to lack of a satisfactory model for describing the responses and behaviors of the spinline with varying frequencies.

CHAPTER 5

EXPERIMENTAL RESULTS AND DISCUSSION

The laboratory work of this study was performed at the fiber spinning facility of the Department of Chemical, Metallurgical, and Polymer Engineering, The University of Tennessee, Knoxville. Equipment for extruding a fiber and winding it onto spools is available. All other equipment used in the current research has either been designed and constructed at UT or purchased from companies to meet certain specifications. A sketch of the melt spinline process with the computer interfaced instrumentation is given in Figure 5.1. The figure shows the on-line measurement system, minicomputer, tensiometer, take-up motor, sound wave device, and all equipment for running a melt spinline. The experimental results reported in this chapter were generated using this equipment for monitoring and controlling the spinline behavior.

5.1 Operating Conditions

Melt spinline. The material being spun for this research was Dupont 7040 polyethylene. The melting point of the polyethylene is 145°C so the extruder temperature was set at 180°C. The mass flow rate through a 0.03 in. die (L/D = 15.97) was set by manually placing the gear pump at its lowest speed which gave a mass flow rate of 3.1gm/min. After setting the mass flow rate, the extruder screw speed was adjusted by the operator to bring the operating

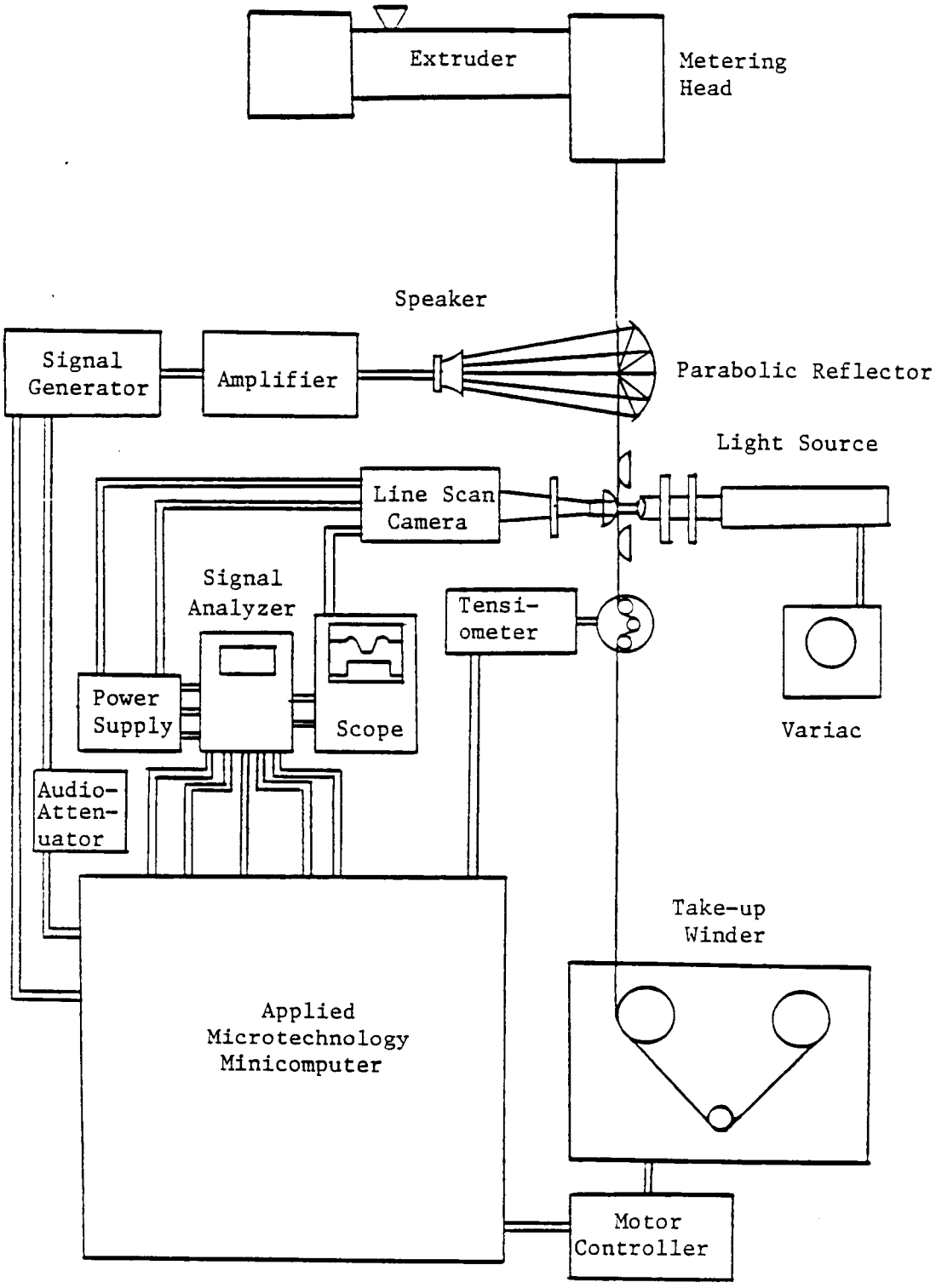


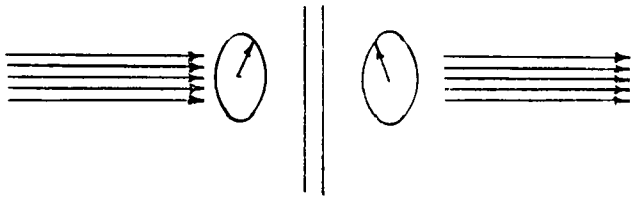
Figure 5.1. Spinline process with all computer interfaced instrumentation.

pressure up to 750psi. The extruder was designed by UT's polymer group from materials purchased from Modern Plastics Machinery Corporation and has a full range operating pressure of 0 to 3000psi.

The extruded fiber was drawn due to the force of a metering drum with the fiber wrapped around it twice. The metering drum was turned by the take-up motor with the speed of the motor set by the computer. From the drum, the fiber was taken up on spools at constant tension by a Leesona take-up winder. The winder had a torque arm, supported by the fiber, that regulated the speed of the take-up bobbin, i.e., as the spinline tension reduced, the arm would drop, increasing the speed of the take-up bobbin and vice versa. The torque arm created a problem because the weak polyethylene would cold work under the weight of the arm. Therefore, the fibers taken up on the spools could not be examined off-line to determine if on-line sensor measurements were correct. Another problem was the start-up time involved with getting the fiber started onto the take-up bobbin. In light of this, it became desirable (in later work) to place an asparator after the metering drum to eliminate the time needed to start the winder. Typical take-up velocities ranged from 500 to 2200m/min.

Sensor. In Chapter 3, development and calibration of the sensor were described, however, specific operating details were not mentioned. The sensor uses a tungsten-halogen 300W lamp which generates a tremendous amount of heat. The heat was dissipated by an intricate system of air hoses directing cool air at the lamp,

chromatic filter, and polarizer. The chromatic filter reduced the white light to a narrow band of wavelengths from 6320Å to 6340Å, or red light. The red light was polarized at 45 degrees to the fiber. After striking the fiber, the light was incident upon a second polarizer rotated 90 degrees to the first polarizer, i.e.,



The lens system was set on lens no. 1 for the experiments presented in this chapter. This magnified the image of the fiber 150 times before striking the line scan camera (Figure 3.1, page 62). Focusing on the moving spinline was very critical due to the lens' narrow depth of field, however, the sharpest average focus was used. The scan rate of the photodiodes was left at the factory setting of 10 milliseconds. The camera's threshold setting, or level of a diode to trigger the beginning or end of the fiber, was set as close as possible to the level of the photodiodes unperturbed by the fiber and not get false signals (Figure 5.2). The final element of the sensing equipment, the tensiometer, was placed on-line directly below the lens system (approximately six inches) and set to have the full range capability from 0-10gm.

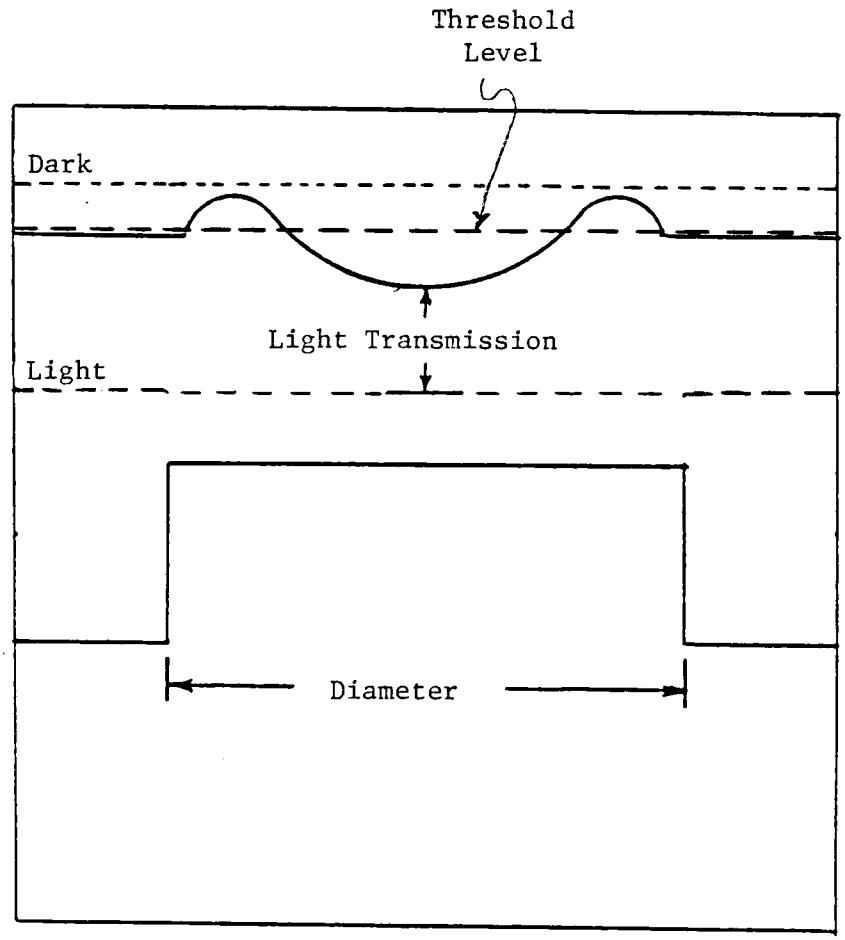


Figure 5.2. Intensity profile with threshold.

5.2 Computer Data Acquisition

An Applied Microtechnology minicomputer was interfaced to the signal analyzer, tensiometer, sound wave frequency generator and amplifier, and take-up motor utilizing nine of the built-in communication ports (including analog to digital and digital to analog converters). Communication to the signal analyzer, requiring five communications ports involved:

1. sending out start and stop signals to indicate the integration limits for determining a light transmission signal corresponding to the center of the fiber;
2. receiving an analog signal (0-5V) corresponding to the diameter of the fiber;
3. receiving a predata signal (0-5V) indicating the starting edge of the fiber on the vector of photodiodes (number of photodiodes scanned left to right). The signal analyzer times the scan from the first diode to the leading edge of the fiber. This time is predata signal. If the signal starts dark (intensity of the first photodiode less than I_o) the fiber is off the vector to the left hand side. If this signal added to the diameter signal is less than or equal to 1024 photodiodes, the fiber is not entirely on the vector, i.e., it is off to the right hand side;
4. receiving a ginal (0-1V) corresponding to the light transmission through the center of the fiber.

Other computer input/output is to receive a value from the tensiometer (0-5V = 1-10gm) and to send values to the frequency generator

(0-5V = 1,000 - 10,000Hz), amplifier (0-1V = 0-100W), and the motor controller (0-5V = 0-4000rpm).

Computer algorithms were written to initiate and monitor all communications in both open and closed loop modes. The code to read and write to the communication ports is found within the program in the appendix. The open loop mode was written for step testing the input variables while monitoring the response of the output variables. The computer code began by initializing an input variable, say motor speed, by setting it to an initial value. The code then stepped the variable by a certain percentage as input by the operator and monitored the system response. The diamter, in microns, was obtained as follows:

$$\text{diameter} = \text{lens factor} \times \left(\frac{\text{voltage}}{5.0}\right) \times 1024 \qquad (5.1)$$

where voltage = 0-5V received from the signal analyzer

lens factor = calibration constant

lens	lens factor
1	0.3758
2	0.3375
3	0.3162
4	0.2913

After determining the diameter, a specific region of the intensity profile must be monitored for retardation, or light transmission. This region has been chosen as the center 20 percent of the fiber for the majority of these experiments. Using simple mathematics and recalling the start and stop integration points are

set from the leading edge of the fiber, a value for the start and stop integration points are calculated. These values are sent out and a value for the light transmission is received. The retardation is determined as

$$\text{Retardation} = 1.8 \times \frac{675}{\pi} \times \left(\frac{\tan^{-1}\frac{Y}{100}}{1-\frac{Y}{100}} + X\right) \qquad (5.2)$$

where $Y = \frac{\text{voltage}}{0.005(\text{stop-start})} \times 100$

X = a multiple of π indicating the order of birefringence found from measuring tension

$$\text{Retardation by tension, } \Gamma_T = \frac{CT}{\pi d} \qquad (5.3)$$

where T = tension on spinline

d = diameter of spinline

c = stress-optical coefficient

X	Γ_T(nm)
0	337.5
$\frac{\pi}{2}$	675.0
π	1012.5

The birefringence is the retardation divided by the diameter.

Tests were also performed with the frequency of sound waves with amplitude fixed. The sound waves were generated using a

Realistic high frequency tweeter (for frequencies >4000Hz) and a 15 in. woofer enclosed in a 1.5 cubic foot cabinet (for frequencies <4000Hz). The speakers are powered by a computer interfaced signal generator and amplifier. Birefringence was collected as a function of frequency for several drawdown ratios.

The computer code for closed loop control was written to include the above calculations for diameter and birefringence along with a strategy for maintaining specific setpoints. That is, calculations were performed to determine the appropriate voltage to send to the take-up motor to obtain a specific diameter (in part, Equation 4.12, page 99). The computer program used in these studies are listed in the Appendices. The program DIACON controlled diameter.

5.3 Open Loop Results

A primary consideration in controller development and tuning is the steady state behavior of the process. The steady state behavior (open loop process with no intentional changes in any inputs) of the spinline is shown at two different motor speeds in Figure 5.3. In these figures, the diameter was sampled at one second intervals with no electronic or statistical filtering. Also, the figures show a nominal movement of ±5 microns, or about 10 percent of the fiber diameter, among the points taken at one second intervals. In the figures for diameters, dashed lines are shown at ±5 microns to illustrate this point.

The melt spinline's average response to changing inputs was as expected. Considerable variations from predicted values were

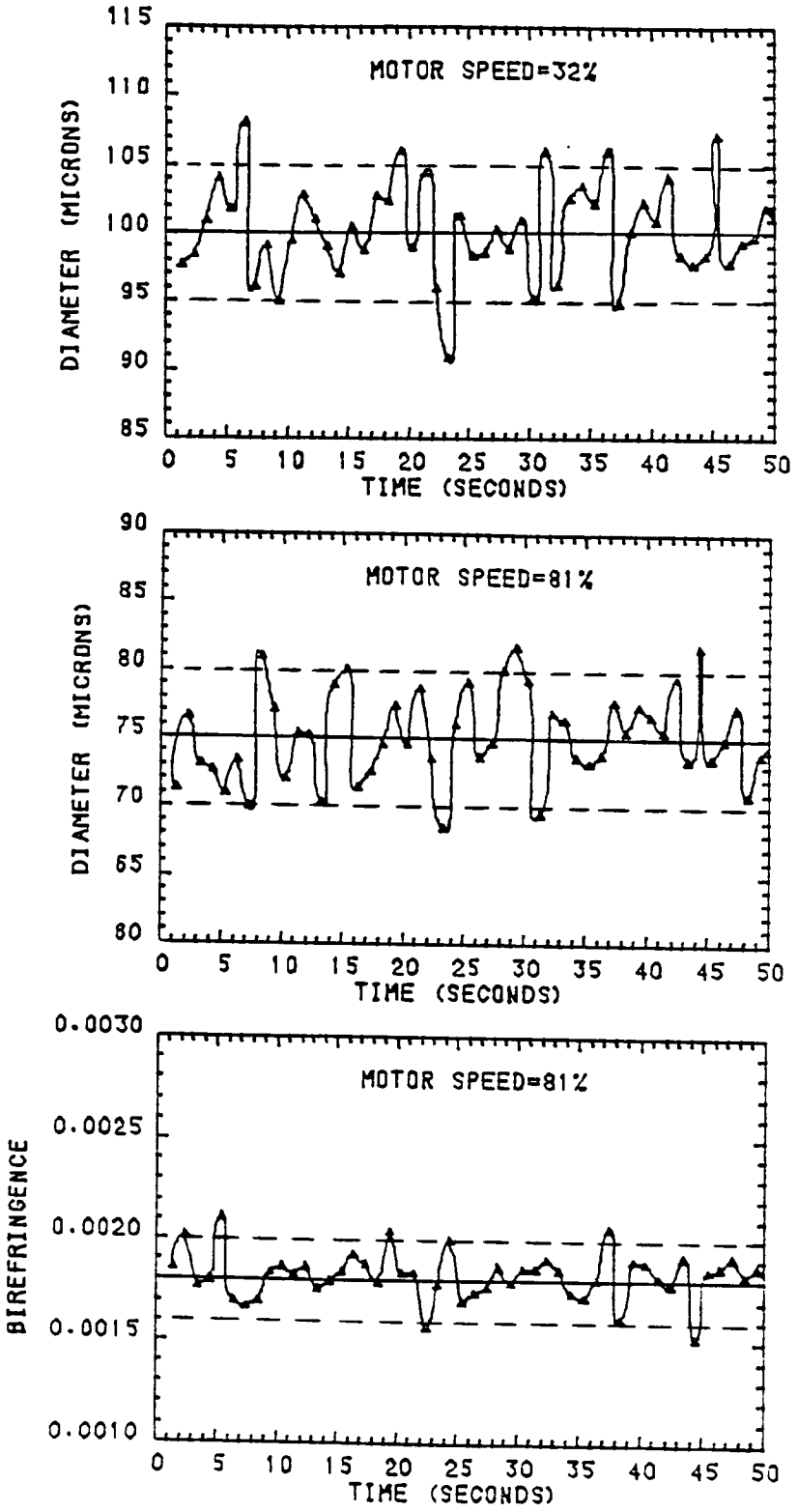


Figure 5.3. Steady state stability of diameter and birefringence.

found in the process output when operated at steady state. Data taken at steady state with one second intervals indicates that some systematic disturbance, either physical or electronic, was taking place. From spinline operating experience, some of the variation in Figure 5.3 is probably physical diameter change. This could arise from pulsations in the gear pump, harmonic vibrations in the equipment, draw resonance, etc. Bench scale operations (off-line) have indicated there is slight electronic noise (Table 3.5, page 82). That is, microscope measured fibers can be measured repeatedly by the sensor with an accuracy of ±2 photodiodes. For a 75 micron fiber magnified to cover three-fourths of the photodiode vector, and error of ±2 photodiodes corresponds to an error of ±0.25 percent. Motor speeds of 32 percent and 81 percent gave data with similar deviations from the mean. Thus, the data offered no reason to suspect a scattering trend with take-up velocity. The scatter of ±5 microns seen in the figure was created by a combination of all the variations. Enhancements in the optical system to increase depth of field (i.e., eliminate sensitivity with respect to the focus) and decrease fiber drag could improve the accuracy of the data. Also, a filter designed to record 10 to 50 data points and average them, could make the diameter measurements even more precise than ±5 microns (or 10 percent error).

Stepping the take-up velocity while monitoring the spinline diameter offers insight into the proper control parameters for maintaining a diameter setpoint. These tests were performed with steps of different sizes, however, only one will be reported (Figure 5.4).

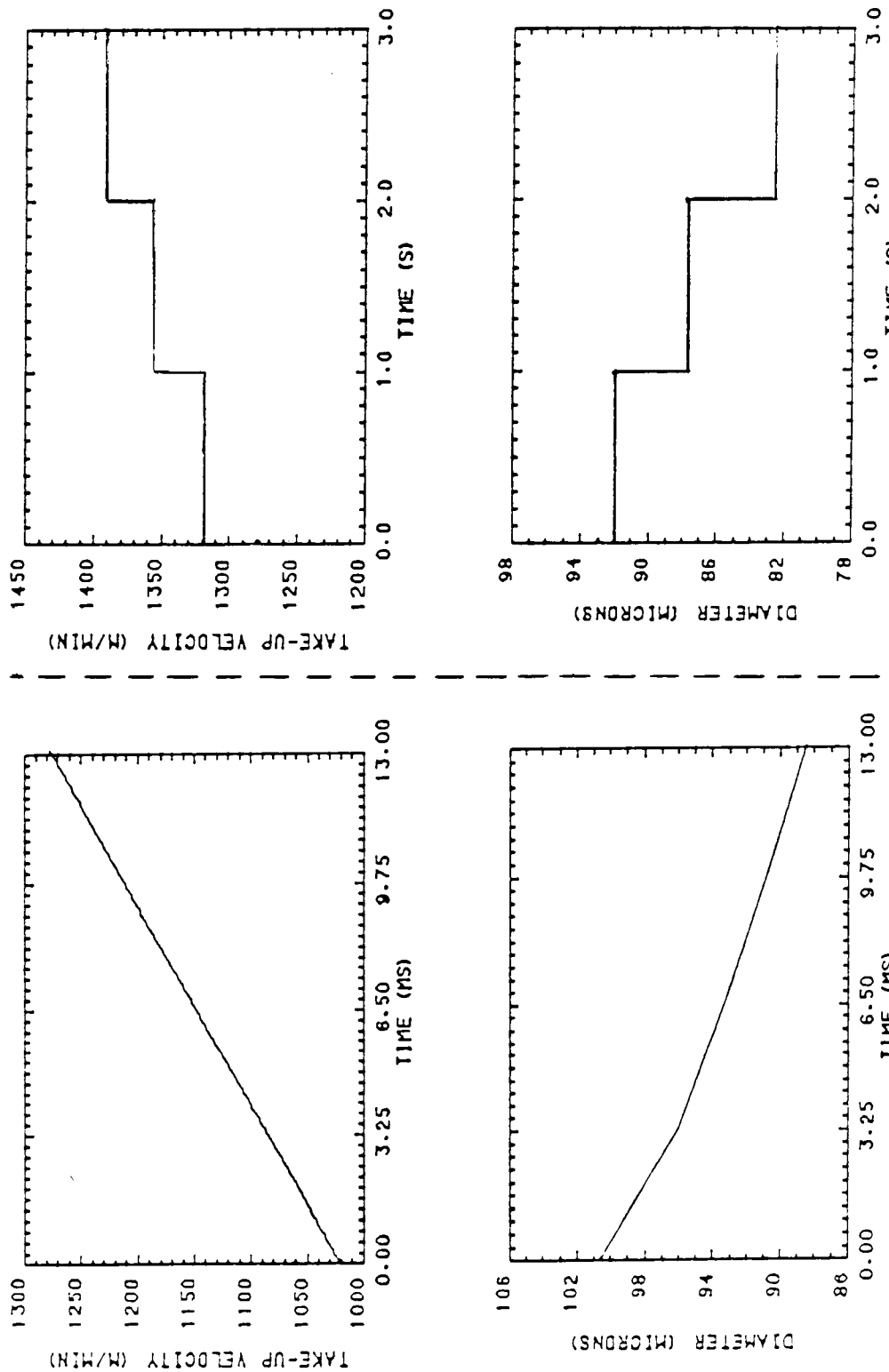


Figure 5.4. Open loop response of diameter to a step change in take-up velocity.
(a) Theoretical response.
(b) Pseudo response.

The system was allowed to reach steady state between successive steps. Due to the response time of the motor, nearly perfect steps of velocity did occur. An overall view of steady state diameter vs. motor speed is given in Figure 5.5. This relationship is mathematically defined in Equation 4.4, page 90, and is used for determining motor speed at given diameter setpoint.

Steps of velocity were also performed while monitoring birefringence. These tests utilized a larger step because significant changes in birefringence were desired (Figure 5.6). Once again, only two tests are reported for brevity. Motor speed setpoints for the birefringence control scheme were obtained from a mathematical equation and verified by experimental data which is plotted in Figure 5.7.

Monitoring spinline response to a step input of motor speed was difficult due to the constraints of available hardware. The motor was designed with a tachometer feedback system to give it the capability for completely responding to a 100 percent step input within 130 milliseconds. The form of the response was a ramp, Figure 5.4(a). The software to monitor a diameter or light intensity, not record or store it, involves reading the I/O port (20 milliseconds), incrementing the array (15 milliseconds), then resetting (10 milliseconds). A total of 45 milliseconds was required for one reading. Therefore, it was not feasible to record the system response to a step of motor speed, say 10 percent which occurs in 13 milliseconds. It was, however, possible to simulate the response using the spinline model, Figure 5.4(a) and 5.6(a).

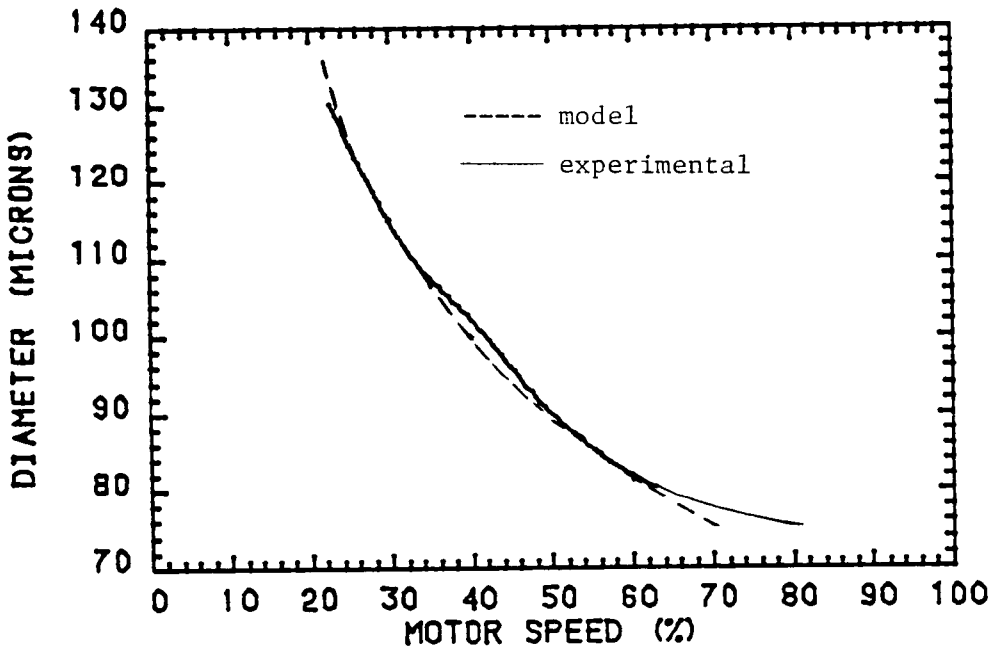


Figure 5.5. Diameter as a function of motor speed for melt spinning under the research operating conditions.

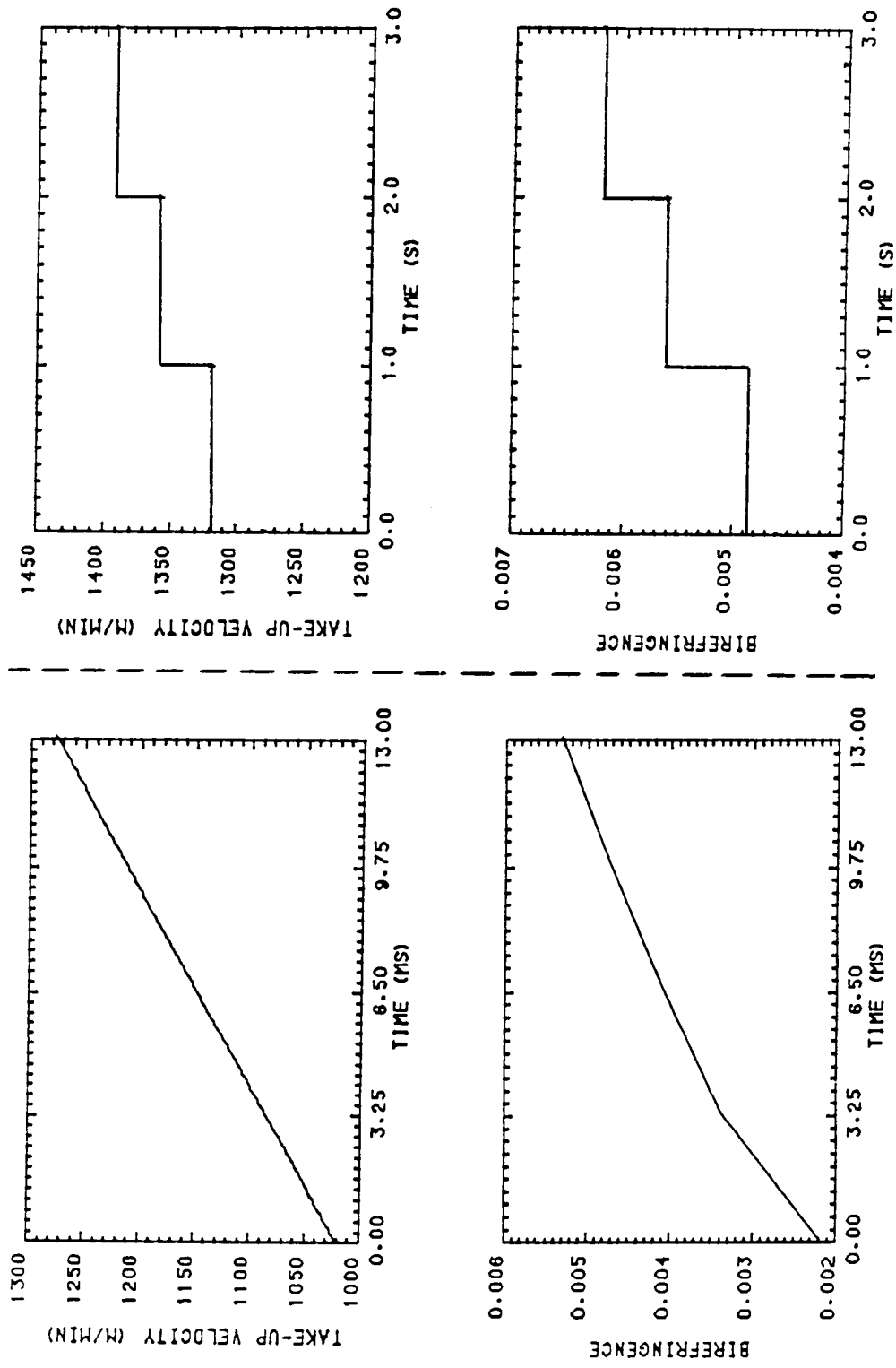


Figure 5.6. Open loop response of birefringence to a step change in take-up velocity.
(a) Theoretical response.
(b) Pseudo response.

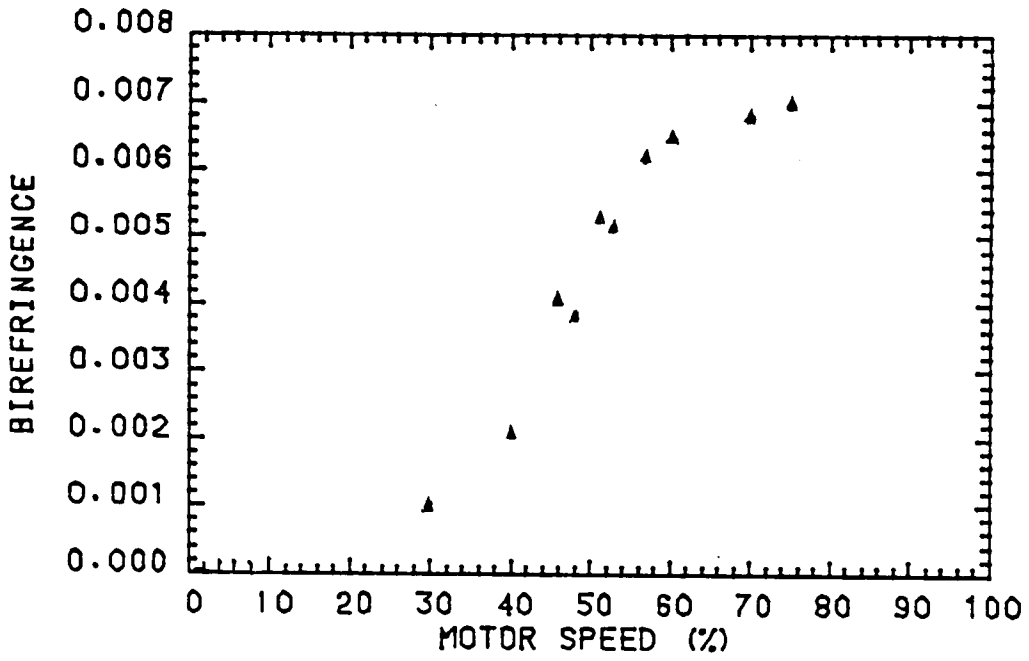


Figure 5.7. Birefringence as a function of motor speed for melt spinning under the research operating conditions.

These figures indicate the diameter and birefringence response to a 10 percent step in motor speed. Diameter decreased and birefringence increased as intuitively expected.

Verifying the predicted response with actual response was to approximate the responses (diameter and birefringence) with small steps (3.33 percent) each second for three seconds. The output was a pseudo-step response, Figures 5.4(b) and 5.6(b). The spinline behavior with the small steps was similar to the response predicted by the actual 10 percent step described above. Therefore, the process behaves closely to a pure gain unless the controller could be run at a sample time near or below 13 milliseconds and have a response described by Table 2.1, page 23.

It has been shown that birefringence as a function of sound wave frequency is not a well defined relationship. To control birefringence by perturbing the spinline with sound waves, it is essential that experiments be performed to clarify their effect on the spinline. Samples taken at different frequencies and drawdowns of 7:1 and 50:1 were analyzed off-line. The steady state results are shown superimposed on the work by Westbrook (42) in Figure 5.8. Dynamic changes with frequency were not determined, however, on-line work with the revolutionary new sensor may reveal insight to a mathematical model of the perturbation.

This testing was to better define the spinline birefringence as a function of sound wave frequency at fixed amplitude. Birefringence was found to change through the range of frequencies tested.

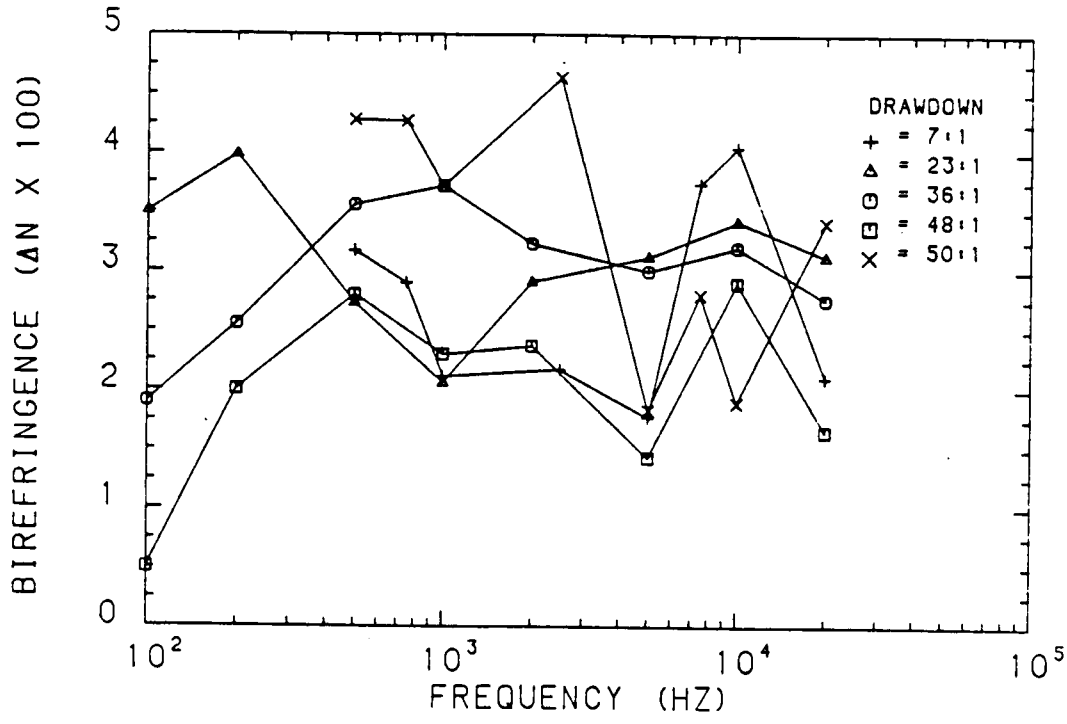


Figure 5.8. Response of birefringence to frequency of perturbing sound waves. Drawdowns of 7:1 and 50:1 were performed in this study.

The test was performed at 8 points from 750 to 20,000Hz, as illustrated, the function is still difficult to determine. Regularly spaced points every 2 to 3Hz are needed to offer more insight into the relationship. The new sensor-computer data acquisition system has this capability.

5.4 Control Loop Responses

Controlling the process begins with exploring the simplest relationship, diameter vs. take-up velocity. Control of this relationship requires the process gain to be well defined. The process gain is easily determined by open loop step tests, or in this case, there is a good model where the process gain for fiber diameter to take-up velocity can be determined. Referring to Figure 2.4(a), page 19, the gain from input to the motor, percent motor speed, to sensor output, d2, is $K_V K_{V_2} K_T$. The relationship of take-up velocity to motor speed is

$$\text{Take-up Velocity} = \text{Motor Speed} \times \text{Drum Circumference} \qquad (5.4)$$

where Motor Speed = 0 - 4000rpm (0 - 100%)

Drum Circumference = 0.655m

so the gain from the motor speed (%) to take-up velocity, V_2, is

$$K_V = \frac{4000\ (0.655)\frac{m}{min}}{100\%} = 26.2\ \frac{\frac{m}{min}}{\%} \qquad (5.5)$$

where K_V = gain of the actuator.

The gain of the sensor, K_T, is 1.0 because the computer converts the sensor measurement into microns. So, an open loop step test in motor speed while measuring the resulting change in fiber diameter would identify the $K_V K_{V_2} K_T$ gain. Alternately, this gain for a given operating point corresponds to the slope at the operating point of the diameter vs. motor speed curve which is given in Figure 5.5, page 117.

Most experiments in this research operated with a fiber diameter setpoint of 75 microns. Taking the slope from Figure 5.5, at 75 microns gives

$$(K_V K_{V_2} K_T)_{expt'l} = -0.411 \frac{\text{microns}}{\% \text{ motor speed}} \quad . \tag{5.6}$$

Solving for K_{V_2} gives

$$(K_{V_2})_{expt'l} = -0.0157 \frac{\text{microns}}{\frac{\text{m}}{\text{min}}} \quad . \tag{5.7}$$

Recalling that K_{V_2} can also be obtained from the linearized model for fiber diameter (Equation 4.8, page 91), at the operating conditions of this research, $d_{1,ref} = 0.000762\text{m}$, $V_{1,ref} = 7.34\text{m/min}$ (as mass flowrate = 3.1gm/min and density = $0.925 \frac{\text{g}}{\text{cm}^3}$), and $V_{2,ref} = 2050\text{m/min}$, the expression gives

$$(K_{V_2})_{theory} = -\frac{d_{1,ref}^2 V_{1,ref}}{2V_{2,ref}^{\frac{3}{2}}}^{1/2} = -0.0090 \frac{\text{microns}}{\frac{\text{m}}{\text{min}}} \tag{5.8}$$

Usually when Equations 5.7 and 5.8 are within a reasonable percentage of each other, it indicates that the process gain has been appropriately defined and the control arguments can continue.

As discussed in Chapter 4, pure I-mode control was employed. According to the closed loop transfer function for I-mode feedback control, the major character of the response is fixed by a process gain and the $\frac{K_C}{T_I}$, called C, in the integral control law. The integral control law is

$$\text{New Motor Speed} = \text{Old Motor Speed} + C\ (d_{2,ref} - d_2) \qquad (5.9)$$

where $d_{2,ref}$ = diameter setpoint

d_2 = measured diameter.

$C = \frac{K_C}{T_I}$

Since the process gain, K_{V_2}, is negative for the case of the spinline, it is known that C must be negative for the closed loop to be stable. The diameter setpoint was entered and used in calculations for the error. Four trials of the spinline integral control with different C values are presented in Figure 5.9. Note the initial starting diameter is not the same on all four.

Control of the spinline diameter with an integral controller offered an effective means of reaching and maintaining a setpoint. A setpoint of 75 microns was studied by varying the controller gain, C. As shown in Figure 5.9, the typical response time for reaching the setpoint from 90 microns was 15 to 35 seconds depending on the value of C. High magnitude values of C gave a large controlling

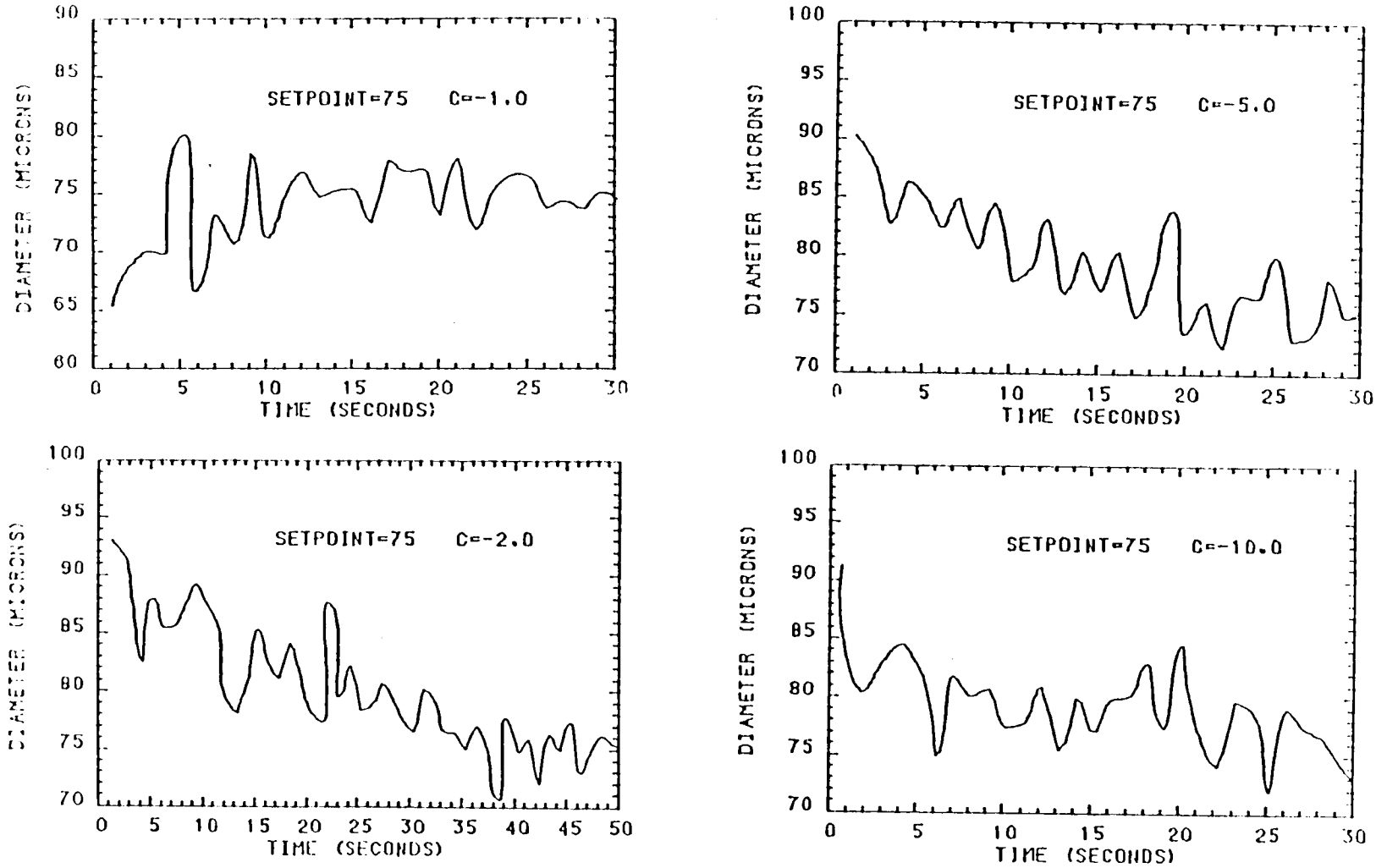


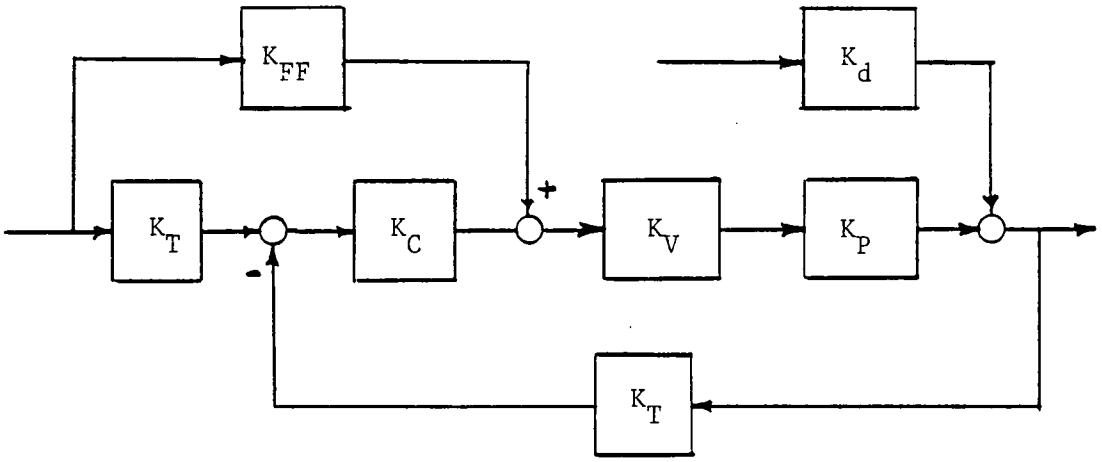
Figure 5.9. Closed loop response of diameter with integral control and varied controller gain.

action, that is, it reached the setpoint fast but has high oscillatory motion due to the multiplication of the spinline "noise" or variations by C. Low magnitude values found the setpoint slowly and gave little oscillation. Recall, that a great deal of the oscillation noted in the figure was due to the steady state variations of the system. Using the integral mode controller, the new motor speed for the new diameter was obtained through several iterations of the control loop, giving the expected first order response. In each iteration, the diameter setpoint was compared to the measured diameter and an amount of the error (as indicated by C) was added to the present motor speed. Since diameter decreased with increasing motor speed, C was negative. Thus, a negative error increased the present motor speed and a positive error decreased it. This action forced the controller to find the correct motor speed setpoint and maintain it there. The results were as good as could be expected for this controller with the process variations (at steady state).

The next logical development is to switch from I-mode to P-mode control with feedforward because of Equation 4.4, page 90. The significant change is that motor speed bias is feedforward. This process is illustrated in Figure 5.10. The control law for this type of control is

$$\text{New Motor Speed} = K_C(d_{2,ref}-d_2) \tag{5.10}$$

Two trials of this controller are illustrated in Figure 5.11. The responses are notably different from integral control due to the



K_{FF} = feedforward gain

K_T = transmitter gain

K_C = controller gain

K_V = activator gain

K_P = process gain

K_d = disturbance gain

Figure 5.10. Block diagram for proportional negative feedback control with feedforward indication of setpoint bias.

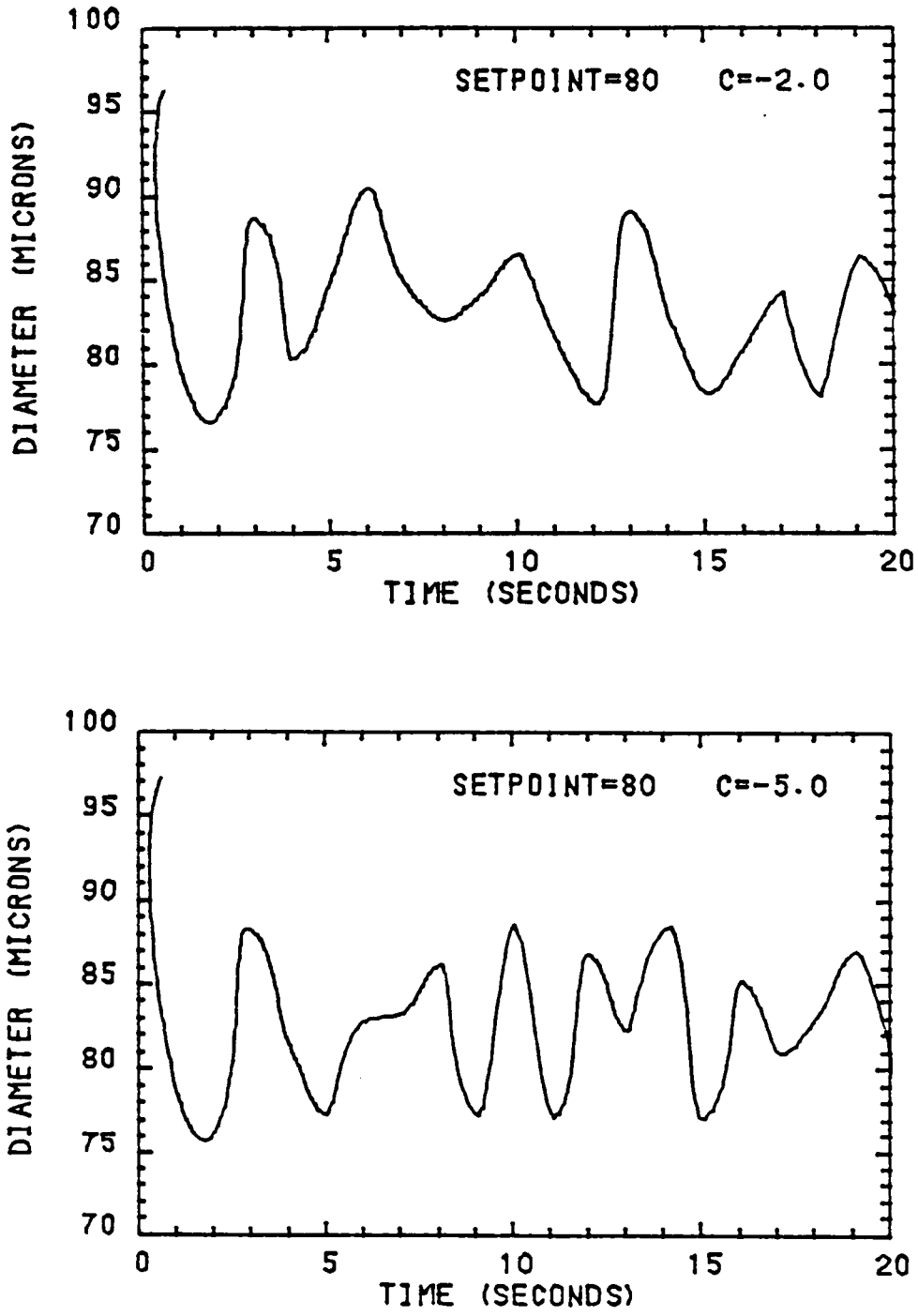


Figure 5.11. Closed loop response of diameter with proportional control and varied controller gain.

feedforward bias. Note there is a small amount of offset because of slight error in the feedforward bias. Also, note that all control action is based on unfiltered diameter readings. A problem with this controller was the offset. Although it reached a new diameter very fast, it was slightly off from the setpoint. The setpoint was 80 microns and the average controlled diameter was 83 microns. The effect of steady state variation was not as great with this controller because the feedforward motor speed bias was not dependent on previous errors.

The next level of development would be to use PI-mode control with feedforward bias. The I-mode would compensate for any errors in the feedforward bias.

Another important relationship studied was the birefringence control by manipulating the take-up velocity. Birefringence was controlled by sending out values to the motor controller that corresponded to the integral control strategy. That is,

$$\text{New Motor Speed} = \text{Old Motor Speed} + C(\Delta n_{2,ref} - \Delta n_2) \qquad (5.11)$$

where $\Delta n_{2,ref}$ = birefringence setpoint

Δn = measured birefringence.

$C = \frac{K_C}{T_I}$

As before, there is only one tuning parameter, C. The birefringence setpoint was entered into the computer code which established a motor speed bias according to the following model:

$$\text{Motor Speed Bias} = C_{\Delta n} \sqrt{\Delta n_{2,ref}} \quad . \tag{5.12}$$

The model of Equation 5.12 was obtained by fitting the data of Figure 5.7 over the range of motor speed of 30 to 50 percent. In this range the square root fit was fairly good. One run with a small C value is presented in Figure 5.12.

The control of birefringence with an integral controller was similar to controlling the diameter. A major difference was in the value of C. Since birefringence increases with increasing take-up velocity, C is positive. The value of the motor speed increased if the error ($\Delta n_{2,ref} - \Delta n_2$) was positive and decreased if it was positive. The run presented in Figure 5.12, illustrates the response. The setpoint of 0.005 was not reached due to an experimental problem that caused the spinline to break. However, all indications are that the setpoint would have been reached. As before, the motor speed bias corresponding to a new setpoint value is not known, so, the contoller iterates to find the value yielding the first order response.

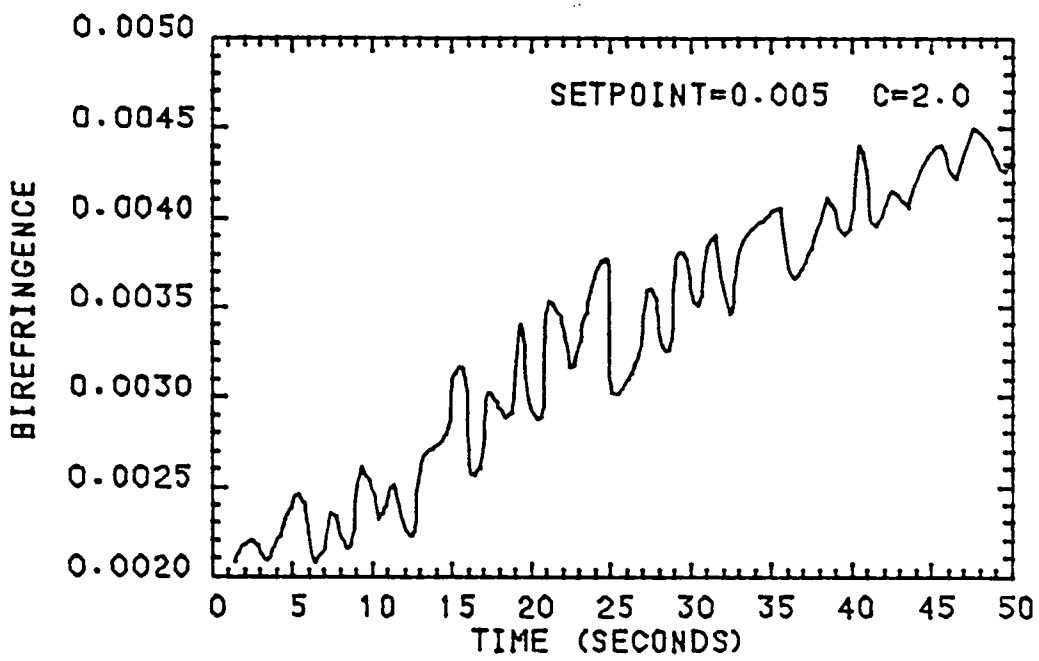


Figure 5.12. Closed loop response of birefringence with integral control.

CHAPTER 6

CONCLUSIONS AND RECOMMENDATIONS

6.1 Conclusions

This work has explored many aspects of process control. The outcome has yielded a novel spinline sensor, description of steady state and transient spinline behavior, investigation of the effect of sound waves on the spinline, and control of spinline diameter and birefringence. The highlights and results of the many areas of research are summarized and specific recommendations are given for future research-performing experiments to meet the control objectives.

An effective sensor has been designed for on-line diameter and birefringence measurements. The sensor indicates values within 2 percent error of actual diameter and 4 percent error of actual birefringence. It's unique capabilities provides application in both research and industrial process control. Outputs of the sensor include fiber diameter, light transmission, fiber position, and spinline tension. Computer interfacing provides for rapid data collection and good process control.

Experiments were performed to determine the response of birefringence to the intentional introduction of energy perturbations (sound waves) near the frost point of the spinline. The results have shown little insight into the relationship due to the small amount of data collected and the very likely complex nature of the relationship or perhaps due to inconsistencies associated with the data. Attempts to maintain a constant birefringence with the sound

waves were not performed because a good controlling strategy requires the system response to be mathematically defined at least near the point around which the birefringence is to be controlled. In spite of no functional description being obtained, a major conclusion is the ability of the sound waves to drive the spinline to different birefringences. The experiments revealed new birefringences but it cannot be said that an optimal change of birefringence was found because there were many frequencies, as well as amplitude, position of focus on the spinline, drawdown ratios, etc., that were not studied. With the new sensor and data acquisition system established, extended on-line studies are now possible to experimentally seek an optimum and provide a data base for model development.

The spinline response to step changing the take-up velocity was studied extensively. The step inputs indicated that diameter changed proportionally to the reciprocal square root of velocity as expected (Equation 4.4). The effect of take-up velocity on birefringence is considerably more complex, however, the birefringence did increase with take-up velocity as expected. A hypothetical (simulated) response was presented for a motor speed change of 10 percent (13 milliseconds) and compared to the experimental response to a series of sall steps on the actual spinline. The results verified the system model, the response of diameter to motor speed is essentially a pure gain, and established the first control strategies.

The proper operation of the new sensor combined with the completion of system step tests indicated that controlling diameter or

birefringence by manipulating the take-up velocity was feasible. Both integral and proportional control with feedback strategies proved to work very well for maintaining a constant diameter. Integral control reached the diameter setpoint slower than the proportional control with feedback, but the setpoint was found and maintained in every test. The proportional controller responded rapidly to a setpoint change, but its response was affected by controller offset. The offset was small and not significant enough for it to be an undesirable controller. The effect of the control parameter C for integral control of diameter was also examined. High values of C (not reported in previous chapters) gave high amplitude oscillation and even led to unstable control (spinline breaking) due to spinline variations. Low values of C proved useful because the response leveled out at the setpoint, however, it was slower (15 to 35 milliseconds) due to small controller action. Birefringence control was successfully performed using an integral controller with a small gain.

The controlled output in all cases showed oscillations which were due to the spinline variations which occurred at steady state, or spinline noise. The noise was monitored at steady state under different spinline velocities. It is felt that the noise was most likely real and created by variations in gear pump speed, harmonic vibrations, etc. In a general sense, controlling melt spinline diameter and birefringence has been proven feasible using modern technological devices and knowledge of applied industrial computer process control on chemical unit operations.

6.2 Recommendations

The melt spinline experiments performed in this work were extensive; however, the demand for better spinline control coupled with the success of this work provides significant motivation to continue research and improve the present operational system. Continuation of this study should include developing a means for improving the quality of collected data, definition of higher level control strategies, and interfacing peripheral equipment to improve spinline stability. The present work has been coined "phase one" of a system that has the potential to revolutionize the production of fibers. The potential has been recognized by Texas Instruments Incorporated, Johnson City, Tennessee, and their interest in phase one has inspired the contribution of TI-530 and CVU 5000, an industrial programmable controller with significant data acquisition, data storage, and graphics capabilities for use in phase two of the project. The donation of $35,000 in equipment has provided a unit with the control capability to handle any foreseeable advanced process control strategies. This upgrade in control equipment should be implemented as soon as possible.

The second phase of the spinline research should begin with review and redesign of the on-line sensor and associated equipment. The steady state variations can be reduced if the principle fiber guide of the sensor was remachined with attention directed at smoothing edges or roughness and reducing friction and spinline vibration. Another important consideration should be the reduction

of sensor vibration by using a dedicated floor mounted stand. The stand could support not only the sensor but all associated interfaces and control equipment. The lens system could be improved by increasing depth of field with an objective lens containing an iris. The iris will decrease light transmission resulting in a need to increase the intensity of the light source, perhaps a 500W Tungsten - Halogen lamp. The use of miniaturized vectors or matrices of photodiodes which are now available should be considered when upgrading the prototype diameter and birefringence sensor. Spinline tension could be more closely monitored by reducing the tensiometer operating range from 0-10gm to 0-1gm. The increase in resolution is desired because the tension is seldom more than 1gm. A more accurate tension will yield a more accurate birefringence measurement. The investigation of a more suitable tensiometer should also be considered because the present sensor imposes excessive spinline drag and causes cold working of the fiber. The overall accuracy of the sensor can be improved if a set of fiber samples corresponding to a known set of standards could be obtained and used to calibrate the sensor. It is also recommended that a new take-up device be obtained, however, until this can be done the aspirator should be retained as a final take-up device because of availability and convenience. The equipment for phase two is shown in Figure 6.1. The use of other computer systems (TI Professional, UTCC Dec-10, etc.) are dedicated to data storage, off-line mathematical analysis, model improvement, and controller communication. All of the equipment shown in this figure will soon be available except for the TI-990.

Figure 6.1. Control configuration for future work.

Definition of Process Variables:

Inputs

Manipulated on-line (real time) variables

A - Take-up motor current
B - Sound wave amplitude
C - Sound wave frequency

Manipulated analog control variables

D - Extruder heater current (zone 1), I_{z1}
E - Extruder heater current (zone 2), I_{z2}
F - Extruder heater current (zone 3), I_{z3}

Manually manipulated by operator

G - Die size
H - Screw gear ratio
I - Detector light source power
J - Magnification

Variable loads

K - Type of polymer
L - Molecular weight distribution of polymer
M - Impurities
N - Room temperature
O - Air velocity
P - Noise level

Outputs

Measured on-line (real time) variables

Q - Diameter of spinline
R - Birefringence of spinline
S - Take-up motor speed
T - Tension of the spinline
U - Take-up motor torque

Measured variables (by operator observation)

V - Pressure in the extruder metering head
W - Temperature of the metering head
X - Temperature of the extruder zones, T_z

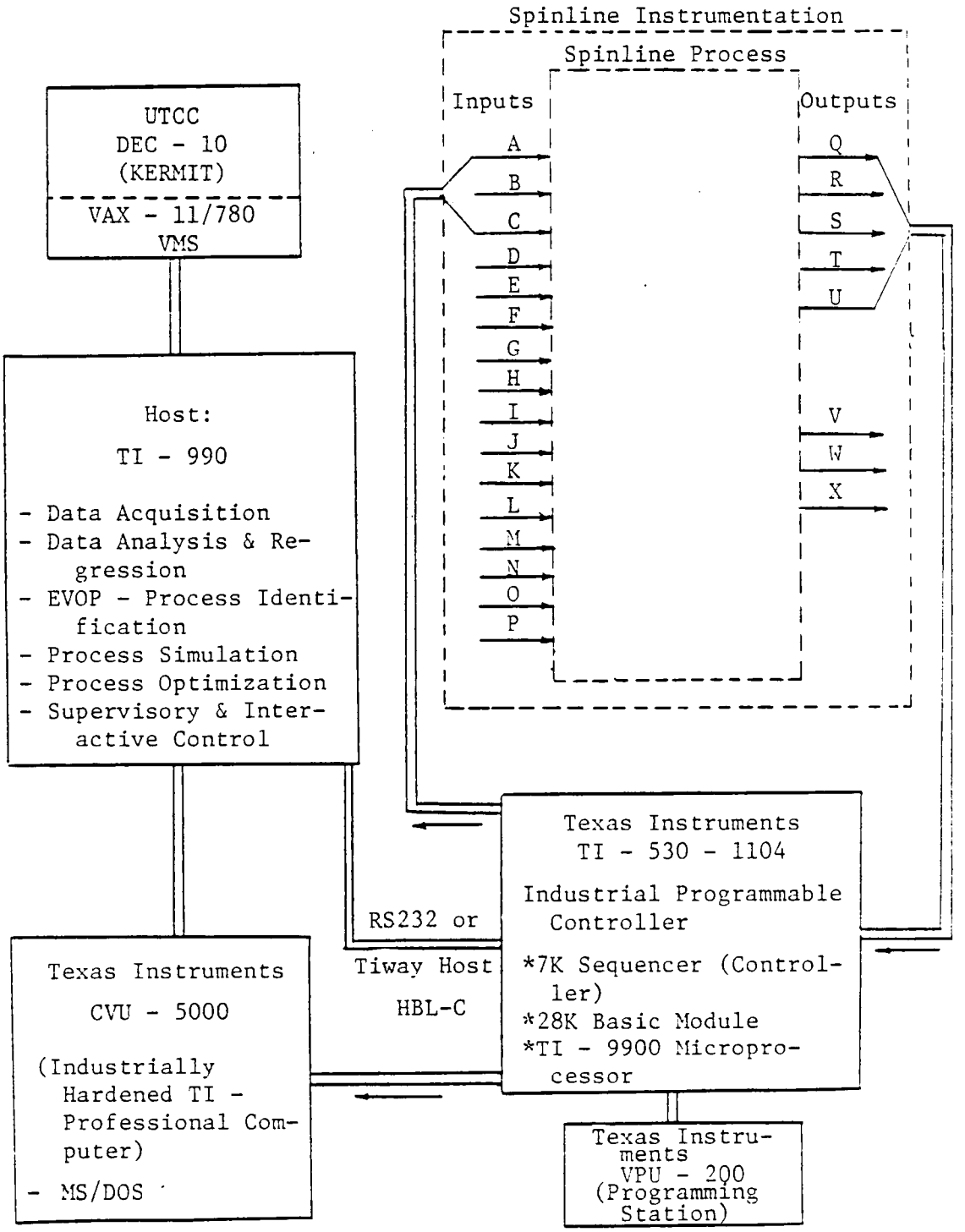

Spinline Instrumentation
Spinline Process
Inputs
Outputs
A
B
C
D
E
F
G
H
I
J
K
L
M
N
O
P
Q
R
S
T
U
V
W
X
UTCC
DEC - 10
(KERMIT)
VAX - 11/780
VMS
Host:
TI - 990
- Data Acquisition
- Data Analysis & Regression
- EVOP - Process Identification
- Process Simulation
- Process Optimization
- Supervisory & Interactive Control
RS232 or
Tiway Host
HBL-C
Texas Instruments
TI - 530 - 1104
Industrial Programmable Controller
*7K Sequencer (Controller)
*28K Basic Module
*TI - 9900 Microprocessor
Texas Instruments
CVU - 5000
(Industrially Hardened TI - Professional Computer)
- MS/DOS
Texas Instruments
VPU - 200
(Programming Station)

Figure 6.1

Improved control will obviously result from the reduction of the noise seen as spinline variations. Characterizing the steady state noise generated by the spinline is important in determining the type of filter that might be used to remove it. An objective could be to reduce the steady state, open loop oscillation to within 1 percent of setpoint with improved equipment and/or filtering. Several filters are available. A numerical averaging of 10 to 50 data points would be effective provided the control loop sample time is large enough to accommodate it. Perhaps, statistically discarding data points that do not fall within one or two standard deviations of the setpoint would yield a vast improvement in the quality of the data. The statistical filter could also include a weighted average of the data, or a differential equation to fit the data. One of the simplest filters is a first order digital filter.

The spinline research should continue the control aspects by a composite of proportional and integral action utilizing feed-forward strategy (14,36). The effect of this action will be an increase in the order of the response, elimination of offset, and a decrease in the oscillatory motion. The PI controller would be tuned with two parameters giving the operator more control of the response.

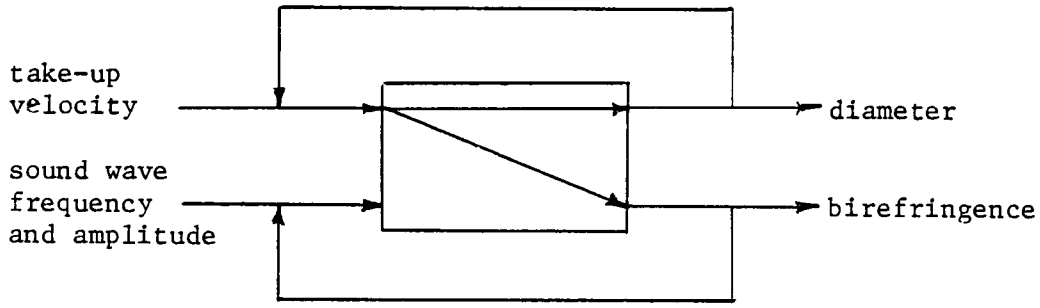
The effect of filtering on PI-control should be determined. The process response to filtered control will give a smoother signal, i.e., low amplitude oscillation. Tuning the controller to give the best process response is much easier, from an operational, as well as a mathematical standpoint, with a low noise signal.

Also, open loop step tests should be performed with a filter. The filtered signal will offer more insight into the process response and challenge the accuracy of the process model.

Another research field is opened up in terms of the relationship of birefringence to the sound wave perturbation. This relationship can be identified with improved process data as a data acquisition system is available and tested. It is recommended that the on-line sensor-computer system be used to obtain a data bank of responses to frequency, amplitude, and location of sound wave focal region with respect to the frost point, with various drawdowns and polymer types. Open loop computer algorithms can be used to drive the system through a series of step tests. The tests should yield an empirical process model of birefringence as a function of sound waves. Exploration of the Lindenmeyer hypothesis should coincide with a major part of this work. That is, define the spinline behavior on a molecular level when high frequency sound waves propagate through it.

Single input-single output control of the spinline can now branch in at least two directions. One direction has been previously explored, controlling diameter and birefringence with take-up velocity. The other direction is to demonstrate control of birefringence with sound waves. Transfer functions for each direction are to be determined using filtered data. The transfer functions concerning sound waves, $\Delta n/\omega$ and $\Delta n/A$, can now be a point of primary interest. Control using these relationships should be developed through proportional and integral algorithms much in the same manner as in this work.

Another realm of spinline control could incorporate a multi-variable control scheme for controlling diameter and birefringence simultaneously. This type of control has been proven very useful with many chemical unit operations and it is feasible that it can be used on the spinline. To control two variables simultaneously, such as the spinline, the degree of interaction between the process variables must be determined.



that is, the manipulation of one input variable can affect more than one output variable. The partial interaction of the spinline can be determined using a relative gain array (RGA) or singular value decomposition (SVD).

Continued research into melt spinline control is to deal with the elimination of steady state process variations created by the extrusion device. Variations in the spinline characteristics can be related to changes in extruder temperature, pressure, mass flow rate, etc. Interfacing these variables with the minicomputer will permit monitoring and perhaps control of the sources of spinline instabilities. It is recommended that necessary equipment for this

expansion be acquired and open loop step tests performed to determine, or better define, the precise relationship of the variables to the spinline instabilities. Models and control development can then be pursued.

LIST OF REFERENCES

LIST OF REFERENCES

1. Bankar, V. G., J. E. Spruiell, and J. L. White, "Melt Spinning of Nylon 6: Structure Development and Mechanical Properties of As-Spun Filaments," Journal of Applied Polymer Science, Vol. 21, pp. 2341-2358, 1977.

2. Barnett, E. H., "Introduction to Evolutionary Operation," Industrial and Engineering Chemistry, Vol. 52, No. 6, pp. 500-503, June, 1960.

3. Berringer, L. D. (editor), "DIALOG Extruder Controls," Plastics World, Vol. 32, No. 6, pp. 36-41, June 17, 1974.

4. Bodaghi, H., J. E. Spruiell, and J. L. White, "The Fibrillar Structure of Melt Spun and Drawn Polypropylene Filaments," PATRA Report No. 199, Polymer Engineering, The University of Tennessee, Knoxville, Tennessee, 1983.

5. Bristol, E. H., "A Philosophy for Single Loop Controllers in a Multiloop World," Chempid Symposium for ISA Chemical and Petroleum Division, May 15-17, 1967.

6. Bristol, E. H., "On a New Measure of Interaction for Multivariable Process Control," IEEE Transactions on Automatic Control, Volume AC-11, No. 1, pp. 133-134, January, 1966.

7. Bristol, E. H., "Process Control: An Application Theorists' View of Control," Control Systems Magazine, pp. 3-8, March, 1982.

8. Brooks, S. H., "A Comparison of Maximum-Seeking Methods," Operations Research, Vol. 1, No. 4, pp. 430-457, 1959.

9. Carey, D. A., C. J. Wust, Jr., and D. C. Bogue, "Studies in Nonisothermal Rheology: Behavior Near the Glass Transition Temperature and in the Oriented Glassy State," Journal of Applied Polymer Science, Vol. 25, pp. 575-588, 1980.

10. Carpenter, B. H., and H. C. Sweeny, "Process Improvement with 'Simplex' Self-Directing Evolutionary Operation," Chemical Engineering, Vol. 72, No. 14, pp. 117-126, July 5, 1965.

11. Choi, K. J., J. E. Spruiell, and J. L. White, "Orientation and Morphology of High-Density Polyethylene Film Produced by the Tubular Blowing Method and its Relationship to Process Conditions," Journal of Polymer Science: Polymer Physics Edition, Vol. 20, pp. 27-47, 1982.

12. Costin, M. H., P. A. Taylor, and J. D. Wright, "A Critical Review of Dynamic Modeling and Control of Plasticating Extruders," Polymer Engineering and Science, Vol. 22, No. 7, pp. 393-401, May, 1982.

13. Coughanowr, D. R., and L. B., Koppel, Process Systems Analysis and Control, McGraw-Hill Book Company Inc., New York, 1965.

14. Coulman, G. A., "Process Reaction Curve Controller Tuning Methods," Cache Corporation, 1976.

15. Danford, M. D., J. E. Spruiell, and J. L. White, "Structure Development in the Melt Spinning of Nylon 66 Fibers and Comparison to Nylon 6," Journal of Applied Polymer Science, Vol. 22, pp. 3351-3361, 1978.

16. DeBusk, R. E., "Experience in Evolutionary Operations at Tennessee Eastman Company," Industrial Quality Control, Vol. 19, No. 4, pp. 15-21, October, 1962.

17. Deshpande, P. D., and R. H. Ash, Elements of Computer Process Control with Advanced Control Applications, Instrument Society of America, pp. 293-302, 1981.

18. Han, C. D., and L. H. Drexler, "Studies of Converging Flows of Viscoelastic Polymeric Melts I. Stress-Birefringent Measurements in the Entrance Region of a Sharp-Edged Slit Die," Journal of Applied Polymer Science, Vol. 17, pp. 2329-2354, 1973.

19. Hassan, G. A., and J. Parnaby, "Model Reference Optimal Steady-State Adaptive Computer Control of Plastics Extrusion Processes," Polymer Engineering and Science, Vol. 21, No. 5, pp. 276-284, April, 1981.

20. Hong, S. D., S. Y. Chong, R. F. Fedors, and J. Moacanin, "Study of Molecular Deformation Mechanisms in the Glassy State. I. Temperature Effect on Stress-Birefringence and Strain-Birefringence Responses of Poly(methyl Methacrylate)," Journal of Polymer Science: Polymer Physics Edition, Vol. 21, pp. 1647-1660, 1983.

21. Hunter, J. S., "Optimize Your Chemical Process with Evolutionary Operations," Chemical Engineering, Vol. 67, No. 10, pp. 193-202, September 19, 1960.

22. Hunter, W. G., and J. R. Kittrell, "Evolutionary Operation: A Review," Technometrics, Vol. 8, No. 3, pp. 389-397, August, 1966.

23. Katayama, K., T. Amano, and K. Nakamura, "Structural formation during melt spinning process," Kolloid-Zeitschrift und Zeitschrift für Polymere, Band 226, Heft 2, pp. 125-134, 1967.

24. Lapidus, L., E. Shapiro, S. Shapiro, and R. E. Stillman, "Optimization of Process Performance," A.I.Ch.E. Journal, Vol. 7, No. 2, pp. 288-294, June, 1961.

25. Luyben, W. L., Process Modeling, Simulation, and Control for Chemical Engineers, McGraw-Hill Book Company, Inc., New York, 1973.

26. Matsumoto, T., and D. C. Bogue, "Stress Birefringence in Amorphous Polymers Under Nonisothermal Conditions," Journal of Polymer Science: Polymer Physics Edition, Vol. 15, pp. 1663-1674, 1977.

27. McCabe, W. L., and J. C. Smith, Unit Operations of Chemical Engineering, 3rd Edition, McGraw-Hill Book Company, Inc., New York, 1976.

28. Nadella, H. P., H. M. Henson, J. E. Spruiell, and J. L. White, "Melt Spinning of Isotactic Polypropylene: Structure Development and Relationship to Mechanical Properties," Journal of Applied Polymer Science, Vol. 21, pp. 3003-3022, 1977.

29. Oda, K., J. L. White, and E. S. Clark, "Influence of Melt Deformation History on Orientation in Vitrified Polymers," Polymer Engineering and Science, Vol. 18, No. 1, pp. 53-59, January, 1978.

30. Perry, R. H., and C. H. Chilton, Chemical Engineers' Handbook, 5th Edition, McGraw-Hill Book Company, Inc., New York, 1975.

31. Shinskey, F. G., Process Control Systems, 2nd Edition, McGraw-Hill Book Company, Inc., New York, pp. 196-221, 1979.

32. Spruiell, J. E., and J. L. White, "Structure Development During Polymer Processing: Studies of the Melt Spinning of Polyethylene and Polypropylene Fibers," Polymer Engineering and Science, Vol. 15, No. 9, pp. 660-667, September, 1975.

33. Spruiell, J. E., and J. L. White, "Structure Development During the Melt Spinning of Fibers," Applied Polymer Symposium, No. 27, pp. 121-157, 1975.

34. Stein, R. S., Newer Methods of Polymer Characterization, p. 173-206, John Wiley and Sons, New York, 1964.

35. Stein, R. S., "Studies of Solid Polymers with Light," Journal of Chemical Education, Vol. 50, No. 11, pp. 748-753, November, 1973.

36. Stephanopoulos, G., Chemical Process Control--An Introduction to Theory and Practice, Prentice-Hall, Inc., New Jersey, 1984.

37. Tipler, P. A., Physics, Vol. 2, Worth Publishers, Inc., 1976.

38. Tsou, J. D., "Dynamics of Isothermal and Non-Isothermal Melt Spinning," Department of Chemical, Metallurgical, and Polymer Engineering, The University of Tennessee, Knoxville, Tennessee, 1983.

39. Wales, J. L. S., "Apparatus for the measurement of flow birefringence of polymer melts at high shear stresses," Rheologica Acta, Band 8, Heft 1, pp. 38-44, 1969.

40. Wales, J. L. S., The Application of Flow Birefringence to Rheological Studies of Polymer Melts, Delft University Press, pp. 58-101, 1976.

41. Wales, J. L. S., and W. Philippoff, "The Anisotropy of Simple Shearing Flow," Rheologica Acta, pp. 25-34, Band 12, Heft 1, 1973.

42. Westbrook, P. A., and J. F. Fellers, "Some Results and Comments on the Experiment to Give a Primative Test to the Modified Lindenmeyer Hypothesis," unpublished.

43. White, J. L., "Dynamics, Heat Transfer and Rheological Aspects of Melt Spinning: A Critical Review," Polymer Engineering Reviews, Vol. 1, No. 4, pp. 297-362, 1981.

44. White, J. L., and J. E. Spruiell, "Structure Development in Fiber Formation From Aliphatic Polyamides and Polypeptides," Journal of Applied Polymer Science: Applied Polymer Symposium 33, pp. 91-127, 1978.

APPENDIX

```
      PROGRAM DIACON
C     ****************************************************************
C
C           PROGRAM FOR COMPUTER CONTROLLED MELT SPINLINE
C
C                                 BY
C                          RICHARD F. ELDRETH
C
C
C          THE FOLLOWING PROGRAM IS THE MAIN ROUTINE FOR CONTROLLING
C     A RESEARCH POLYETHYLENE MELT SPINLINE.  THE ALGORITHM
C     RECEIVES ONE INPUT VARIABLE (DIAMETER) AND MANIPULATES ONE
C     OUTPUT VARIABLE (TAKE-UP RATE). THE COMPUTER MONITORS THE
C     INPUT VARIABLE, COMPARES IT TO THE SETPOINT AND
C     MANIPULATES THE OUTPUT VARIABLE TO COMPENSATE FOR
C     ANY DEVIATION FROM THE SETPOINT.  ALSO, THIS ROUTINE
C     INCORPORATES A TENSIOMETER READING FOR INDICATING THE
C     STRESS IN THE SPINLINE.
C          THIS PROJECT IS PERFORMED IN PARTIAL FULFILLMENT OF THE
C     REQUIREMENTS FOR A MASTER OF SCIENCE DEGREE IN CHEMICAL ENG-
C     INEERING.  SUPERVISORS FOR THE PROJECT ARE DR. D. D. BRUNS AND
C     DR. J. F. FELLERS, BOTH OF THE UNIVERSITY OF TENNESSEE, DEPART-
C     MENT OF CHEMICAL, METALLURGICAL, AND POLYMER ENGINEERING.
C
C                          OCTOBER, 1984
C
C     ****************************************************************
C
      EXTERNAL ADC,ADINIT
      DIMENSION VA1(500),INV(500)
      DIMENSION FMICRO(500),FMOTOR(500),FIMTR(500)
      DIMENSION GRAMS(500),STRESS(500),IMTR(500)
      REAL LENS
      CALL ADINIT
      ICHAN0 = 0
      ICHAN1 = 1
      ICHAN2 = 2
      L=1.0
C
C     THE FOLLOWING 58 LINES OF THIS PROGRAM READ IN THE OPERATING
C     PARAMETERS FROM THE KEYBOARD AND SET UP ALL INITIAL VALUES
C     FOR CALCULATIONS AND DATA RETRIEVAL.
C
500   WRITE(1,10)
10    FORMAT(1X,' ')
      WRITE(1,25)
25    FORMAT(1X,'ENTER DIAMETER TO BE MAINTAINED (50.0-200.0 MICRONS)
     &: ')
      READ(1,26)DIA
26    FORMAT(F8.4)
      WRITE(1,27)
27    FORMAT(1X,'ENTER CONTROLLER GAIN, KC (0.0-1.0): ')
      READ(1,28)FKC
28    FORMAT(F7.4)
```

```
      WRITE(1,30)
30    FORMAT(1X,'ENTER SAMPLE TIME (0.1 - 15.0 SECONDS): ')
      READ(1,32)DLY
32    FORMAT(F7.4)
      IDLY=(DLY*1000.0)*(255.0/15000.0)
      CALL MSDLY(IDLY)
      WRITE(1,33)
33    FORMAT(1X,'WHICH LENS IS BEING USED (1-7)? ')
      READ(1,34)ILENS
34    FORMAT(I6)
      IF(ILENS.EQ.1.0)LENS=0.3758
      IF(ILENS.EQ.2.0)LENS=0.3375
      IF(ILENS.EQ.3.0)LENS=0.3162
      IF(ILENS.EQ.4.0)LENS=0.2913
      IF(ILENS.EQ.5.0)LENS=0.2976
      IF(ILENS.EQ.6.0)LENS=0.2590
      IF(ILENS.EQ.7.0)LENS=0.2375
      WRITE(1,38)
38    FORMAT(1X,'SEND THE OUTPUT TO DISK FILE 7 (1=YES,2=NO)? ')
      READ(1,39)IDISK
39    FORMAT(I6)
      IF(IDISK.EQ.2.0)GO TO 41
      WRITE(1,43)
43    FORMAT(1X,'ERASE OLD AND START NEW (1) OR ADD TO OLD (2)? ')
      READ(1,44)IERA
44    FORMAT(I6)
41    WRITE(1,35)
35    FORMAT(1X,'ENTER THE INITIAL MOTOR SPEED (0-100%): ')
      READ(1,37)MOTOR
37    FORMAT(I6)
      IMTR(1)=(MOTOR/100.0)*2047.0
      CALL OUTPUT(21,20,IMTR(1))
      IC=0.0
54    WRITE(1,55)
55    FORMAT(1X,'ENTER "0" WHEN CONTROL IS TO BEGIN: ')
      READ(1,56)INT
56    FORMAT(I6)
      IF(INT.NE.0.0)GO TO 54
      CALL HEADIN
C
C     THE FOLLOWING 80 LINES INCORPORATE THE CONTROLLING
C     ALGORITHM.  THEY CONTROL THE SYSTEM BY MONITORING CONTROL
C     VARIABLES AND CHANGING MANIPULATED TO COMPENSATE FOR
C     DEVIATIONS FROM THE SETPOINT.  THE 80 LINES ARE REPEATED
C     500 TIMES OR UNTIL THE PROGRAM IS FLAGGED TO STOP.
C
5     SUM=0.0
      DO 900 I=1,30
910   CALL ADC(ICHANO,IRDG)
      IF(IRDG.LE.100.0)GO TO 910
      SUM=IRDG+SUM
900   CONTINUE
      FDIA=SUM/30.0
      IC=IC+1.0
```

```
         VA1(IC)=(FDIA/2.0)*(1960.0/2047.0)
         FMICRO(IC)=VA1(IC)*LENS
         CALL IBCD(INVAL)
         INV(IC)=INVAL
         CALL ADC(ICHAN2,IRDG)
         GRAMS(IC)=(FLOAT(IRDG)/2047.)*10.
         STRESS(IC)=(GRAMS(IC)/(3.14159*((FMICRO(IC)/2.0)**2.0)))*
     &98067000000.0
         FMOTOR(IC)=(IMTR(IC)/2047.0)*100.0
         WRITE(1,51)FMICRO(IC),FMOTOR(IC),GRAMS(IC)
51       FORMAT(1X,F6.1,F10.2,F11.3)
         J=IC+1.0
C
C        THE NEXT 10 LINES MANIPULATE THE MOTOR SPEED TO ALTER
C        THE DIAMETER.
C
         IMTR(J)=IMTR(IC)+FKC*(DIA-FMICRO(IC))
         IF(IMTR(J).GT.2047.0)IMTR(J)=2047.0
         CALL OUTPUT(21,20,IMTR(J))
2200     IF(IC.EQ.500)GO TO 410
C
C        THE NEXT SIX STATEMENTS INCORPORATE THE DELAY BETWEEN
C        SAMPLE TIMES AND MONITOR THE KEYBOARD FOR FLAGS THAT STOP
C        ITERATIONS (S) OR KILL THE PROGRAM (K).
C
1000     ISYNC=INP(195)
         IF(ISYNC.NE.1)GO TO 1000
         IST=INP(01)
         IST=IST.AND.127
         IF(IST.EQ.83)GO TO 410
         IF(IST.EQ.75)GO TO 410
         GO TO 5




C
410      IF(IDISK.EQ.2.0)GO TO 450
         IF(IERA.EQ.2.0)GO TO 415
         IOLD=0.0
         GO TO 420
415      READ(7,417,REC=1)IOLD
417      FORMAT(I6)
420      ICNT=IOLD+IC
         WRITE(7,425,REC=1)ICNT
425      FORMAT(I6)
         ENDFILE 7
         WRITE(6,430)(FMICRO(I),FMOTOR(I),GRAMS(I),STRESS(I),INV(I)
     &,I=1,IC)
430      FORMAT(G10.4,F8.2,G10.4,E10.4,G10.4)
         ENDFILE 6
450      IF(IST.EQ.75)STOP EXIT
C
C        THE FINAL PORTION OF THE PROGRAM DISPLAYS THE DATA FROM THE
```

```
C       PRESENT RUN ON THE SCREEN, IF DESIRED.  IT IS COMPLETE WITH
C       TITLES AND ANY SPECIFIED NUMBER OF DATA POINTS.
C
800     WRITE(1,700)
700     FORMAT(1X,' ')
        WRITE(1,710)IC
710     FORMAT(1X,'THERE ARE ',I5,' DATA POINTS ON THIS RUN.  WOULD')
        WRITE(1,720)
720     FORMAT(1X,'YOU LIKE TO SEE ANY OF THE DETAILED RESULTS (1=YES
     &,2=NO)? ')
        READ(1,730)ISEE
730     FORMAT(I6)
        IF(ISEE.EQ.2.0)GO TO 500
        WRITE(1,740)IC
740     FORMAT(1X,'ENTER START,STOP POINTS (1-',I5,'): ')
        READ(1,755)ISEESR,ISEESP
755     FORMAT(2I6)
        WRITE(1,750)
750     FORMAT(8X,' DIAMETER   MOTOR    TENSION    STRESS   PREDATA')
        WRITE(1,760)
760     FORMAT(8X,' (MICRONS)   (%)     (GRAMS)  (DYN/CM2) (DIODES)')
        DO 770 I=ISEESR,ISEESP
        WRITE(1,780)I,FMICRO(I),FMOTOR(I),GRAMS(I),STRESS(I),INV(I)
780     FORMAT(1X,I5,F9.1,F10.2,F14.3,E10.2,I8)
770     CONTINUE
        WRITE(1,796)
796     FORMAT(1X,' ')
        GO TO 800
        END
C
C       THE SUBROUTINE "OBCD" CONVERTS A DECIMAL NUMBER TO
C       BINARY CODED DECIMAL THEN OUTPUTS THE HI BYTE TO THE
C       HI PORT AND THE LO BYTE TO THE LO PORT.
C
        SUBROUTINE OBCD(INTEG,IHPRT,ILPRT)
        N=INTEG
        NTEMP=N/10*10
        IUNIT=N-NTEMP
        N=NTEMP/10
        NTEMP=N/10*10
        ITENS=N-NTEMP
        N=NTEMP/10
        NTEMP=N/10*10
        IHNDS=N-NTEMP
        N=NTEMP/10
        NTEMP=N/10*10
        ITHS=N-NTEMP
        IBCDH=(16*ITHS)+IHNDS
        IBCDL=(16*ITENS)+IUNIT
        CALL OUT(ILPRT,IBCDL)
        CALL OUT(IHPRT,IBCDH)
        RETURN
        END
C
```

```
C       THE SUBROUTINE "MSDLY" INITIALIZES THE PARAMETERS FOR
C       THE DELAY ROUTINE.  THEREFORE, "MSDLY" MUST BE CALLED
C       BEFORE THE DELAY ROUTINE (SYNC) CAN BE CALLED.
C
        SUBROUTINE MSDLY(IDLY)
        CALL OUT(195,87)
        CALL OUT(194,87)
        CALL OUT(193,87)
        CALL OUT(192,87)
        CALL OUT(195,148)
        CALL OUT(194,IDLY)
        CALL OUT(193,4)
        CALL OUT(192,125)
        RETURN
        END
C
C       THE SUBROUTINE "OUTPUT" DIVIDES A 12 BIT DECIMAL NUMBER
C       INTO A HI BYTE AND A LO BYTE.  THE HI BYTE IS SENT TO
C       THE HI PORT AND THE LO BYTE IS SENT TO THE LO PORT.
C
        SUBROUTINE OUTPUT(IHPRT,ILPRT,IFREQ)
        ILO=IFREQ.AND.255
        IHI=(IFREQ.AND.65280)/256
        CALL OUT(ILPRT,ILO)
        CALL OUT(IHPRT,IHI)
        RETURN
        END
C
C       THE SUBROUTINE "IBCD" READS AN ADC AND SENDS THE NUMBER
C       TO THE MAIN ROUTINE.  THE HI AND LO BYTES ARE READ, AND
C       USED TO FIND THE DECIMAL DECADES WHICH ARE COMBINED TO
C       FORM A DECIMAL NUMBER.
C
        SUBROUTINE IBCD(INVAL)
        ILO=INP(32)
        IHI=INP(33)
        ILO=ILO.AND.255
        IHI=IHI.AND.255
        ITHS=(IHI.AND.240)/16*1000
        IHNDS=(IHI.AND.15)*100
        ITENS=(ILO.AND.255)/16*10
        IUNIT=ILO.AND.15
        INVAL=ITHS+IHNDS+ITENS+IUNIT
        RETURN
        END
C
C       THE SUBROUTINE "HEADING" PRINTS THE HEADING AT THE
C       TOP OF THE DATA TABLE.
C
        SUBROUTINE HEADIN
        WRITE(1,10)
10      FORMAT(1X,'DIAMETER   MOTOR    TENSION')
        WRITE(1,20)
20      FORMAT(1X,'(MICRONS)    (%)    (GRAMS)')
```

```
RETURN
END
```

VITA

Richard F. Eldreth was born in Kingsport, Tennessee on October 15, 1960. He graduated from Sullivan Central High School in June 1978 and then entered The University of Tennessee, Knoxville in September of that year. In December 1982 he graduated with a Bachelor of Science degree in Chemical Engineering. He continued his education in the area of process control at The University of Tennessee and was awarded a teaching assistantship in June 1983. He received his Master of Science degree in Chemical Engineering in March 1985. He is a member of the American Institute of Chemical Engineers, Smoky Mountain Astronomical Society and Bays Mountain Amateur Astronomers.